QATAR UNIVERSITY

COLLEGE OF ENGINEERING

MODELLING AND OPTIMIZATION OF A MULTI-POPULATION, SINGLE-CHAMBER MICROBIAL FUEL CELL OPERATING IN A CONTINUOUS FLOW MODE AT STEADY-STATE

BY

HAFSA MOHAMMED ASHRAF

A Thesis Submitted to

the College of Engineering

in Partial Fulfillment of the Requirements for the Degree of

Master of Science in Environmental Engineering

January 2022

COMMITTEE PAGE

The members of the Committee approve the Thesis of

Hafsa Ashraf defended on 18/11/2021.

Prof. Ibrahim Abu-Reesh
Thesis/Dissertation Supervisor

Prof. Riyadh Al-Raoush
Committee Member

Approved:

Khalid Kamal Naji, Dean, College of Engineering

ABSTRACT

ASHRAF, HAFSA M., Masters : January : 2022, Masters of Science in Environmental Engineering

Title: Modelling and Optimization of a Multi-population, Single Chamber Microbial Fuel Cell Operating in a Continuous Flow Mode at Steady-State

Supervisor of Thesis: brahim M. Abu-Reesh.

There is no doubt that energy demand has been increased in the last decade due to the economic revolution. However, this revolution is based on the fossils fuel which are going to be depleted. Microbial fuel cells are one the proposed technologies to provide renewable energy and treat wastewater simultaneously. The stumbling block for this technology is the low power production compared to conventional fuel cells. Modelling and optimization is carried out on a multi-population, single chamber microbial fuel cell operating in a continuous flow under steady state conditions for the first time in the literature. Microsoft Excel and Matlab computational tools were used to optimize three objective functions which are: power density, current density and substrate removal efficiency. Five parameters were varied around specified ranges for the optimization which are: dilution rate, external resistance, anodophilic and methanogenic bacteria concentration and substrate concentration. Results showed that all the objective functions converged to an optimum point at which power density, current density and substrate removal efficiency were 157 mW/L, 251 mA/L and 99%, respectively. The optimum point was at 2 day^{-1} dilution rate, 25 Ω external resistance, anodophilic and methanogenic bacteria concentration of 510.5 and 2 mg/L, respectively and 0.01 mg/L substrate concentration. From the local sensitivity analysis on power density, the most impacting factors of the studied parameters were external resistance and anodophilic bacteria concentration. This was agreed with the response surface methodology contour plots using Minitab software. Finally, variance-based global

sensitivity analysis was carried out studying six parameters which are maximum specific anodophilic growth rate, number of electrons transferred per mole of mediator, decay rate constant of anodophilics, half rate constant of both mediator and anodophilic bacteria. Following this analysis, first and total indices of each parameter were computed using Matlab and was coupled with Monte Carlo simulations. Maximum specific anodophilic growth rate and number of electrons transferred per mole of mediator were the most impacting factors on power density having total indices of 0.74 and 0.624, respectively. The findings herein are critical in understanding and further model improvement of microbial fuel cells.

DEDICATION

To my beloved family, a major reason this work saw the light. To all scholars in this complex and vital field.

ACKNOWLEDGMENTS

I would like to gratefully thank Allah, by his blessing good deeds are accomplished. Gratefully too, I would like to thank my supervisor Prof. Ibrahim Abu-Reesh for his valuable time, knowledge and limitless support. I am grateful for all people in the field of MFC which my research was built on their precious knowledge. Gratitude to Chemical Engineering Department at Qatar University for their great cooperation, collaboration and support. Finally, special thanks to all: Eng. Jamal Hannun, Eng. Najmath Ottakth and Eng. Salman Ismail for providing some computational tools. The findings achieved herein are solely the responsibility of the author.

TABLE OF CONTENTS

LIST OF TABLES

LIST OF FIGURES

CHAPTER 1: LITERATURE REVIEW

1.0.Introduction

There is no doubt that the energy demand has been increased in the last decade due to the economic revolution [1]. However, this revolution was based on non-renewable energy source of fossils fuel which is polluting the environment and about to be depleted [2]. Nowadays, researchers are seeking to develop new alternative technologies to serve the energy requirements and save the environment as well [3]. One of the proposed technologies is using microorganisms as catalysts for electricity generation which is known for several years [4]. This technique can be harvested in bio-electrochemical cells just as microbial fuel cells (MFCs) and microbial electrolysis cells (MECs) [5]. MFC is a promising sustainable technology which can directly recover chemical energy in bio-convertible wastewater and produce energy simultaneously. This is achieved by exploiting biocatalyst activity and utilising the microorganisms to degrade nutrients in either industrial or domestic wastewater [5]. The process of waste degradation (oxidation) by microorganisms produces electrons that is used as a renewable energy source [6]. It is worth mentioning that this potential source of renewable electrical energy cannot be recovered by using conventional techniques or chemical processes [7]. Therefore, MFCs are considered as climate-neutral technology for wastewater treatment and electricity production [8]. In fact, the amount of energy that can be recovered from urban wastewater exceeds the amount of energy that is currently used to treat it by nine times using the best technology; that can recover only one fourth of that recoverable energy of urban wastewater [9]. The ability of microorganisms to adopt in different environments and systems boosts the feature of utilizing different compounds as a source of essential needs from nitrogen, carbon and hydrogen [10]. Thus, by this methodology microorganisms (bacteria) are

decontaminating the polluted environments and benefiting from that as a source for their living, sustaining and producing more cells while producing energy [11]. For these aspects, environmentally friendly processes are developed to maximize the sustainability of energy production processes and resolve the global problem of emitting greenhouse gasses and global warming [12]. MFCs can utilize one or more species of microorganisms to achieve more than one objective [13]. For example, electricigenics (anodophilic bacteria) can be used as a single population to optimize the power density and electricity generation, while a multi-population of methanogens and electricigenic under a controlled environment of temperature and pH can be used to boost the substrate removal efficiency [14]. MFCs can be designed to be a dual chamber of both anode and cathode with proton exchange membrane (PEM) separating the two chambers or a single chamber of anode [15]. For maximizing the power production, it is preferred to use a dual chamber with PEM. This prevents the crossover of reactants and allows higher reactant concentration, hence, increasing the power production [4]. The anodic compartment of MFC contains the microorganisms, electron transfer mediators and nutrient (substrate). Microorganisms are considered as the biocatalyst in the system which are either suspended or exist as a biofilm. While mediators such as NADH and NAD^+ are responsible for electron transfer and can enhance the efficiency of the cell based on their molecular structure, dissociation and polarization [16]. While PEM are used for dual chamber MFC to ease the transport of H^+ ions from the anodic compartment to the cathodic compartment [1]. Also, there is the outer circuit connecting both electrodes together and eases the electrons flow for electricity generation. The main reaction in cathode is the reduction reaction in which electrons, protons and electron acceptor combine. If oxygen is the electron acceptor then the by-product which is produced is fresh water [16]. Based on microbial culture used in the

anode compartment the other by-products of MFC can be identified. If methanogens and anodophilics are used, then the other by-products are off-gases containing methane and carbon dioxide [17]. Although MFCs are attractive and renewable energy source which reduce the aeration pumping cost that comprises between (45-75) % of the total plant operating cost in conventional wastewater treatment plant [18], the bottleneck is that the MFC technology is not commercialized and used in large industrial scale. This is due to the low amount of power density produced compared to other conventional fuel cells [18]. Therefore, optimizing the performance of MFCs is a mandatory application. The optimization of the operating conditions in MFC is a topic that is covered by scholars since mid-90s. This can be carried out by using different tools such as mathematical modelling and computational methods as well as the experimental methods [19]. Mathematical modelling and computational methods for optimization are rare in MFC optimization although it is inexpensive and fast methodology [20]. Mathematical modelling can vary all the parameters together and define the interrelationships among them which helps identifying the important and most impacting parameters. In contrast, limitations are associated with the classical experimental optimization method as all the studied factors cannot be varied together which takes more time and effort [21]. The impact of parameters on the objective function can be tracked by using software such as Minitab and Matlab. Empirical equations which are used mostly for mathematical modelling of MFC are stated in Table 1-1.

Table 0-1. Empirical equations used for MFC [22]

Name	Governance variables	Equation
Monod Kinetics	Microbial growth	$\mu = \mu_{max}\frac{S}{K_s+S}$
Butler-Volmer	Voltage difference	$i = i_0[\exp\left(\frac{\alpha_n nF}{RT}(E - E_{eq})\right) - \exp(-\frac{\alpha_c nF}{RT}(E - E_{eq}))]$
Tafel plot	Overpotential	$E = E_{eq} + \frac{RT}{(1-\alpha)nF}\ln\left(\frac{i}{i_0}\right)$
Ohm's law	Voltage, external resistance, current	$V = IR$
Faraday's law	Mass transport	$J = zF\theta$
Nernst equation	Electron transfer	$E = E_0 - \frac{RT}{(1-\alpha)nF}\ln(Q)$

1.1.Thesis organization

This thesis study is started with a bibliometric analysis to show the scholars the vitality of the field. Then continued by a literature review on MFC system design. After that a DoE of Minitab specifically response surface methodology (RSM) is used to expect the optimization field using contour plots and generate equations for the output functions with respect to the studied parameters. Optimization of MFC is applied using Matlab and Microsoft Excel. This is followed by local and global sensitivity analysis using variance based Sobol's method.

1.2.Literature review

1.2.1. Bibliometric analysis of MFC over the last decade (2010-2020)

In this section, a quantitative bibliometric study is conducted to analyse the published content and literature related to MFC. It is one of the important analyses to be conducted before any study; as it reveals the importance of the study, the hot spot areas in the field of study and the competence of the topic to be studied. Sampson et al.

(2014) [23] stated that periodical analysis of a certain topic over the journals opens perspectives for researchers and provides different paths for discovering the professional literature related to a field. 8,065 journal articles and review papers were published in MFC field only in the last decade in English. 90.17 % which is 7,272 of the papers were scientific articles while the balance is review papers. The search was limited to review papers and articles for more reliable results [24]. This study is important as it gives an indication that this is a hot spot field of interest which is grabbing a good attention. The main objectives of this section are:

1- To map the science related to MFC and reveal the importance of this thesis topic.
2- Reveal the hotspot areas in the field of MFC and future research direction.

For bibliometric analysis, the number of publications per year, most publishing journals, authors and countries in addition to keywords analysis and most cited papers are discussed.

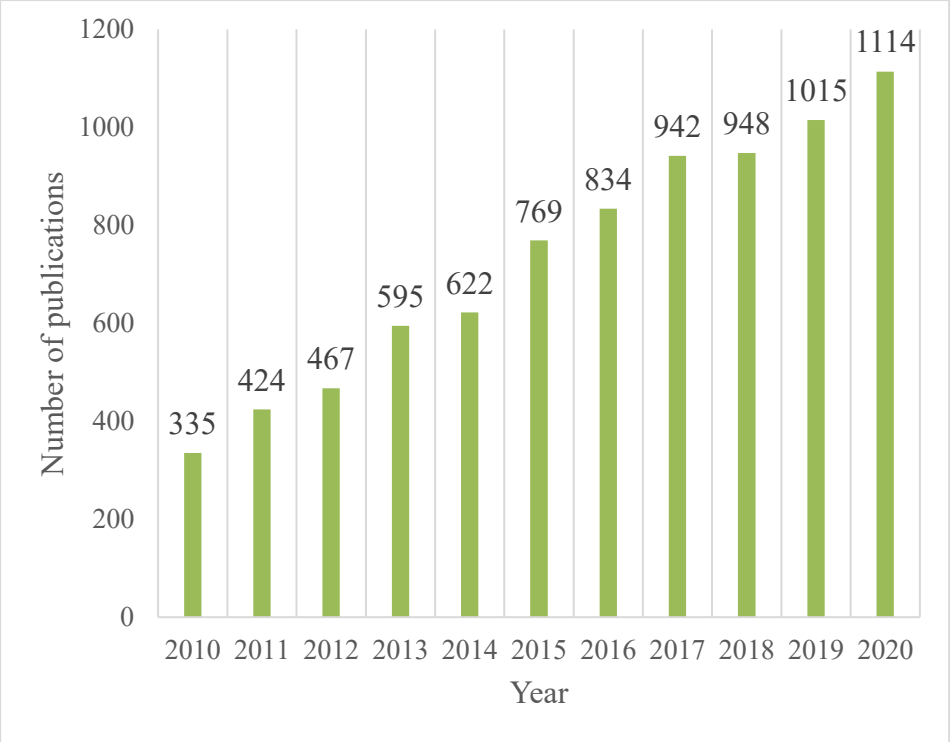

Figure 0-1.The number of publications per year [25]

Figure 1-1 shows the number of publications per year which shows the rate of publishing documents in the field. This is an important parameter to reveal the dynamicity, growth and the affinity of the scholars to publish in the field. It can be noticed that a year after another there is a considerable growth in number of publications. From 2010 to 2020 the number of publications has increased 3.30 times. This is an important sign that the field is growing considerably, and it is expected to grow in the future. Therefore, publishing in this field is getting interest, however, the fields of interest must be revealed too. This is achieved by both keywords and most cited papers analysis. The topic turned into a keen interest as the power of sustainability in wastewater treatment technologies has increased. Analysing all leading journal is another technique for quantitative literature review. Table 1-2 states all the leading journals in MFC publications. This is critical for young scholars to be updated about the new journal papers, research areas and topics in the field by following most

publishing journals. Ten top publishing journals in MFC are shown in Table 1-2 below. The leading journal in the field is Bioresource Technology which published 809 papers proceeded by Journal of Power Sources and International Journal of Hydrogen Energy with 352 and 317 journal papers, respectively. While Table 1-3 shows the most publishing countries in MFC field. China, the United States and India are the top three in publishing while the United States is the leading in citations. China and States are already the leading countries in renewable energy production and consumption. Chines government gives priority and attention to finding alternative methods solving variety of issues such as air and water pollution and wastewater treatment [26].

Table 0-2. Top 10 most publishing journals in MFC [25]

Journal	Documents	Citation contribution (%)
Bioresource Technology	809	18.71
Journal of Power Sources	352	9.64
International Journal of Hydrogen Energy	317	6.70
Chemical Engineering Journal	174	18.89
Biosensors And Bioelectronics	171	3.58
Electrochimica Acta	170	3.08
Bioelectrochemistry	164	2.97
Rsc Advances	147	6.60
Science of The Total Environment	117	1.42
Environmental Science And Technology	111	5.43

Table 0-3. Most publishing countries and their contribution of citations [25]

Country	Documents	Citation contribution (%)
China	2694	21.04
USA	1566	29.70
India	913	4.16
South Korea	561	5.81
United Kingdom	455	3.88
Germany	273	2.62
Japan	271	3.12
Spain	268	2.00
Malaysia	241	1.25
Taiwan	237	1.88

Leading authors in terms of the number of publications in MFC field is one of the most important bibliometric parameters as it shows the experts of the field. This is due to the importance of their earlier contribution discovering the field from the time that the field start seeing the sunshine till today. Top 10 most publishing authors are shown in Figure 1-2 below, and the most prolific authors in the field are Logan, Bruce E., Ghangrekar, M.M. and Greenman, J. who published 180, 122 and 113 scientific papers in MFC in the last decade respectively.

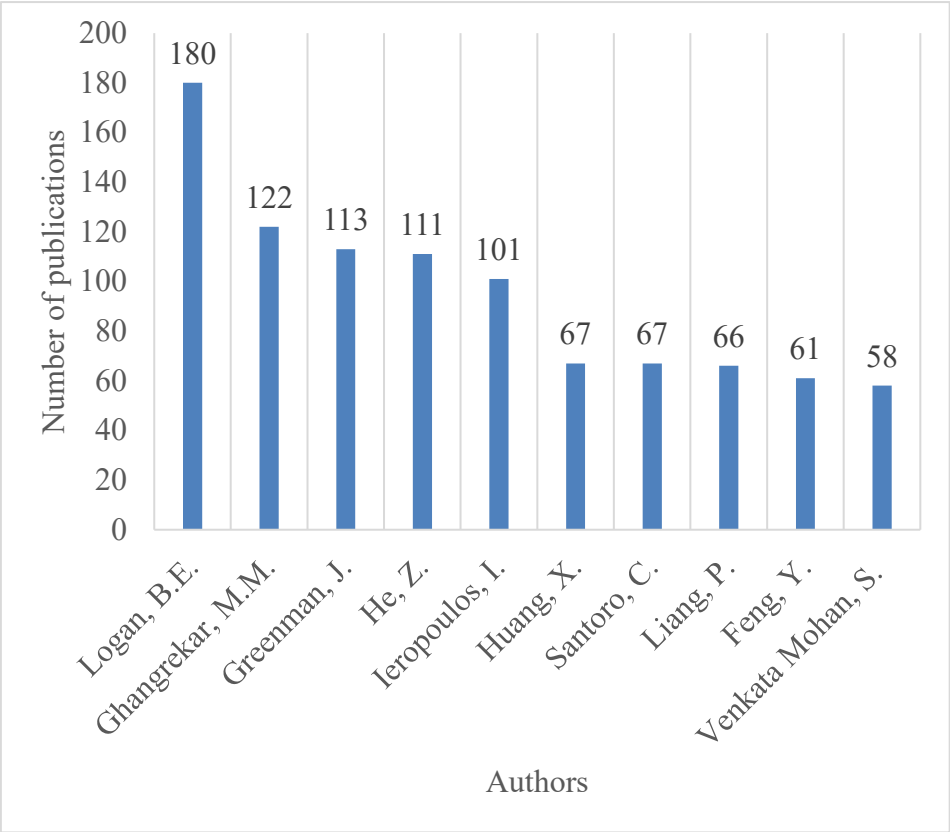

Figure 0-2.most publishing authors in MFC field (2010-2020) [25]

Divulging most frequently used keywords in the field of MFC is critical to increase the visibility of articles. Research engines utilize the keywords for results filtration and matching the best to the research. Therefore, young scholars could make use of most frequently keywords in their scientific papers to increase the visibility, thus increase the chances of citations. Figure 1-3 shows the most frequently used keywords in the last decade in MFC field and the frequency of appearance based on Scopus.

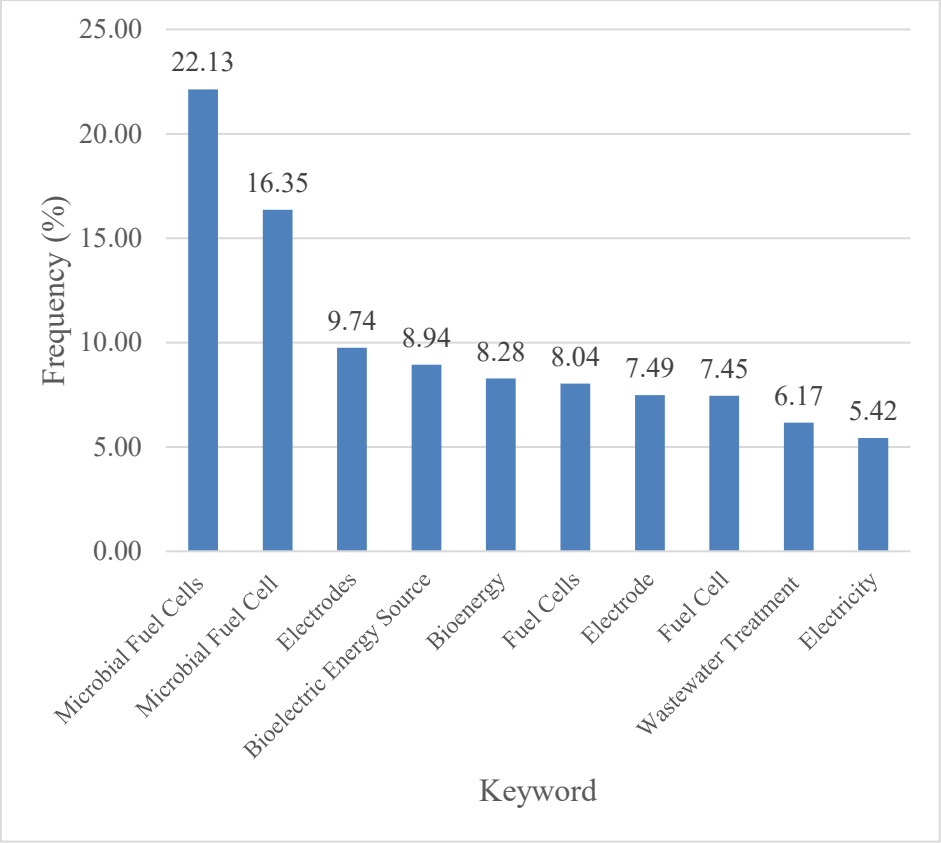

Figure 0-3. Top 10 most frequently used keywords in MFC field (2010-2020) [25]

"Microbial Fuel Cells" and "Microbial Fuel Cell" are the most frequently used keywords to give an indication that the article is related to MFC. Also, "Electrodes" is another keyword that has a frequency of 9.74%. Electrodes are one of the most important parts of MFC and impact the power productivity. The performance of MFC is directly related to the type and size of the electrode, the spacing between electrodes and bacteria on the surface of the electrodes. Hamed, M. et al. (2020) [27] have published a paper that studies the impact of electrodes on the performance of MFC [27]. The performance of MFC is main challenge towards commercializing its use in wastewater treatment industry. Scholars have shown a growing interest in the field of bioenergy of MFC, and that is reflected on the number of publications and the frequency of using the keyword "Bioelectric Energy Source" and "Bioenergy". Performance

improvement of MFC another hotspot in which some scholars proposed using nanoparticles, nanotubes and algae. The performance of MFC was studied in many publications. One of the studies was conducted by Konovalova, E. Yu. et al. (2018) [28] in which they studied the impact microorganism on the performance of MFC [28]. With respect to MFC industrial applications, wastewater treatment and heavy metal removal is one of the most discussed topics in MFC field. This is reflected by the keywords too, as wastewater treatment is one of the most frequently used keywords with a frequency of 6.17%. Finally, revealing the most cited papers in MFC field in the timespan of (2010-2020) is a crucial practice, and new scholars in the field should be aware of it. High citations of a paper are an indication that this paper includes critical, important and valuable information that help to settle an exact idea about a topic. Highly cited papers can be seen from Scopus. In the field of MFC, the most cited paper in the specified time is a review paper with title: “A review of the Substrates Used in Microbial Fuel Cells (MFCs) for Sustainable Energy Production” for Pant, Deepak; Van Bogaert, Gilbert; Diels, Ludo; Vanbroekhoven, Karolien which is published in 2010 with total citations of 1201 from the day it was published till the day of this data extraction.

1.2.1.1.Research trends in MFC

The leading research areas in MFC are energy fuels, biotechnology, engineering, and control. The overall design of MFC including electrodes, chamber and configuration is the top research topic. While the leading research topics in the area are wastewater treatment, optimization, management, and the industrial application and commercializing of this renewable source of energy. Mathematical modelling of system containing biofilms and the chemistry development topics have grown at a very high rate since the last two decades.

1.2.1.2.Conclusions

In conclusion, 8,065 journal articles and review papers in MFC field over the timespan of (2010-2020) were reviewed in a bibliometric analysis using Scopus. The major findings can be concluded as: 2020 is the year with the highest number of publications in the field of MFC. 87% of the contribution of research articles is related to the last decade which is the decade of this study. 90.17 % of the published documents were research articles while 9.83% were review papers. In the domain of this field, 145 study categories are involved with energy fuel as the leading subject. Frequently used keywords were analysed also and found that “Microbial Fuel Cells” is the most used with a frequency of 22.13%. Finally, power and electricity generation, optimization and commercialization are the hot topics in the area in the last decade. The field of MFC is one the growing fields in sustainable wastewater treatment and electricity generation.

1.2.2. Microbial fuel cell system

MFCs are a renewable bio-electrochemical cells or devices that are used with the contribution of bacterial culture to convert the reserved chemical energy in the fed nutrients to electrical energy [29]. Microbial fuel cell is like other fuel cells consists of chambers of anode and cathode. Based on the structure of the cathodic chamber can be classified as a single or dual chamber MFC. According to the existence of the membrane, MFC can be classified as a membrane-type or membrane-less. MFC is a chamber that contains a bio-anode and/or a bio-cathode which are separated from one another by a proton exchange membrane and both compartments of the cell are connected with an outer circuit to ease the electrons transfer [30]. At the anode compartment the oxidation of the organic material takes place as most of the MFC use the organic substances as the electron donors and carbon dioxide and/or methane will be produced, protons and electrons. The electron flux transfers to the cathode either

directly or via a mediator. Based on the electron acceptor, the reduction reaction occurs, if the oxygen is the electrons acceptor, then pure water will be produced. A charge balance occurs in MFCs due to the transfer of electrons through the outer circuit and protons from the anode through the membrane if there is any [31]. MFCs can be classified based on many criteria as shown below in Figure 1-4. While both configurations (dual chamber and single chamber) of MFC are shown in Figures 1-5 and 1-6, respectively.

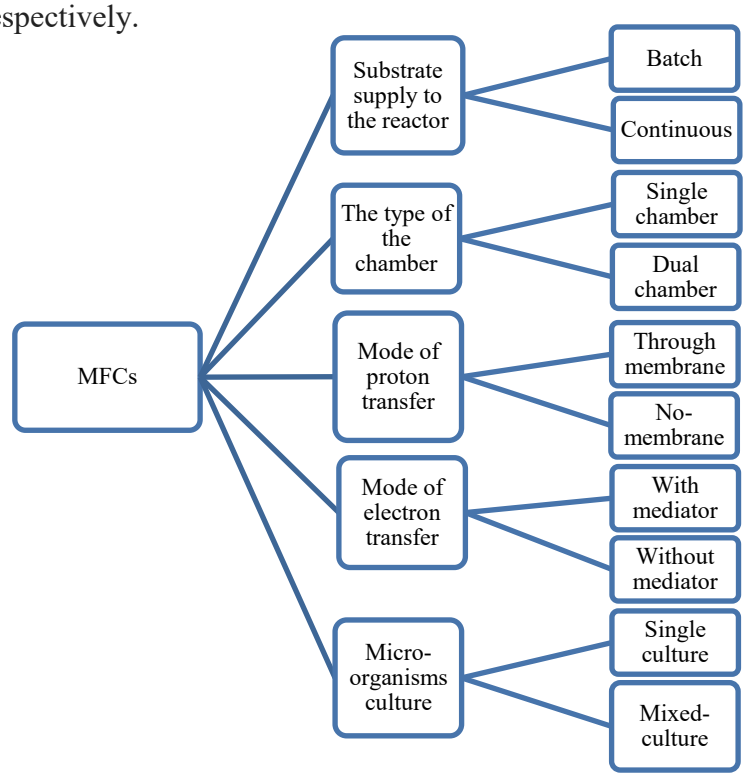

Figure 0-4. MFCs classification

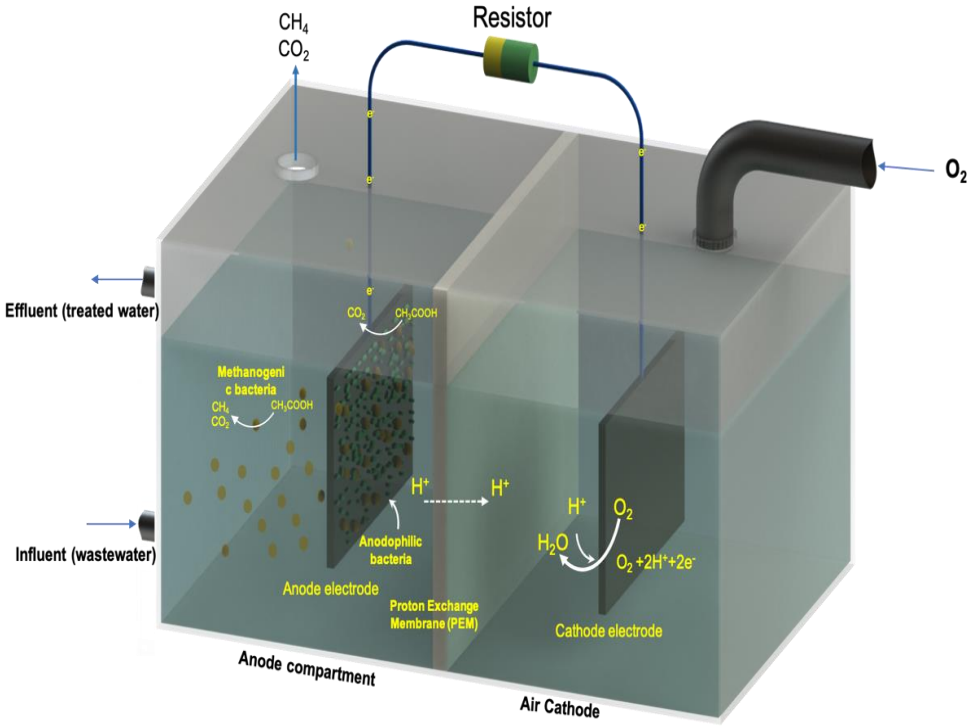

Figure 0-5. Dual chamber MFC

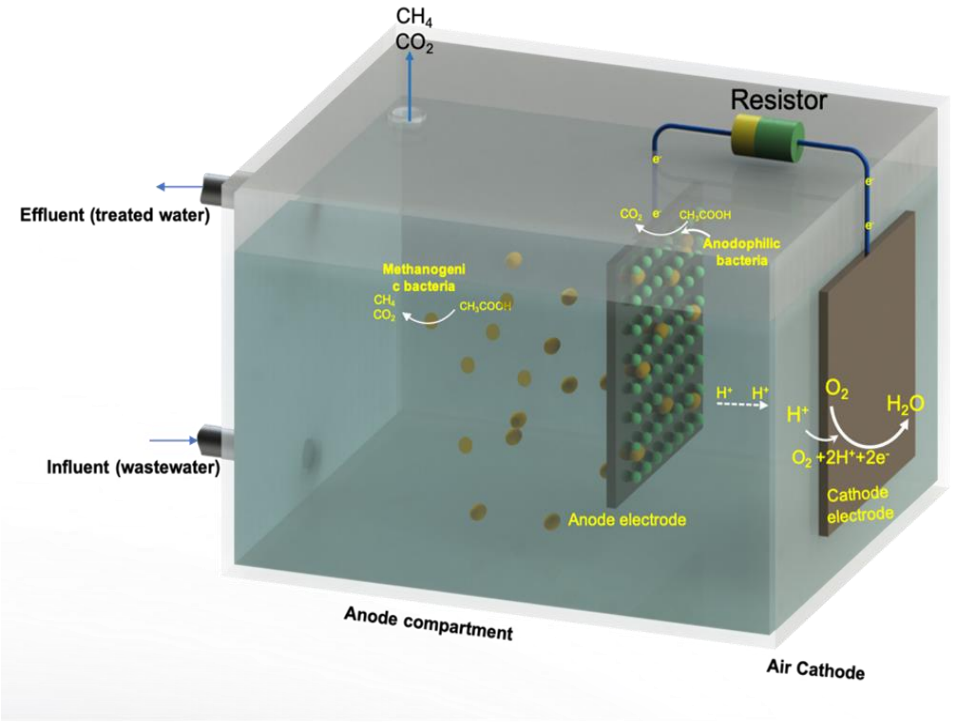

Figure 0-6. Single Chamber MFC

1.2.2.1. Microorganisms

Microorganisms are used in MFCs in the anode compartment for the degradation of the available substrate, very limited information have been provided in the literature for the composition of the microbial community in the cell. The bacterial community could be composed of single culture or multiple culture. Also, they could be suspended in the liquid bulk or attached forming a biofilm above the electrode. However, microorganisms that are attached to the cathode electrode are not well-defined. MFCs promote the growth of obligate anaerobic bacteria such fermentative or methanogenic microorganisms [32].

1.2.2.1.1. Electricigenic bacteria

Electricigenic bacteria, or anodophilic bacteria or exoelectrogens, are the microorganisms that are used in the anodic compartment for electron production. These microorganisms under microaerobic or aerobic conditions are able to transfer electrons through the cell envelop to electron acceptors as electrodes, inorganic compounds or other microorganisms in a process called Extracellular Electron Transfer (EET) [33]. In addition, EET is used by bacteria to gain energy for other cellular activities such as reproduction and growth. As stated earlier, electricigenic bacteria oxidize organic substrate and produce electron, therefore they are the main driver for power generation. The power generation mechanism depends on the type of anodophilic bacteria that is used in the cell, hence the electron transfer mechanism. Theoretically, different anodophilic bacteria can be inoculated in MFC for substrate oxidation and electron production. However, some bacteria have strong cell wall peptide bonds which hindrance the movement of electrons out of the body of the microorganism and increase the non-conductivity of the bacterial community. Gram negative electricigenic bacteria are considered as the lowest electrogenic and more non-conductive among other

anodophilic bacteria due to their thick cell envelops. This issue can be solved by the addition of redox mediators which can help to transfer and increase the transfer rate of electrons from the bacteria to the anodic electrode. Such mediators are thionine and soluble quinone which are easy to flow however, most of them are considered as toxic [34]. Table 1-4 summarises different electricigenic bacteria, the type of electron transfer, the used redox mediator and terminal electron transfer [35].

Table 0-4. Electricigenic bacteria and metabolism type, electron transfer type, terminal electron acceptor and redox mediator

Electricigenic bacteria	Metabolism type	Electron transfer type	Terminal electron acceptor	Redox mediator	Ref.
Rhodoferax ferrireducens	Oxidative	Membrane-driven (no mediator)	Cytochrome	-	[35]
Clostridium butyricum	Fermentative	Membrane-driven	Cytochrome (putative)	-	[36]
Escherichia coli	Oxidative	Mediator-driven	Hydrogenase	Neutral Red (NR)	[37]
Desulfovibrio desulfuricans	Fermentative	Mediator-driven	S^{2-}	Iron chelator (Fe(III)CyDTA)	[38]
Pseudomonas aeruginosa	Oxidative	(Mediator-driven) secondary metabolites	Pyocyanin phenazine carboxamide	-	[39]

1.2.2.1.2. The mechanism of power production

Power generation in MFC requires a major of five processes. First process is the biological oxidation of the electron donor (substrate). The substrate is fed to the anodic compartment of the reactor which is oxidized by the means of the microbial culture. Based on microbial community the products of the oxidation reaction would be electrons, protons and metabolites. The second process is the anode reduction, which

occurs by the transfer of the produced electrons to the electrode surface directly or via mediators. The third process is the electron transfer through the outer circuit from the anodic electrode to the cathodic electrode. The fourth process is the proton transfer from the anodic compartment to the cathodic electrode. Finally, the fifth process is the reduction reaction of the electron acceptor which takes place on the surface of the cathode electrode [40].

1.2.2.1.3. Respiratory metabolism for power production

Electricigenic bacteria oxidize organic substrate and produce electrons using metabolism and respiration processes. The respiration and metabolic pathway determine the flow of electrons and electricity production, hence the power productivity and MFC performance. In addition, substrate, extracellular mediator and anode potential all play a decisive role in the metabolism process [41]. Based on the anodic potential, the metabolism can be classified as high, medium, or low redox potential metabolism. Electrons and protons are travelled through external mediators as cytochrome, NADH and coenzyme Q at high anode potential when microorganisms use the respiratory chain. While at low anodic potential, electrons look for other electron acceptors and find a path to follow, such electron acceptors are sulfate, nitrate and oxygen [42]. If no electron acceptor is available, the microorganism follows a fermentation metabolic process which releases a very small amount of electrical energy. This can be translated as the selective pressure on electricigenic bacteria for electricity generation [43]. For respiration process, the produced electrons are accepted by a non-organic matter as a terminal electron acceptor [44]. The organic matter is completely degraded and produces carbon dioxide, water and ATP molecules which depend on substrate type. Electrons are transferred to the terminal acceptor using electrons transport chain processes using a system of enzymes and co-factors. The movement of

negatively charged electrons induce the transport of positively charged protons and generate a charge gradient which perform as a driving force [28].

1.2.2.1.4. Anodic reduction

Once the substrate dissociates in the anode, the electrons are produced and should be transferred to the (final) terminal electron acceptor in the cathode. The flux of electrons will transfer from the microbe to the anodic electrode. This process is known as anode reduction, and it impacts the power production and performance of MFC. Four main modes of electron transfer are available and discussed in literature: direct contact transfer, nano-wire mechanism, in-situ oxidation transfer and electron shuttle transfer. The former methods are biofilm mechanisms while the latter processes are electron shuttle mechanisms [45].

1.2.2.1.5. Biofilm electricity generation mechanism

Microorganisms accumulate on electrode surface and form a biofilm. This helps in the direct contact and nano-wire mechanisms for electron transfer. Mediator-less MFC are based on this technique for electron transfer. However, microbes cell membrane should be thin and be in a spatial and direct contact with the electrode to ensure the electron transfer and power production. Contact efficiency of microbial community and the electrode is the key of enhancing the power generation using this method. The mechanism is as follows: by the bacterial cell, the substrate is oxidized, and the electrons are transferred using metabolic respiration chain via intracellular NADH dehydrogenase and coenzyme Q and other enzymes. First the electrons reach to the inner membrane of the cell then to the outer membrane via C-type cytochrome. Finally, electrons will be directly transferred from the outer cell membrane to electrode surface. Based on the bacterial community, two theories were made for the last step of electrons transfer to the electrode: first is the direct cell membrane contact to with electrode, the

second is the nanowire assist which is assigned for longer distance travel [46].

1.2.2.1.6. External circuit electron transfer

Electrons travelled to the anode electrode, will be transferred to the cathode electrode through the external circuit producing a current and electrical potential. External resistance levels have a critical impact on power generation in MFC. External resistance impacts the internal resistance, microbial metabolism, hence the substate consumption. According to Ohm's law, increasing the load of MFC, decreases the generated current, with small internal consumption and results in high voltage. With low external load, the migration of electrons will be easier, the rate of electron transfer will be higher with higher internal consumption which results in higher current generation [47]. The study conducted by Menicucci et al. (2006) [48] showed that the limiting factor for electron transfer in MFC is external resistance when its high, while for lower loads, the limiting factors will be the mass transfer and internal resistances [48].

1.2.2.2. Anode

Oxidation reaction of substrate takes place in the anode compartment via bacterial culture. This means that the material of construction of anode electrode should not be toxic to the bacterial community. Also, it must be chemically stable and biocompatible. Different materials are used for the electrode such as non-corrosive stainless steel, graphite and glassy carbon. The material of construction of anode and its properties impacts the performance of MFC; by impacting the biofilm that is formed on the electrode and anaerobic bacterial metabolism rate. Therefore, it is impacting the interfacial area of electron transfer [49]. The simplest and inexpensive material that can be used is the carbon (graphite plates) which ultimately has a well-defined surface area. It is shown that the current increases with increasing the overall available surface area of the material used for the electrode. With carbon-based anode electrode specifically

carbon brushes, the highest power density achieved was 2110 ± 68 mW/m^2 [50]. While graphite-felt macro anode electrode was used in a CSTR reactor to treat Cassava mill wastewater found to enhance the treatment and increase the power generation to be 1771 mW/m^2 [51]. Enhanced functionalized nitrogen-doped carbon-based anode electrodes show a better performance of maximum power density 2777.7 mW/m^2 [52]. It is found that carbon is a promising material for anode electrode and power generation enhancement in addition being cost-effective. In addition to other unique properties like the large surface area and porosity made them feasible for the anodophilic bacteria growth [36]. Metal-based anode is another promising material type for electrode construction. This is due to their conductivity, durability, corrosion resistance and large reactive surface area of some metal oxides. These are preferred properties for anode electrode for performance boosting and electrons transfer easing [53]. Such materials are silver, aluminium, molybdenum, copper and others. It is found that molybdenum anode electrode produced a power density of 1296 mW/m^2 [54].

1.2.2.3. Cathode

For the cathode electrode, oxygen is one of the most suitable and used electron acceptor for MFC [55]. This is because of its low cost (air), availability and high oxidation potential. Also, the most important feature is that when it is reduced, pure water is produced. The material of construction of the cathode electrode impacts the overall performance of the cell by impacting the oxygen reduction reaction. To increase the oxygen reduction reaction, cathode electrode kinetics must be increased. Platinum electrodes are generally used as a catalyst in oxygen reduction reaction which occurs at the cathode. However, it can cause surface poising for the bacterial community [56].

1.2.2.4. Membrane

For most of the MFCs membranes are used to separate the electrodes from one another

unless it is not special single chamber design or naturally separated system such as sediment MFCs. Membranes are used for crossover prevention of effluents, oxygen, proton and carbon dioxide. Different types of material are used for membrane synthesis in MFC. Such materials are polymer electrolyte membranes (PEM), ceramics and fibers [57]. Oxygen diffusion, internal resistance, biofouling and loss of nutrients are some important parameters to be taken into consideration for membrane. PEM are especially synthesized for easing the proton exchange process from the anode to the electron acceptor reaction compartment and are categorised as perfluorinated polymer membranes, composite membranes and hydrocarbon membranes [58]. The most used membrane is Nafion based, or an alternative cost effective could be Ultrex CMI-7000 [18].

Below, Table 1-5 summarises different material for anode electrodes, cathode electrodes and membranes used for MFC and corresponding performance, to reveal the impact of construction material.

Table 0-5. Anode, cathode and membrane material type and the performance

Anode	Cathode	Membrane	Performance (mW/m^2)	Ref.
Carbon-based: Carbon cloth	Air cathode	Membrane-less	2110 ± 68	[59]
Carbon-based: Graphite-fiber brushes	Air cathode-graphite-fiber doped with (nitrogen, and phosphorus)	Membrane-less	879 ± 16	[60]
Carbon-based: Nitrogen-doped porous carbon	Carbon-based: Carbon brush	PEM	2777.7	[61]
Metal-based: Alumina and nickel particles-dispersed using	Polymer alumina and nickel nanoparticles	Membrane-less	1270 ± 30	[62]

Anode	Cathode	Membrane	Performance (mW/m^2)	Ref.
carbon nanofiber	with air cathode			
Metal-based: MW CNTs/SnO_2/GCE	Metal-based: Pt cathode	Nafion 117	1421	[63]
Metal-based 3D graphene/Platinum	Metal-based Pt	Nafion membrane	1460	[64]

1.2.3. Parameters governing the performance of MFCs

The performance of MFC is evaluated based on different objective (desired) functions to be maximized. Power density is one of the most studied functions in the literature of MFC. Many scholars studied experimentally the different factors that impact the value of MFC power density. While others assess the performance based on the substrate removal efficiency for wastewater treatment or using the current density. In this section, power density is used for performance evaluation and the most impacting factors are stated. It is worth mentioning that the mentioned performance in this section is the real performance of MFC not the ideal performance. The main difference between the ideal and real performance is that the ideal performance relays on the electrochemical reactions that produces uncertain voltage. This is due to the transfer of electrons through a complex respiratory chain that is poorly understood and differs from one microbe to another based on the environmental conditions. The actual performance of MFC takes into consideration the irreversible losses which are activation polarizations losses on available electrodes, Ohmic losses and concentration losses. There are many factors impacting MFC performance such as substrate type and conversion rate, microorganisms, microorganisms metabolism, the mechanism of electron transfer, anodic and cathodic overpotential, chambers design and finally operating conditions

[65].

1. **The substrate conversion**

Substrate conversion rate impacts the power generation through different means. The higher the substrate conversion by anodophilic bacteria, the more electrons are available to be transferred. Thus, the higher the generated power theoretically, with no consideration for external and internal resistance values. This factor depends on the bacterial kinetics constants, hence the bacterial type. Maximum specific growth rate, half rate constant of substrate saturation, bacterial affinity constant towards the substrate and the biomass loading rate are some of the constants that specify the influence of substrate conversion on power density [66]. A study conducted by Rahimnejad, M. et al. (2009) [67] to figure out the effect of different substrate types on MFC performance. They concluded that the open circuit potential of grape juice was higher than that of why and molasses over the time by using Saccharomyces cerevisiae [67].

2. **Microbial culture**

Bacterial community can be divided based on their requirement for mediator just as bacteria require mediator or mediator-less. While the inoculated community can be pure or mixed culture. Mixed cultures add more value to MFC being more adaptable and stress resistance. Based on the required objective of the cell, the bacterial community is chosen [68]. In systems where power density is required to be maximized, the anodophilic bacteria must dominate in the culture for boosting the amount of generated electricity after using fermentative or methanogenic bacteria to recover the metabolic products and to recover electrons. Exo-electrogenic bacteria as stated earlier can oxidize the substrate and transfer the produced electrons to the anodic electrode. Activated sludge is well-known example of mixed cultures that has been studied in

literature [69]. Yates, M. et al. (2012) [70] studied bog-inoculated and wastewater-inoculated MFCs to compare the amount of produced power based on their different types of bacteria. The study concluded that bog sediment produced power density that is higher than the other MFC before completing the first 20 cycles [70].

Table 1-6 below, shows how the performance of MFC is impacted based on the microbial community and the substrate type. Using the same substrate with different bacterial culture such as glucose with Proteus Vulgaris and Rhodoferax ferrireducens show very different performance based on the power density generation while the electron donor is the same.

Table 0-6. Impact of bacterial culture and substrate type on MFC performance

Type of the bacterial culture	Bacterial culture	Substrate type	Performance (mW/m^2)	Ref.
Single	Proteus Vulgaris	Glucose	4.5	[71]
Single	Rhodoferax ferrireducens	Glucose	8	[72]
Mixed culture	Mixed Consortium	Glucose	494	[73]
Single	Shewanella putrefaciens	Lactate	0.00032	[74]
Mixed culture	Activated sludge	Lactate	5.3	[75]
Mixed culture	Activated sludge	Wastewater	8	[76]

3. Internal resistance

Internal resistance is vital impacting factor on MFC performance. It depends on the external resistance, the followed mathematical model and the model experimental parameters. However, it mainly occurs due to the losses such as activation, ohmic and

concentration losses. Experimentally investigated and found that concentration losses are the largest contributor to the internal resistance compared to other losses which can be neglected. Ohmic losses found to be constant for the whole current density range while the activation losses found to be increased for higher currents and reach to a constant value [77]. Zhang, P. et al. (2010) [78] experimentally concluded that concentration losses contribute the maximum to the internal resistance and take almost 50% of the total value of the internal resistance. Since internal resistance impacts the produced current, concentration losses impact the current too. Increasing the limiting current value of the system is found to be an efficient method to decrease the concentration losses value and boost the performance of MFC [78]. Other factors impact the internal resistance are the membrane and electrolyte resistance. For reducing this resistance, anode and cathode electrodes must be as close as possible.

4. Proton Exchange Membrane (PEM)

Dual chamber MFC consist of PEM which found to be a critical factor in power generation of the cell. Two types of PEM are commonly used in MFC which are porous proton exchange membranes and dense membranes which are nonporous. Nafion membrane is one of the traditional PEM types which achieves the ion equilibrium between anolyte and catholyte. PEM thickness and available area for mass transfer impact the produced power density [79]. The study conducted by Rahimnejad, M. et al. (2014) [80] deliberate the impact of mass transfer area on power generation by using Nafion PEM. 3.14 cm^2, 9 cm^2 and 16 cm^2 are the mass transfer surface areas. Results show that the maximum power density generated was using a PEM of 16 cm^2 surface area. This is due to increasing the available surface area for proton transfer to the cathode and allow the reduction reaction to take place more [80]. Rahimnejad, M. et al. (2010) [81] conduct another study to see the impact of PEM thickness on MFC power

generation. They used Nafion 117 and Nafion 112 which have pre-defined thicknesses of 0.183 mm and 0.0508 mm, respectively. The generated power density is found to be inversely proportional with the thickness of PEM. Increasing the PEM thickness decreases the generated power density, as it is found the generated power density for Nafion 117 was less than that of Nafion 112 with values of 9.95 mW/m^2 and 31.32 mW/m^2, respectively [81].

5. Anode electrode

In electron transfer mechanism, the role of anode electrode is shown to be critical in electrons transfer to the outer circuit then to the cathode. Therefore, the electrode material characteristics are vital to ease the electron transfer process which is a great impact of power production. Essential characteristics of electrode are stability, conductivity, available surface area, nontoxicity and biocompatibility. Commonly used materials for anode electrode are copper, steel and carbon. Copper electrodes when they are compared to steel and carbon electrodes are found to produce low power, they produce 2 mW/m^2. While carbon and steel are producing 880 mW/m^2 and 12 mW/m^2, respectively. Carbon cloth despite its non-conductive as metals, the available specific surface area is higher compared to metal mesh [82].

6. Cathode electrode

The performance of MFC is impacted by the type of cathode electrode used. The electrode is used to catalyse the reduction reaction of the terminal electron acceptor which is oxygen in air cathode. Platinum (Pt) as cathode electrode is preferred over carbon and graphite and it is used commonly despite it is expensive and unsustainable [83]. However, carbon electrodes (carbon nanotubes (CNTs)) is functionalized with nitrogen (meso-porous nitrogen-rich) which can replace Pt electrodes. For improving the performance air cathode with oxygen side must be hydrophobic to increase the

diffusivity and avoiding solution leakage while the water side must be hydrophilic [84]. Lou, Y. et al. (2011) [85] weighed the influence of design and size of cathodic electrode. They found that by using wastewater in MFC, doubling the area of the cathode increases the produced power more than 60% [85]. Santoro, C. et al. (2012) [86] compared the power density generation of two different types of cathode electrodes: Pt-based and Pt-free cathodes. At start-up, Pt-based cathode produced a power density of 330 mW/m^2 which was higher compared to Pt-free cathode. While the performance difference vanished after a couple weeks of operation [86].

1.2.4. Different models for MFC

Different models were proposed for MFCs, such as the mathematical models based on the mechanism such as bulk liquid model, electrochemical model and biofilm model and other such as optimization and control models. Below in Table 1-7 different MFC model types are discussed. While the difference between mechanism-based models is illustrated in Figure 1-7.

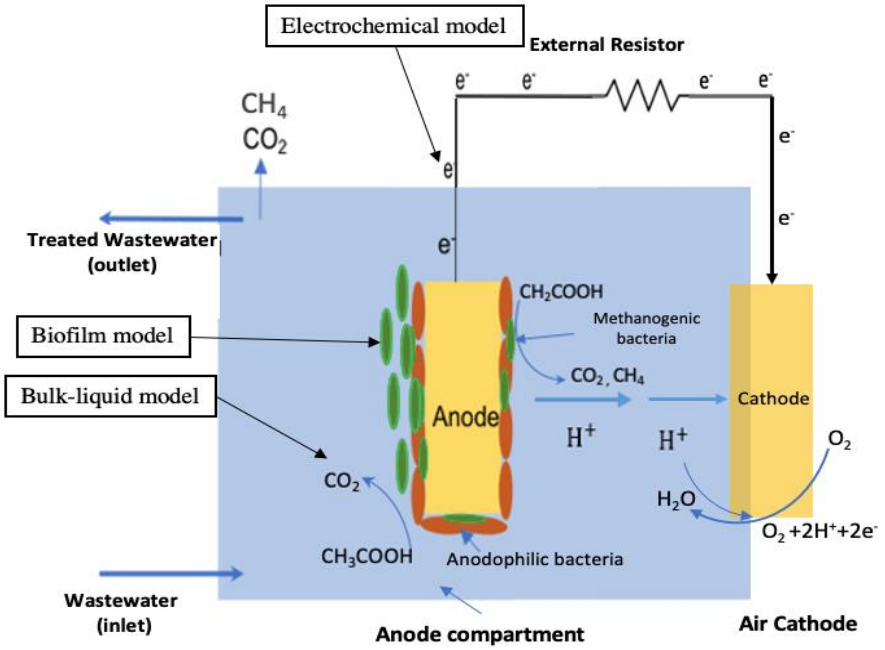

Figure 0-7. MFC and the different mechanism-based models

Table 0-7. Different MFC model types

Model Type	Model	Model description	Ref.
Mechanism-based models	Bulk-liquid model	This model renders the fundamental process of MFC on a macroscale. This is based on the mass balances of bacterial community, substrate and mediator (if available).	[87]
	Electrochemical model	Electrochemical models are based on the electrical characteristics of MFCs depending on the theory of electrochemistry to evaluate the electrical performance of the cell. Herein, the model is based on Ohm's law as in input equation and voltage, current density, external resistance as output functions in addition to using electron balance.	[87]
	Biofilm model	The biofilm model studies the related specification of the biofilm such as the thickness fluctuation and the bacterial distribution. Progressively go from anode biofilm modelling to cathode biofilm modelling.	[88]

Model Type	Model	Model description	Ref.
	Special model	The model used the LRC electrical performance of the circuit to determine the pH of the anode chamber as a function of time. This model depends on substrate consumption as an impacting variable for the anode pH which are connected using Monod-type kinetics and microbial culture concentration.	[89]
Application-based models	Controlling, learning and optimization model	Black box models are developed without a deep knowledge of the MFC. They rely on massive requirement of experimental data and results is used to simulate the MFC. Numerous modeling techniques are specified to improve the accuracy of prediction of the outcomes while reducing the time it takes to learn new models. Non-parametric modeling approaches of this sort minimize modeling complexity while emphasizing the relevance of learning sample and methodologies. As a result of the experimental data collecting techniques and learning process, the resulting models differ. Furthermore, the controlling models differ somewhat in that just a few important responses are considered.	[90]

While the different proposed models which are based on the application and performance are the optimization models. These models vary in their complexity or simplicity, studied dimensions, bacterial community and others. However, all these models are specialized to serve the optimization purposes and are built on the models of Table 1-7. Different models are shown in Table 1-8 below.

Table 0-8. Optimization models of MFC

Model	Model type	MFC type	Kinetics type	Bacterial community	Electron transfer mode	Ref.
Pinto, R.P. et al. (2012)	Biofilm	Single chamber	-Double Monod -Nernst -Butler	Mixed	Direct and mediator	[1]

Model	Model type	MFC type	Kinetics type	Bacterial community	Electron transfer mode	Ref.
			Volmer			
Zhang and Halme (1995)	Bulk-liquid Ideal mixing	Single chamber	Monod Nernst Tafel	Single	Mediator	[91]
Ha, H. et al. (2010)	Electrical	Single chamber	-	-	-	[92]
Recio-Garrido, M. et al. (2014)	Electrical and biofilm	Single chamber	-Double Monod -Nernst -Butler Volmer	Mixed	Direct and mediator	[93]

Some of the real applications of MFC using real wastewater are shown in Table 1-9.

Table 0-9. Bacterial culture, MFC design and results of real used for real wastewater treatment activities

Bacterial culture, substrate concentration	MFC specifications	Results	Ref.
Dairy wastewater treatment factory. COD concentration: 1000mg/L.	Annular single chamber MFC (ASCMFC). Anode: metal-based stainless steel with coating material of graphite. Cathode: carbon-based carbon cloth.	Substrate (COD) removal efficiency of (26.87% -91%) with maximum columbic efficiency. Maximum power density: 20.2%.	[79]
Local wastewater (COD 1000-1500mg/l)	Dual chamber MFC with 20 L volume. Anode: carbon-based graphite rods on plastic base. Cathode: Copper and cobalt based manganese dioxide and platinum based.	Pt cathode: 213mW/m^2 Cu-MnO_2 cathodes: 465 mWm^{-2}. Co-MnO_2 cathodes: 500 mWm^{-2}. The power generated increased as the number of electrodes increased.	[184]

Bacterial culture, substrate concentration	MFC specifications	Results	Ref.
Activated sludge inoculated local wastewater	Salt bridge separates two chambers (MFC): Anode: cylinder of graphite Cathode: graphite bar with pores.	Maximum power density: 25mWm^{-2}.	[29]
Dairy wastewater: COD concentration: 3700 mg/l. BOD concentration: 2200 mg/L.	Anode: carbon-based graphite. Cathode: carbon-based graphite. Membrane: Nafion.	Carbohydrates removal efficiency: 91.98% Proteins removal efficiency: 78.07% Turbidity relief: 99.02% Removal efficiency of COD: 95.49% Production of maximal volumetric power: 1.10 Wm^{-3}; 308 mV; 1.78 mA.	[80]
Brewery wastewater	Pilot microbial fuel cell with a 90 L stacking volume. Anode: a titanium wire is braided with carbon brushes. Cathode: activated carbon. Membrane: textile separator.	At stage 2. 0.097 kWhm^{-3}, the COD and SS removal efficiencies were 87.6% and 86.3%, respectively.	[185]
Paper-plant wastewater treatment: COD concentration: 506 mg/L	Anode: carbon cloth Cathode: carbon-based (brush) using 0.5 mg/cm^2 Pt treated using ammonia gas in hydrophilic side. While has four diffusion layers in hydrophobic side.	Using a 6h, 5.9 ± 0.2 Wm^{-3} HRT, COD cathodewas reduced by 26 ± 2%.	[186]

1.3.MFC model description

The mathematical model of MFC implemented in this study was developed by

Pinto et al. (2012) [1] which can be implemented for optimizing productivity [1]. The model of Pinto et al. (2012) is a simple, one dimensional, unified model which can be applied on bioelectorchemical cells to optimize either the power generation of MFC or hydrogen generation of MEC. The model combines biochemical reactions in the anode compartment, ordinary differential equations of mole balances of substrate, anodophilic bacteria and methanogenic bacteria, Monod kinetics for growth kinetics and Butler–Volmer equation. The model considered the co-existence of microbial population of anodophilic (electricigenic) and methanogenic bacteria in a single anode chamber, air cathode, membrane-less that is operating in a continuous flow mode. Acetate was the only substrate in the system prefered over other substrates, because of its complete degradation and both microorganisms are competing for it [15]. A uniform distribution of both carbon source and microbial population is proposed in the anode compartment with ideal mixing. The anodophilic microorganisms are the only electron producer in the model [94]. The anodophilic are placed attached to the biofilm on the anodic electrode. While the methanogens are both attached to the biofilm and suspended. Intracellular mediators (NAD^+/NADH) are assumed to be involved in the charge transfer process from the carbon source (acetate) [95]. The proposed model focuses on the bio-electrochemical reactions in the anode compartment and its associated kinetics are considered as the rate-limiting of MFC [1]. A schematic diagram of the used MFC is shown in Figure 1-6. A combination of electrochemical and biochemical reactions is taking place in MFC. Electrochemical reactions deal with electron production and transfer from the oxidation of organic matter, while biochemical reactions deal with the microorganisms metabolism and substrate reduction [94]. The main model assumptions and considerations are listed as follows [1]:

The biofilm effect is considered in the design equations and the substrate gradient

through the biofilm is neglected.

Direct and indirect (NAD^+/NADH) mechanisms for electron transfer from the carbon source (acetate) to the anode electrode are used.

A balance between the microbial poppulation in the biofilm is assumed.

Stationary phase is assumed so that equilibrium will be achieved between biofilm growth and washout so that the biofilm will reach its steady state thickness and washout will be equal to the net biofilm growth.

Substrate degradation and electron generation reactions by anodophilic bacteria are illustrated in Equation 1. Figure 1-8 provides a schematic diagram for the anode compartment presenting all the associated reactions [96].

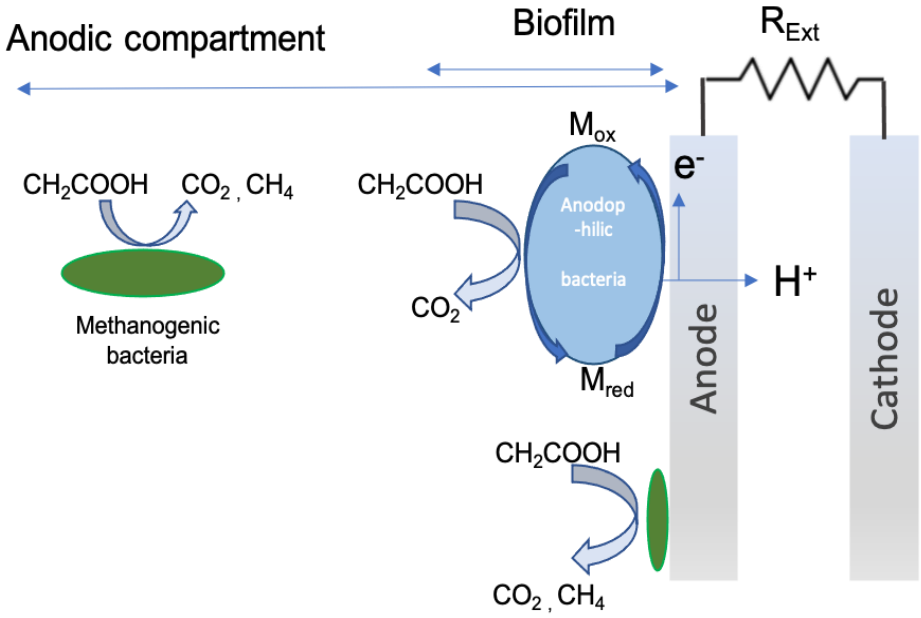

Figure 0-8. Reactions in the anode compartment of MFC

In Figure 1-8, anodophilic bacteria are represented in blue and they are attached only to the biofilm, they oxidize the substrate (acetate) which releases electrons that are transferred directly or indirectly by mediators as shown in Equation 2. Equation 3

shows the reduction reaction of electron acceptor (oxygen) in the cathode compartment. While methanogenic bacteria are represented in green and they are both attached to the biofilm and suspended in the bulk. The substrate conversion by methanogenic bacteria is represented by Equation 4. The conceptual reactions for oxidizing the substrate are as follows: If the substrate is acetate, then the reaction over the anode and cathode for anodophilic microorganisms is shown as follows [1]:

Anode:

$C_2H_4O_2 + 2H_2O + 4\ M_{ox} \rightarrow 2CO_2 + 4\ M_{red}$ (1)

$4\ M_{red} \rightarrow 8H^+ + 8e^- + 4\ M_{ox}$ (2)

Air Cathode:

$O_2 + 4e^- + 2H_2O \rightarrow 4\ OH^-$ (3)

While methanogenic bacteria reaction is as follows:

Anode:

$C_2H_4O_2 \rightarrow CO_2 + CH_4$ (4)

Mathematical model of a Single chamber MFC

Anode compartment material balances [1]**:**

The model balances equations used in this paper are represented as follows:

$$\frac{dS}{dt} = -q_a X_a - q_m X_m + \frac{F_{S_0}}{V_A}(S_0 - S) \quad (5)$$

$$\frac{dX_a}{dt} = \mu_a X_a - k_{d,a} X_a - \alpha D X_a \quad (6)$$

$$\frac{dX_m}{dt} = \mu_m X_m - k_{d,m} X_m - \alpha D X_m \quad (7)$$

Where:

S and S_0 are the substrate concentration and initial substrate concentration respectively (mgS/L); X_m and X_a are methanogenic and electricigenic microorganism respectively (mgX/L); t is the time (d); D is the dilution rate (1/d) which is defined as ($D=F_{in}/V_A$);

V_A is the volume of anode (L); F_{in} inlet flow rate; μ_{max} is the maximum specific growth rate (1/d); q_{max} is the maximum substrate consumption rate (mgS/mgX.d) and $k_{d,a}$, $k_{d,m}$ are decay rates constants for anodophilics and methanogens respectively (1/d).

In this model, the biofilm impacts in the anode compartment are taken into consideration based on two-phase biofilm growth model. For the effects of biomass formation and retention in the layer, α which is the biofilm retention constant that is calculated below, assuming the cell is at the stationary phase and the biofilm reached its steady state thickness. The maximum attainable biomass concentration (X_{max}) is hold in the biofilm at this phase.

$$\alpha = \begin{cases} \frac{\mu_a X_a + \mu_m X_m}{X_a + X_m}; & if\ (x_a + x_m \geq X_{max}) \\ 0; & otherwise \end{cases} \quad (8)$$

Intracellular material balance:

Intracellular mediators are used for electrons transport; therefore, they exist in both oxidized and reduced forms. The material balance of the intracellular mediators per anodophilic microorganisms is as follows:

$$\frac{dM_{ox}}{dt} = -Y_M q_a + \frac{\gamma I_{MFC}}{V_A m F x_a} \quad (9)$$

Given that:

$$M_T = M_{ox} + M_{red} \quad (10)$$

Where:

M_{ox} is the oxidized mediator fraction per anodophilic microorganism (mgM/mgX_a); M_{red} is the reduced mediator fraction per anodophilic microorganism (mgM/mgX_a); M_T is the total mediator fraction per microorganism (mgM/mgX_a) which is a constant known value tabulated in the nominal values table. Y_M is the mediator yield (mgM/mgS); I_{MFC} is the MFC current (mA); F is Faraday constant (Ad/mole$^-$); m is the number of electrons transferred per mol of mediator; γ is mediator molar mass

(mgM/molM).

Kinetics equations:

$$\mu_a = \mu_{max,a}\left(\frac{S}{S+K_{s,a}}\right)\left(\frac{M_{ox}}{k_M+M_{ox}}\right) \quad (11)$$

$$q_a = q_{max,a}\left(\frac{S}{S+K_{s,a}}\right)\left(\frac{M_{ox}}{k_M+M_{ox}}\right) \quad (12)$$

$$\mu_m = \mu_{max,m}\left(\frac{S}{S+K_{s,m}}\right) \quad (13)$$

$$q_m = q_{max,m}\left(\frac{S}{S+K_{s,m}}\right) \quad (14)$$

Where:

μ_m, μ_a are the specific growth rates of methanogens and anodophilics microorganisms, respectively (1/d); $\mu_{max,m}, \mu_{max,a}$ are the maximum specific growth rates for both methanogens and anodophilic microorganisms, respectively (1/d); q_m, q_a are substrate consumption rate by methanogens and anodophilic microorganisms, respectively (mgS/mgXd); $q_{max,m}, q_{max,a}$ are the maximum substrate consumption rate by methanogens and anodophilics microorganisms, respectively (mgS/mgXd).

Electrochemical equations

Theoretically, the MFC output voltage (E_{MFC}) can be calculated by open circuit potential (E_{OCV}) and removing from it the losses which are mainly concentration losses (η_{conc}), ohmic losses (η_{ohm}) and activation losses (η_{act}).

$$E_{MFC} = E_{ocv} - \eta_{ohm} - \eta_{conc} - \eta_{act} \quad (15)$$

Activation losses can generally be neglected, as from the optimization the internal resistance is aimed to be equal to the external resistance. This simplifies the equation of MFC voltage to:

$$E_{MFC} = E_{ocv} - \eta_{conc} - R_{int}I_{MFC} \quad (16)$$

Where the open circuit potential, concentration losses, internal resistance and MFC

current are calculated theoretically as follows:

$$E_{OCV} = E_{min} + (E_{max} - E_{min})e^{\frac{-1}{K_r}} \quad (17)$$

$$\eta_{conc} = \frac{RT}{mF} ln\left(\frac{M_T}{M_{red}}\right) \quad (18)$$

$$R_{int} = R_{min} + (R_{max} - R_{min})e^{-K_r X_a} \quad (19)$$

$$I_{MFC} = \left(\frac{E_{OCV} - \eta_{conc}}{R_{ext} + R_{int}}\right)\left(\frac{M_{red}}{M_T \varepsilon + M_{red}}\right) \quad (20)$$

Where ε is a constant and it is approximately equated to zero; then the current of MFC is reduced to:

$$I_{MFC} = \frac{E_{OCV} - \eta_{conc}}{R_{ext} + R_{int}} \quad (21)$$

The power density of MFC can be calculated as:

$$P_{MFC} = \frac{I_{MFC} * E_{MFC}}{V} \quad (22)$$

Where E_{OCV} is the open circuit potential (V); R_{max} and R_{min}: are the maximum and minimum internal resistance (Ω); γ is the mediator molar mass (mgM/molM); E_{MFC} is the MFC voltage (V); η_{conc} is the concentration losses (V); R is the universal gas constant (J/K.mol); K_r is the curve steepness factor (L/mgX); P_{MFC} is the power density of MFC (mW/L). Table 1-10 below shows the nominal values of all the constants used for the optimization model.

Table 0-10. Nominal values of MFC parameters [1]

Constant	Symbol	Unit	Value
Volume of the anode compartment	V	L	0.05
Faraday constant	F	A.s/mol of e	96485.33
Ideal gas constant	R	J/Kmol	8.314472
MFC Temperature	T	K	303.15
Mediator Yield	Y_M	mgM/mgS	34.85
Maximum anodophilic reaction rate	$q_{max,a}$	mgS/mgXd	13.14
Maximum methanogenic reaction rate	$q_{max,m}$	mgS/mgXd	14.12
Maximum anodophilic growth rate	$\mu_{max,a}$	1/d	1.97
Maximum methanogenic growth rate	$\mu_{max,m}$	1/d	0.3
Half rate constant of anodophilics	$K_{s,a}$	mgS/L	20
Half rate constant of methanogens	$K_{s,m}$	mgS/L	80
Electron transferred per mol of mediator	m	$mole^-$/molM	2
Mediator molar mass	γ	mgM/molM	663400
Mediator fraction	M_T	mgM/mgX	0.05
Mediator half rate constant	k_M	mgM/L	0.01
Decay rate of anodophilic	$k_{d,a}$	1/d	0.04
Decay rate of methanogens	$k_{d,m}$	1/d	0.002
Maximum attainable biomass concentration	X_{max}	mgX/L	512.5
Curve steepness factor	K_r	L/mgX	0.006
Minimum internal resistance	R_{min}	Ω	25
Maximum internal resistance	R_{max}	Ω	2025
Minimum open circuit voltage	$E_{OCV,min}$	V	0.01
Maximum open circuit voltage	$E_{OCV,max}$	V	0.68

CHAPTER 2: OPTIMIZATION OF SINGLE CHAMBER MFC

2.0. Modelling and optimization

In this chapter, response surface methodology (RSM) based in the experimental data of the model and optimization are applied to MFC model that is described in the previous section. Many studies applied (RSM) using Minitab on MFC by involving an assemblage of mathematical and statistical techniques for studying the factors impacting the objective functions [97]. The complex relationships and the relative significance of each factor are evaluated. Tartakovsky, B. and Guiot, S. R. (2006) [98] applied full factorial design using RSM by studying the impact of two-factors, two-level with one centre point on a dual-chamber continuous flow MFC. They evaluated the impact of cathode oxygenation by air and hydrogen peroxide on the power density (mW/m^2). Zhang, Y. and Angelidaki, I. (2011) [99] used Plackett–Burman 2-level screening design by studying the effect of seven-factors on current density (mA/m^2) on a Submersible microbial fuel cell sensor. The investigated factors include operating condition such as temperature and pH, airflow and stirring rate, nitrate and sulfate concentration (mg/L) on the objective function. For optimization of MFC, not all proposed mathematical models are suitable to be implemented and used for optimization purposes. Zhang, X. and Halme, A. (1995) [91] proposed a model for optimizing the power density of a single population, single anodic chamber MFC in a continuous flow operating in unsteady state mode. They revealed the impact of substrate concentration and mediator on the power density. Later models such as the one developed by Zeng, Y. et al. (2010) [100] for optimizing the power density for a dual-chamber, single species and mediator less MFC under both transient and steady-state conditions.. They developed easy to be used model which is relying on anodic bio-electrochemical reactions, charge and mass balances and Butler-Volmer equations. By

using the proposed model, they studied the impact of changing the feed flow rate on the produced power density. In this chapter, optimization is applied using Microsoft Excel, Matlab and Minitab using Pinto, R.P. et al. (2012) unified model [1]. The model considers the coexistence of two microorganisms which are electricigenic and methanogenic in the biofilm in a single-chamber MFC operating in a continuous flow mode under steady state conditions. Power density, current density and substrate removal efficiency are the studied objective functions by varying dilution rate, external resistance, substrate concentration, anodophilic bacteria concentration and methanogenic bacteria concentration. RSM was computed using Minitab to estimate the objective functions in term of decision parameters; and to produce contour plots based on the proposed model which can assist in the optimization problem. RSM is very important tool to illustrate the objective functions in mathematical equations in terms of the parameters of the study. This reveals the impact of each parameter in the model on the objective function.

2.1. Mathematical Modelling: Design of Experiments (DOE)

Mathematical modelling of MFC is simpler method for representing complex bio-electrochemical systems depending on the interactions within the cell. The interactions among microbial species, biofilm and mass transport set the major hurdles in developing MFC community. Mathematical modelling was accomplished to determine the various electrochemical redox processes, factors and interactions to enriches the performance of MFC in practical applications [101]. Design of experiments (DoE) is a systematic statistical method of experimentation to vary different independent variables simultaneously tracking a certain response over a set of experiments [96]. Using Minitab software, DoE was applied in this section. DoE is in opposition to One Factor At Time (OFAT) method [102]. In DoE the effect of each of the factors is evaluated on

the response at all the levels of other factors simultaneously, therefore, both single impacts of the factors on the system and the impacts based on the interactions among the variables are investigated and taken into consideration in the predicted model for the entire experimental domain [103]. On the other hand, in OFAT method only one factor is investigated at time, as a result, the predicted models by RSM and DoE are more accurate and reliable [104]. RSM is used for modelling and optimization of three main MFC performance commercialization factors. Applying RSM methodology on MFC is coupled with many advantages just as saving resources and time in experiments in such a complicated system [105]. Despite these advantages, applying DoE and RSM for studying MFC systems is rare and limited. Power density, current density and substrate removal efficiency are the main objective functions (responses) in this study. Three main basics for DoE were considered while designing the experiments: replication, randomization and blocking [106]. Main steps of DoE after defining the response and the factors, is screening. Screening of the factors can be carried out to cull the significant factors out of all other factors and simplify the model [107]. Since MFC are very complicated systems due to the co-occurrence of biological and electrochemical processes with interrelations of parameters affecting the output of the system. Therefore, screening designs are essential and effective in investigation stages of parameters using minimum resources and time. Plackett–Burman Method (PBM) [108] is the chosen screening design for determining the most impacting factors on each of the objective functions over the other screening design method which is the Definitive Screening (DS) to make a simple screening for the factors and not complicate the model. The main difference between the two screening methods is the ability of DS to study the main impacts as well as the quadratic and two-variable interactions in the model [108]. Finally, based on previous literature of studied response and impacting

factors on MFC, an appropriate DoE method for design can be chosen depending on MFC type under study either for optimization or screening purposes. Therefore, for further DoE study and analysis, Factorial, Response Surface, Mixture and Taguchi designs could be used. For full factorial optimization design under which central composite (CCD) and Box–Behnken (BP) are categorised could be used. Most popular method for optimization applications is response surface in particular CCD [109]. Table 2-1 shows a summary of some applications of DoE on MFC systems which can assist to choose a DoE design. More complex analysis should be carried out for optimization purposes. RSM is used to obtain the optimum factors specifically central composite design and Box–Behnken method.

Table 0-1. Literature review of DoE and MFC

MFC type	DoE type	Factors of the study	Response of the study	Major results	Ref.
Membrane-less, single chamber, air cathode with mediator	Central composite: five levels with four factors	• Temperature • Carbon to nitrogen (C/N) ratio • pH • Hydraulic retention time (HRT)	Short chain fatty acid production (SCFA)	The maximum response of SCFA was at: 37°C of 6 days HRT at pH of 8.	[110]
Mediator-less, single-chamber, air cathode	Central composite: five-levels with three factors	• Temperature • pH • Pentachlorophenol-glucose concentration	• PCP-glucose degradation (%) • Power density (W/m^2) • CE (%)	Optimum PCP-glucose degradation was found to be 73% with power density 23.08 W/m^2 and %CE 49%. The Temperature was 20°C, PCP-glucose concentration of 70–2,500 mg/L and pH of 7.5.	[111]
Dual chamber	Plackett–Burman design of screening: two-levels with seven factors Box–Behnken design: three-levels and three factors	Screening design: • Glucose concentration • $NaHCO_3$ concentration • NH_4Cl concentration $MgSO_4$ concentration • KCl concentration • Yeast extracttion • Mixture of minerals and vitamins concentration Behnken design: • Glucose concentration • $NaHCO_3$ concentration • KCl concentration	• Power density (mW/m^2) • Voltage (mV) • CE (%)	Optimum result for voltage was 738.72 mV at glucose concentration of 8.5 g/L, $NaHCO_3$ concentration of 0.2 g/L and KCl concentration of 0.8 g/L.	[112]
Dual chamber	Box–Behnken design: three-levels and three factors	• Cathode surface area • Catholyte buffer solution concentration. • Catholyte pH	Power density (mW/m^2)	• Only surface area has a major impact on the response	[113]

MFC type	DoE type	Factors of the study	Response of the study	Major results	Ref.
				• No significant interaction was shown among the parameters	
Dual chamber	Box–Behnken design: three levels and three factors	• Oxyfluorfen (OF) concentration • Temperature • pH	Degradation of (OF) (%)	Optimum degradation was 94.95% and achieved at a temperature of 31.96°C, pH of 7,65 and OF concentration of 120.05 mg/L.	[114]
Dual chamber	Full factorial design: two-levels with three centre points and three factors.	• Influent COD concentration • Influent pH • HRT	• COD removal (%) • Power density (mW/m^3)	Optimum conditions were found to be the same for both objectives: 1- Influent COD concentration (2,150–2,350 mg/L) 2- HRT (22–24 h) 3- Influent pH of 8.0.	[115]
Dual chamber continuous flow	Full factorial design: two-levels with two factors and one centre point.	Cathode aeration rate by: Oxygen Hydrogen peroxide concentration	Power density (mW/m^2)	The optimal power density achieved is: 22 mW/m^2 at oxygenation rate of 300 mL/d using 0.30% hydrogen peroxide.	[116]
Dual chamber MFC with anode effluent fed	Full factorial and central	• Influent COD concentration	• Phosphor us	The MFC was operating at a COD	[117]

MFC type	DoE type	Factors of the study	Response of the study	Major results	Ref.
into the cathode chamber	composite design: two-levels and two factors	• Cathode aeration rate	precipitation (%) • Power density (kW·h/m^2) • CE (%) • COD removal (%) • Cathode pH	concentration of 1,700 mg/L and a cathode aeration rate of 210 mL/min achieved phosphorus precipitation of 95% and a power of 1.62 kW·h/m^2	
Dual chamber	Taguchi method: four-levels with two factors	• Anolyte pH • Catholyte pH	Power density (mW/m^3)	Optimum power density was 2,491.42 mW/m^3 at anolyte pH of 8 and catholyte pH of 1.	[118]
Constructed wetland–MFC	Taguchi method: five-levels with five factors	• DO concentration in the cathode • HRT • External resistance • Effluent reflux ratio • Volume ratio of graphite in substrate	• Power density (mW/m^3) • COD removal (%) • NH3-N, TN, TP removal (%)	HRT was the most impacting factor for pollutants removal, while the external resistance was the most influential impact on power generation	[119]

In the current study, screening was carried out using PBM, after that CCD. In fact, screening design reveals the most impacting factors which are used further in CCD. However, in this study all factors used in PBM are used in CCD even insignificant ones on the objective functions, to compare the linear and quadratic modelling.

2.1.1. Screening design Plackett–Burman method (PBM)

Plackett–Burman method is a screening method that was discovered by Robin Plackett and J. Burman in 1946 [120]. The master idea behind this technique is investigating the most impacting independent factors on dependent responses, with taking (L) level of study. This is carried out by reducing the variance of the response and estimating the factors using very limited number of experiments without taking into consideration the interactions between any pair of factors [121]. For this study, a 2-level design with 1-center point was constructed to study the impact of 7 factors on different responses such as power density, current density and substrate removal efficiency of MFC. The designed matrix of Plackett–Burman for this design study is shown in Appendix 1Table 1. The designs are randomized by Minitab to reduce the noise in the results [122].

- **Pareto chart of the standardized effects**

Pareto chart mainly ranks the factors (parameters) based on their importance on impacting the response. Figure 2-1 shows the pareto chart from screening design for all the three factors using $\alpha = 0.1$. From Figure 2-1, a, the most impacting factor on power density as ranked in pareto chart are: anodophilic bacteria concentration, external resistance, mediator per anodophilic bacteria concentration, feed substrate concentration and substrate concentration respectively. While dilution rate and methanogenic bacteria have insignificant impact on power density compared to others. While for the current density, in addition to the factors impacting the power density,

feed substrate concentration and substrate concentration appear to be other impacting factors which is shown in Figure 2-1, b. Finally, for the substrate removal efficiency, only feed substrate concentration and substrate concentration are impacting this function. The results are reasonable, as anodophilic bacteria are defined to be electrochemically active bacteria which is responsible of electron production after oxidizing the substrate. It can transfer the produced electrons to extracellular electron acceptors (mediators) and result in power and current density. In addition, it is well known from physics (Ohm's law) that external resistance is linked to the produced power and current. This is by regulating the flow of electrons from the anode electrode to the cathode. Increasing the external resistance decreases the mobility of electrons in the outer circuit, reducing the produced current and power density.

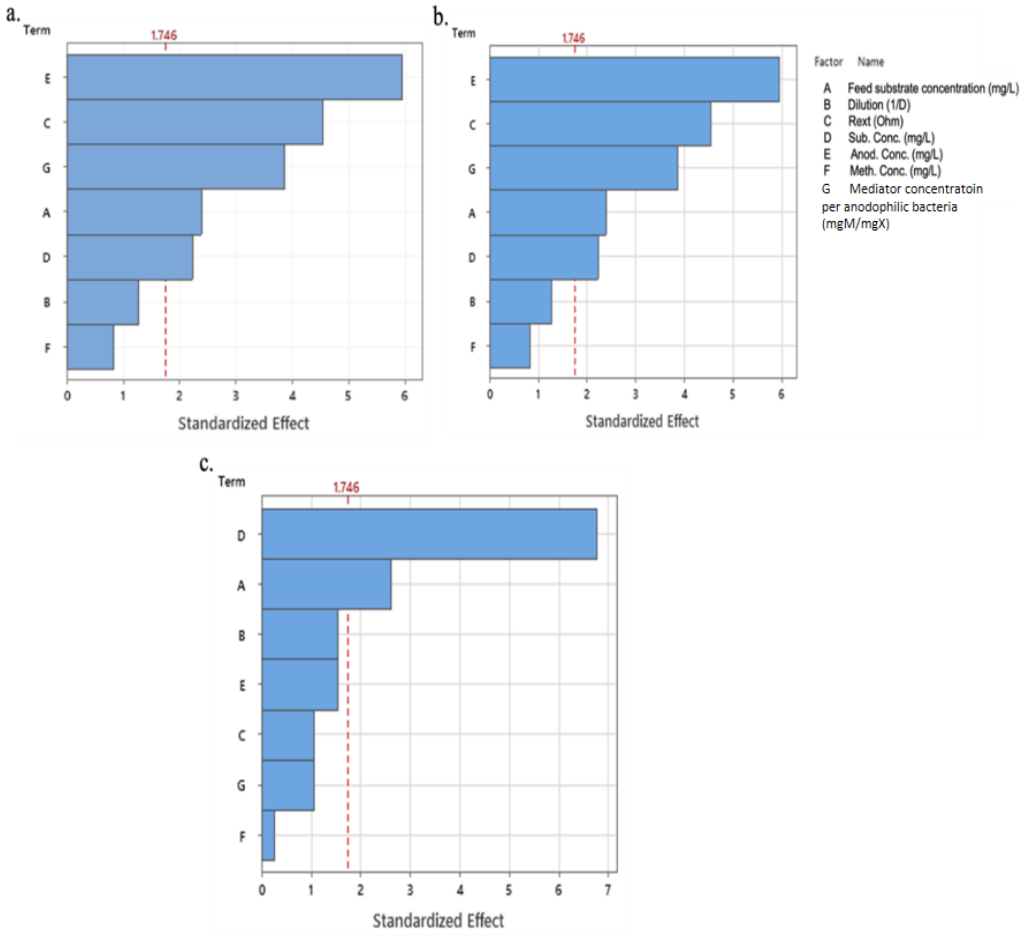

Figure 0-1. Pareto chart for screening design: a. pareto chart of power density response; b. pareto chart of current density response; c. pareto chart of substrate removal efficiency response

It is worth mentioning that the screening methods do not take into consideration the impact of binary interactions of factors and it is considered as very simple method to show the which factors are the most impacting on the output function and this is shown from low R^2 values. Analysis of variance (ANOVA) study, which is shown in Table 2 in Appendix 1, shows p-values of all factors which defines the significance of impacts. Anodophilic bacteria concentration, external resistance and mediator per anodophilic bacteria concentration have p-values less than 0.01 based on DoE which is

based on experimental results of the model proposed by Pinto, R.P. et al. (2012) [1], being the most factors influencing the power density. P-value represents the probability to measure the evidence against null hypothesis for the model. While for current density, most of the factors are impacting its results. The resultant linear models for the power density, current density and substrate removal efficiency from the screening design are generated as shown in Equations (23), (24) and (25) respectively with the R^2 of each model:

Power Density (mW/L)= -35.7 +0.0483 X_1 (mg/L) -0.226 X_2 (1/d) - 0.0980 X_3 (ohm)+0.0494 X_4 (mg/L)+0.2055 X_5 (mgX_a/L)+0.0274 X_6 (mgX_m/L)+16437 X_7(mgM/mgX_a) -64.8 Ct Pt (23)

S	R^2	R^2 (adj)	R^2 (pred)
12.81	88.19%	78.58%	66.73%

Current density (mA/L)= -1753 + 2.367 X_1 (mg/L) - 11.07 X_2 (1/d) - 4.81 X_3 (ohm) + 2.42 X_4 (mg/L) + 10.08 X_5 (mgX_a/L) + 1.34 X_6 (mgX_m/L)+ 806213 X_7 (mgM/mgX_a) - 3180 Ct Pt (24)

S	R^2	R^2 (adj)	R^2 (pred)
11.21	86.29%	76.81%	65.12%

Substrate removal efficiency (%)= 82.1 + 0.0386 X_1 (mg/L) + 0.200 X_2 (1/d) - 0.0167 X_3 (ohm)- 0.1094 X_4 (mg/L) - 0.0389 X_5 (mgX_a/L) - 0.0062 X_6 (mgX_m/L)+ - 3299 X_7 (mgM/mgX_a) - 26.0 Ct Pt (25)

S	R^2	R^2 (adj)	R^2 (pred)
29.9140	76.50%	63.28%	40.65%

The R^2 values for power density, current density and substrate removal efficiency are 88%, 86% and 76.5% respectively. It can be concluded that the model explains almost 88% of the variations for these data for power density and 86% of current density and almost 77% for the substrate removal efficiency. The R^2 value indicates that the model gives a good fit of the data using only linear modelling. Therefore, the model using second-order interactions as well be shown in CCD is expecting to enhance the mathematical models further. This is shown in the next section. It is preferred not to remove the insignificant terms from models resulted in screening design as they impact the overall value of the response.

2.1.2. Central Composite design (CCD)

Central Composite Design (CCD) is a factorial design which is a part of DoE in Minitab software. CCD is statistical toolbox that offers a systematic design and efficient data analysis method to solve multivariate problems in an empirical and statistically way. CCD is a part of Response surface methodology (RSM) and it is called this way because the resulting models are especially suitable for robust mapping of the response. The increased precision and forecasting are a result of the higher order polynomials which are resulted from this method, and therefore CCDs are used for optimization purposes. The main difference in 2-level factorial design and CCD is the accuracy based on the degree of the polynomial. The 2-level factorial design suits more screening purposes which can create at most a first-order model in relating the input factor (X) to the response (Y) as shown in PBD in the previous section. While, CCD have enough treatments to create a second-order polynomial, therefore, CCD is more elaborate. While comparing three-level factorial design with CCD, both designs give very similar results with fewer experimental trials using the later method [123]. CCDs can be either

ordinary central composite designs or face centred central composite designs in this study an ordinary CCD was computed. Evaluation point types gives a huge importance for CCD. The points could be factorial points, axial points and centre points and each one of the points has a great and different significance in the design [124]. Centre points contribute to error estimation and precision of the model, axial points are estimating the pure factors interactions in quadratic terms and the distance from the centre points and finally factorial points estimate linear terms, two- and three-way interactions of different factor [125]. While in the design the value of alpha (α) which represents the distance between the centre point and the outer most points, depends on the number of the factors. In this study CCD is based on one-centre point with 2-levels study and six variables with randomized experiments of two replicates and spherical design. The coded levels of the variables are shown in Table 2-2 below. Polynomial regression equations were developed for each of the responses based on CCD finding a relationship between the objective functions and the studied factors. A second order model of the response surface was developed by means of Multiple Linear Regression (MLR) to minimize the sum of squares of the residuals [126], the model of the response is calculated by the following equation:

$$Y = \beta_0 + \sum_{i=1}^{7} \beta_i X_i + \sum_{i=1}^{6} \sum_{j=i+1}^{7} \beta_{ij} X_i X_j + \sum_{i=1}^{7} \beta_{ii} X_i^2 + \xi \quad (26)$$

Where Y is the predicted response by the model, X_i and X_j refers to the independent variables or factors, β_0, β_I, β_{ii}, β_{ij} and ξ, are regression coefficients and statistical error respectively [127]: Finally, Analysis of Variance (ANOVA) was applied for the model regression and the quality of the fit which is expressed by coefficient of determination (R^2, adjusted R^2 and predicted R^2). The model was visualized using contour plots to analyse the most important factors.

Table 0-2. The coded levels of the variables for CCD

Levels	X_1[b]	X_2[b]	X_3[b]	X_4[b]	X_5[b]	X_6[b]
$-\alpha$[a]	7.7	-0.83	7.17	-----	7.17	-0.83
-1[a]	10	2	10	0.01	10	2
0[a]	505	51	405	-----	261.25	257.25
$+1$[a]	1000	100	800	X_1	512.5	512.5
$+\alpha$[a]	1002.83	102.83	802.83	-----	515.33	515.33

[a] 0 = centre value, +1 = high value, 1 = low value, +/−α = axial point value.

[b]Where: X_1: feed substrate concentration (mg/L); X_2: dilution rate (1/day); X_3: external resistance (ohm); X_4: substrate concentration (mg/L); X_5: anodophilic bacteria concentration (mg/L); X_6: methanogenic bacteria concentration (mg/L)

Table 2-2 is based on five-levels, in which (0) is the centre value in the defined range of each variable based on the upper and lower bounds which are defined as +1 and -1. Alpha represents the axial points in which α is calculated as follows:

$$\alpha = (2^k)^{0.25} \quad (27)$$

Where k is the number of the studied factors. Then + α can be calculated as the upper limit of the variable added to the value of alpha while - α is the lower limit subtracts the alpha value.

In the model suggested by Pinto (2012) [1] which is studied in this paper, the value of mediator concentration per anodophilic concentration is constant under steady-state conditions, therefore, this term was dropped out in CCD despite its great impact on the power density. CCD first is carried out for all the factors not only the important factors from screening model as CCD reveals binary impacts which are not shown in the screening design. Therefore, the binary impacts are captured in CCD to see if any binary impact is significant. Following is the half normal plot of the standardized effects

for all the three functions as shown in Figure 2-2.

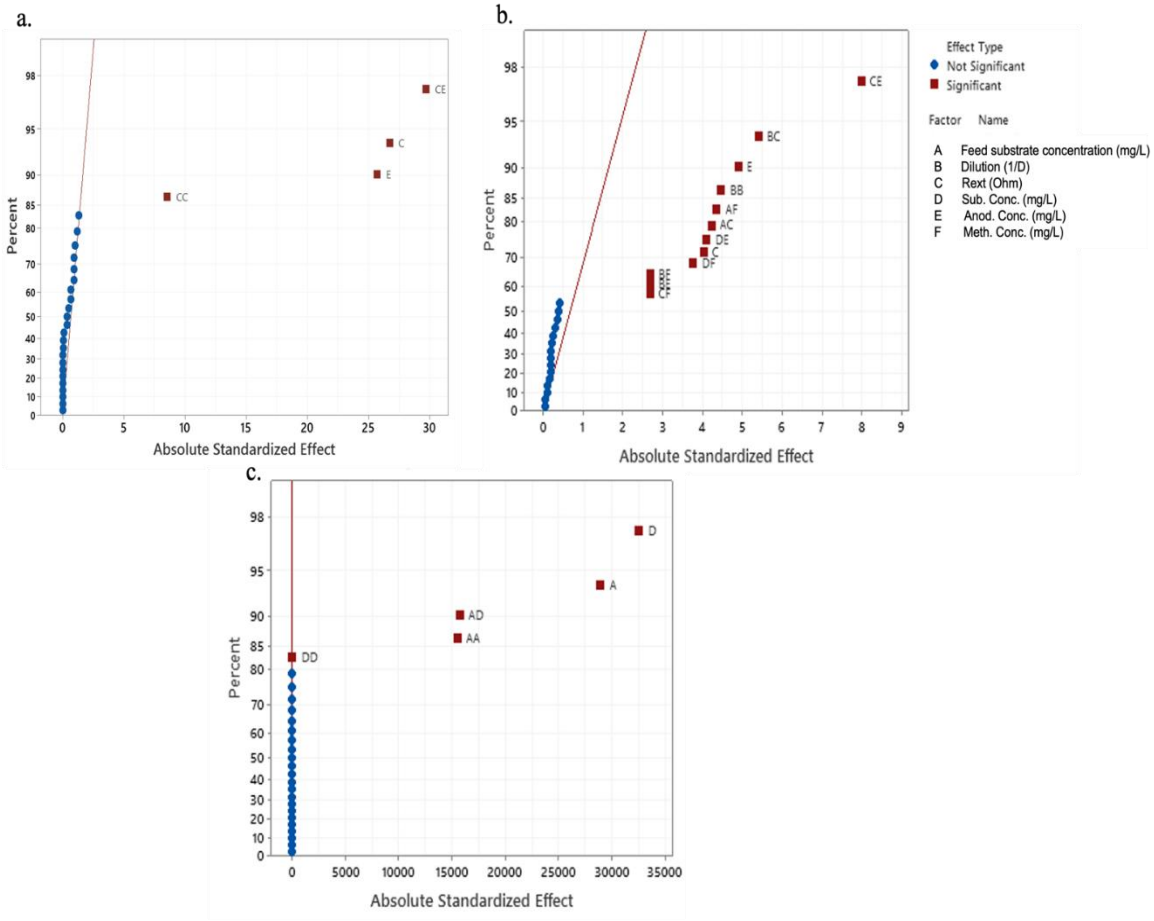

Figure 0-2. Half normal plot of the standardized effects using α=0.1 for: a. Power density, b. current density, c. substrate removal efficiency

From Figure 2-2, a which represents the half normal plot of power density, anodophilic bacteria concentration and external resistance are factors of most impacting the power density (that was also suggested by the screening analysis) with their single impacts as well as the interactions. While, from Figure 2-2, b, it can be noticed that besides anodophilic bacteria concentration and external resistance, many binary interactions are impacting the current density. External resistance and dilution interaction, dilution rate and dilution rate interaction, feed substrate concentration and methanogenic bacteria concentration interaction, feed substrate concentration and external resistance

interaction, substrate concentration and anodophilic bacteria concentration, substrate concentration and methanogenic bacteria concentration interaction, dilution rate and methanogenic bacteria concentration interaction, dilution rate and anodophilic bacteria concentration interaction and finally the external resistance and methanogenic bacteria concentration interaction. For the substrate removal efficiency, feed substrate concentration are the most important impacting factors as expected, including binary interactions which is represented in Figure 2-2, c. the analysis of variance (ANOVA) for all the functions is shown in Table 3 in Appendix 1 in which the importance of each of the linear and quadratic models is clearly represented. The resultant second order predicted models for all the three functions are shown in Equations 28, 29 and 30 with the determination coefficient (R^2).

Power Density (mW/L)=

$$32.68 + 12.5\,X_1\left(\frac{mg}{L}\right) - 3.8\,X_2\left(\frac{1}{D}\right) - 410.6\,X_3\,(ohm) + 0.0322\,X_4\left(\frac{mg}{L}\right) + 480.9\,X_5\left(\frac{mg}{L}\right) - 0.0412\,X_6 + 2.1X_1^2\left(\frac{mg}{L}\right) - 50.8\,X_3^2(ohm)^2 - 0.211\,X_4^2\left(\frac{mg}{L}\right) + 7.6X_5^2 + 0.008X_6^2\left(\frac{mg}{L}\right) + 0.003\,X_1\left(\frac{mg}{L}\right)X_2 - 50.8\,X_3^2(ohm)^2 + 54.3\,X_3\,(ohm) * X_5\left(\frac{mg}{L}\right) \quad (28)$$

S	R^2	R^2 (adj)	R^2 (pred)
10.491	98.04%	97.18%	96.22%

Current density (mA/L)=

$$45 + 26X_1\left(\frac{mg}{L}\right) - 2.127\,X_2\left(\frac{1}{D}\right) - 169.2\,X_3\,(ohm) - 2.7\,X_4\left(\frac{mg}{L}\right) + 61.3X_5\left(\frac{mg}{L}\right) + 3.5\,X_6\left(\frac{mg}{L}\right) - 0.36\,X_4^2\left(\frac{mg}{L}\right)^2 + 2.095X_2^2\left(\frac{1}{D}\right) + 7.X_3^2\,(ohm) - 1.51X_4^2\left(\frac{mg}{L}\right) + 3.02\,X_5^2 + + 0.0294X_6^2\left(\frac{mg}{L}\right) - 0.0027\,X_1\left(\frac{mg}{L}\right) * X_2\left(\frac{1}{D}\right) + 0.0289X_1\left(\frac{mg}{L}\right) * X_3\,(ohm) + 0.187\,X_1\left(\frac{mg}{L}\right) * X_4\left(\frac{mg}{L}\right) + 0.08X_1\left(\frac{mg}{L}\right) * X_5\left(\frac{mg}{L}\right) + 0.0436X_1\left(\frac{mg}{L}\right) * X_6\left(\frac{mg}{L}\right) + 0.0241X_2\left(\frac{1}{D}\right) * X_3(ohm) + 0.00141X_2\left(\frac{1}{D}\right) * X_4\left(\frac{mg}{L}\right) - 0.001898\,X_2\left(\frac{1}{D}\right) *$$

$$X_5\left(\frac{mg}{L}\right) - 0.001870\,X_2\left(\frac{1}{D}\right) * X_6\left(\frac{mg}{L}\right) + 0.0027\,X_3(ohm) * X_4\left(\frac{mg}{L}\right) - 0.0702\,X_3\,(ohm) *$$

$$X_5\left(\frac{mg}{L}\right) - 0.232\;X_3\,(ohm) * X_6\left(\frac{mg}{L}\right) - 0.000504\,X_4\left(\frac{mg}{L}\right) * X_5\left(\frac{mg}{L}\right) + 0.0456X_4\left(\frac{mg}{L}\right) * X_6\left(\frac{mg}{L}\right) +$$

$$0.000013\,X_5\left(\frac{mg}{L}\right) * X_6 \quad (mg/L) \tag{29}$$

S	R^2	R^2 (adj)	R^2 (pred)
12.828	94.02%	87.88%	75.47%

$$\textbf{Substrate removal efficiency}\ (\%) = 20.001 +$$

$$297.5909X_1\left(\frac{mg}{L}\right) - 0.000004\,X_2\left(\frac{1}{D}\right) + 0.000007\,X_3\,(ohm) - 371.906X_4\left(\frac{mg}{L}\right) +$$

$$0.000011\,X_5\left(\frac{mg}{L}\right) + 0.000012\,X_6\left(\frac{mg}{L}\right) - 0.000247\,X_7\left(\frac{mg}{L}\right) \tag{30}$$

S	R^2	R^2 (adj)	R^2 (pred)
0.0014164	99.99%	99.99%	99.99%

The determination coefficient (R^2) for all the functions was greater than 90%, which gives an indication that the model is suitable and explains the results. The models are interpreted into contour plots which can gives insights for optimization and maximization of each function at some constant and variable factors. The contour plots are extracted for each function for the most impacting factors.

2.1.3. Comparison between PBM and CCD models

PBM design predicted each of the functions using linear modelling while CCD took the binary interactions into consideration. R^2 values for CCD are larger than the one of PBM for all the functions. Therefore, binary interactions represented by the factor duplicated or the interactions of the factors with one another. The R^2 for power and current density jump from 88% and 86.29% respectively for PBM to 98% and 94% in CCD respectively. Therefore, CCD boosts the models which can predict better results than PBM while the later can be used if simplicity is a condition. For substrate removal

efficiency, CCD showed a way better model with R^2 almost 100% which was 76.50% in PBM.

2.1.4. Contour plots

Contour plots for the responses are generated based on the models proposed using CCD which are built on MFC model discussed by Pinto et al. (2012) [1]. The contour plots help in optimization purposes in which the response value can be predicted based on the variation of two variables. It was noticed that the external resistance and the anodophilic bacteria concentration are the most impacting factors that affect the value of the power density generated by MFC. Using the model generated by CCD, a contour plot showing levels of both variables (external resistance and anodophilic concentration) and the response of the generated power density which is represented in Figure 2-3.

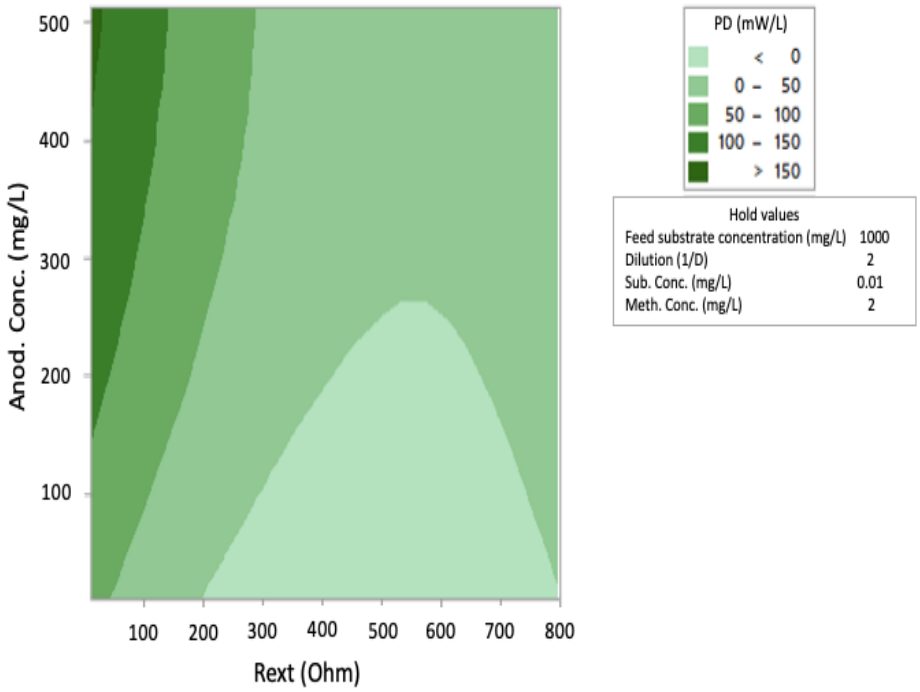

Figure 0-3. Contour plot of power density (mW/L) VS external resistance (Rext)(X_3) of MFC and Anodophilic bacteria concentration (Anod. Conc.) (X_5)

It is known that anodophilic bacteria are electrogenic and produce electrons from the oxidation reaction of an electron doner which is the substrate. To increase the power density, the one should increase the microbial electrogenicity. This is by either using only electrogenic pure community in MFC anode compartment, increase the concentration of electrogenic bacteria if mixed culture is used or use high performance electrogenic bacterial community. Li, M. et al. (2018) [68] conducted a review paper for enhancing the power generation performance by enhancing the electrogenic bacterial community. In this paper, they gathered all electrogenic bacteria and rank them based on their ability for power generation. γ- Proteobacteria of species Shewanella oneidensis, gram negative is one of the most producing power bacteria with an ability to produce 3000 mW/m^2 [68]. While external resistance which is the opposing

force to the flow of a steady electric current. Increasing the opposing force decreases the flow of the current and hence the generated power density. Therefore, decreased resistance is preferable to maximize the power generation [128]. One study showed that external resistance also impacts the anodic biofilm microbial community by affecting the rate of electrons retransferred from the anode, inevitably impacting the microbial metabolism and biofilm structure, hence the power generation [129]. The results of this model in studying the relationship between power density and the external resistance are compatible with the studies accomplished by Abu-Reesh, I. (2020) [130] and Katuri, K. (2011) [131] which showed that increasing the external resistance decreases the generated power density. Opposing results were shown in Zhang, L. et al. (2011) [132] study in which the obtained power of MFC increased from (1.96 -6.05) mW when the external resistance was increased from (10-50) ohm. The fluctuation in the results is due to the fact that the relationship of the external resistance and power density is extracted from the model which differs from one study to another and the interactions with the internal resistance which is not a system constant; and depends on the external resistance value [132]. For current density function, from ANOVA analysis it was noticed that most of the factors are impacting the current density. Selectively, some factors are chosen to be represented in contour plots. The impact of external resistance and feed substrate concentration on the current density is shown in Figure 2-4 below. It can be noticed that the external resistance shows the same behaviour as in Figure 2-5. Increasing the external resistance will lead to decreasing in current density values, while the opposite is applied for the feed substrate concentration.

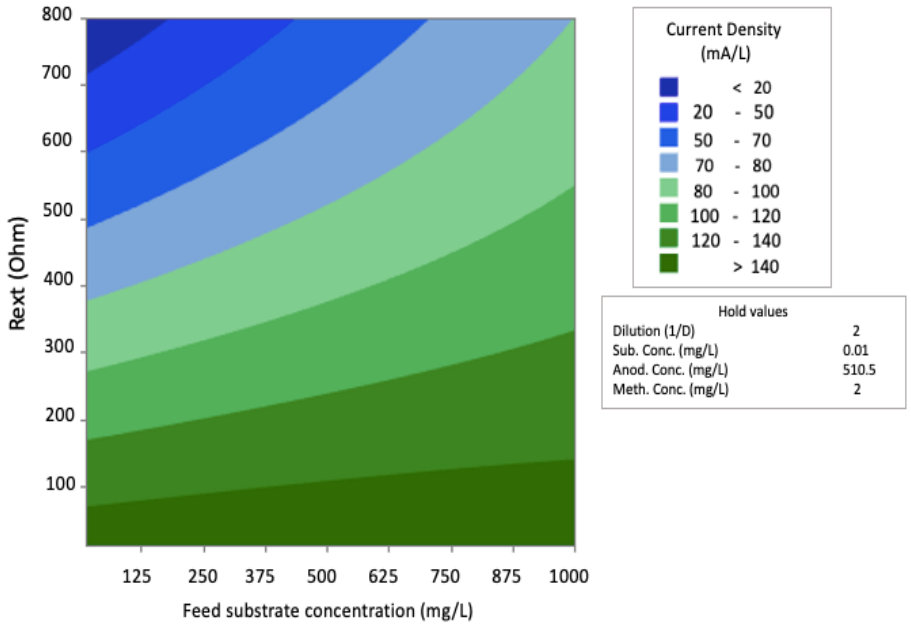

Figure 0-4. Contour plot of current density (mA/L) VS feed substrate concentration (X_1) and external resistance (Rext)(X_3) of MFC

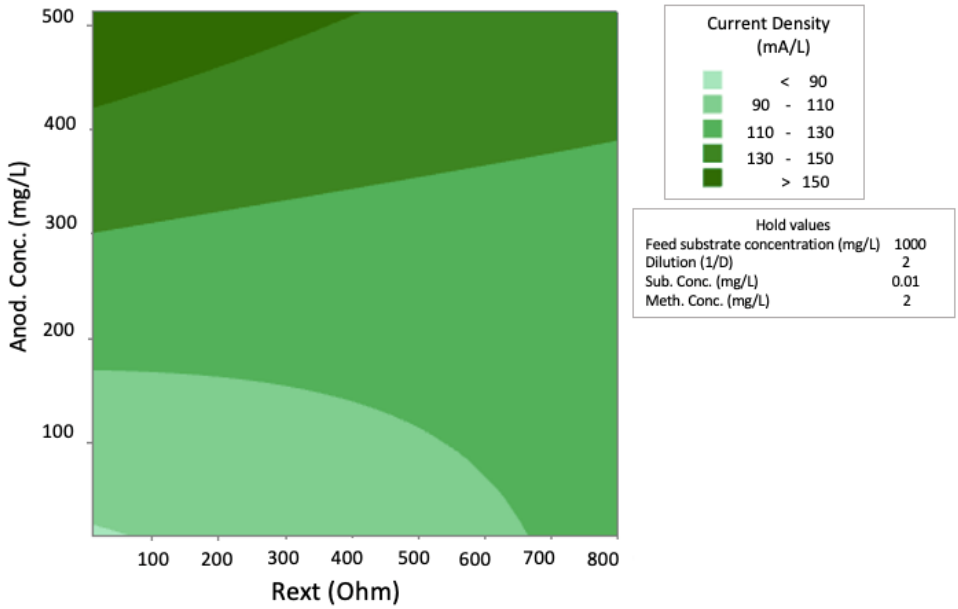

Figure 0-5. Contour plot of current density (mA/L) VS external resistance (Rext)(X_3) and anodophilic bacteria concentration (Anod. Conc.)(X_5) of MFC

The behaviour of external resistance in Figures 2-3,2-4 and 2-5 gives an indication about the relationship of the current and the power density that both functions are going in the same path (i.e., increasing and decreasing together). While for the substrate removal efficiency, from ANOVA results almost feed substrate and substrate concentration are impacting the function. Feed substrate concentration VS the anodophilic bacteria concentration is plotted as shown in Figure 2-6 in relation with substrate removal efficiency. Feed substrate can be defined as the available oxidation material for anodophilic bacteria to produce the electrons and cause power generation. Therefore, the substrate removal % depends on the amount of the feed substrate added to the system and available for bacteria.

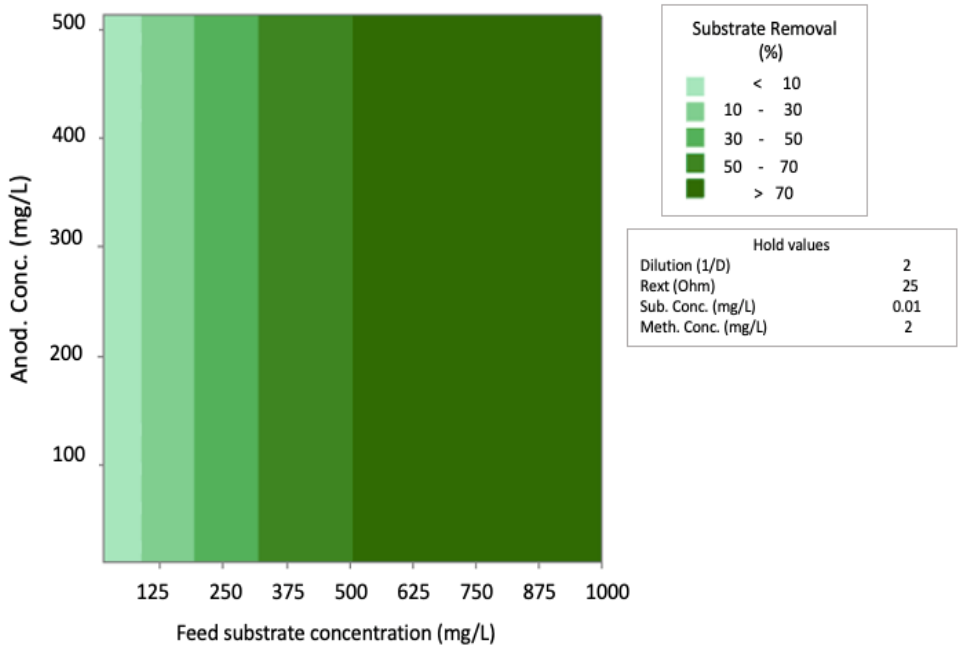

Figure 0-6. Contour plot of substrate removal efficiency (%) VS feed substrate concentration (X_1) and anodophilic bacteria concentration (Anod. Conc.)(X_5) of MFC.

2.1.5. Conclusions

In conclusion, the importance of RSM in modelling and optimization of MFC is significant. PBM screening method and CCD as advanced RSM helped in modelling

three important performance factors of MFC which are power density, current density and substrate removal efficiency. PBM screening method predicted a linear model for all functions revealing the linear and single impacts of variables on each of the functions. While CCD predicted quadratic models for each of the functions by revealing the interactions between the factors. The predicted model of PBM was linear based on all the defined factors which was further enhanced by CCD predicted model and this was shown in R^2 of each of the functions in the model. This modelling helps further in optimization purposes, by using contour plots the one can predict where could a function be maximized under some defined conditions.

2.2.Optimization of MFC

Gomez, A. et al. (2004) [133] define the optimization as "doing the most with the least" [133]. Optimization is the process of finding the best design that achieves certain criteria within given constraints for a certain system, maximizing or minimizing a certain objective. While computer-based optimization is using computer assistance in decision making via different software and technology for finding the best solution for a system objective function. Optimization of MFC operating conditions is studied using two main methods as discussed before: experimental and mathematical modelling [134]. Over the past decades, extensive experimental studies about MFC design operational conditions, materials, electrodes and microbial population which lead to a great understanding of the system [135]. Yet, challenges of scaling-up, low power density production, low volumetric performance need to be addressed and solved. Model-based optimization is a perfect tool for further improving the performance operational conditions towards commercialization. Many studies were previously developed investigating the optimization of MFC using either experimental or computational techniques. Table 2-3 shows the different model types that were used to

study modelling and optimization field of MFC. While Table 2-4 shows different studies of MFC optimization.

Table 0-3 modelling and optimization methods for MFC in the literature

Modelling type	Govern equation type	Potential variables of the model	Ref.
Statistical method	DOE, factorial design, central composite design, screening designs	External resistance, pH, bacteria concentration	[136]
Black box method	Adaptive neuro-fuzzy interface system	Ionic strength, pH, operational conditions	[137]
Biological method	Electrons, substrate, bio-electrochemical balances	Biofilm catalytic activity, overpotential	[138]
Sensitivity analysis	Ordinary differential equations, partial differential equations	Operational conditions, external or internal resistance	[139]
Polarization model	Butler-Volmer equations	Electrochemical kinetics	[140]
Electrochemical simulation method	Nyquist plots, EIS	Substrate concentration, external resistance, electrode spacing	[141]
Conceptual methods	Tafel equation	electrode spacing and surface area	[142]

Table 0-4 MFC models in the literature

MFC type	Type of the study	Modelling approach	Microbial population	Objective function	Decision parameters	Type of electron transfer	Ref.
Single anode chamber	-One dimensional -Dynamic	Ordinary differential equations (ODE)	Single population	Current density	-Substrate concentration -Mediator concentration	External mediator	[91]
Single anode chamber	-One dimensional -Dynamic	Ordinary differential equations (ODE)	Single population	-Substrate concentration -Open circuit anode potential - Cathode potential	-	-	[143]
Single anode chamber	- One dimensional -Dynamic -Steady-state	ODE	Multi-population	-Power density	-External resistance -Coulombic efficiency	Intercellular	[15]

MFC type	Type of the study	Modelling approach	Microbial population	Objective function	Decision parameters	Type of electron transfer	Ref.
Single anode chamber	- One dimensional -Dynamic	ODE	Multi-population	-Charge storage	-External resistance	Intercellular	[144]
Dual chamber	- One dimensional -Dynamic -Steady-state	ODE	Single population	-Voltage -fuel concentration	-Power output	-	[100]
Dual Chamber	- One dimensional -Steady-state	ODE	Single population	-Current density -Biofilm thickness -Performance	-Cell voltage -Substrate concentration and temperature	-	[13]
Dual Chamber	- One dimensional -Dynamic -Steady-state	ODE	Single population	-Voltage -Current	-Lactate concentration	External	[145]
Dual Chamber	- One dimensional -Steady-state	ODE	Multi-population	-Cell voltage, -Power density -Temperature	-Process parameter	-	[146]
Single chamber	- One dimensional -Steady-state -Dynamic	Partial differential equation (PDE)	Single population	-Biofilm related growth	-Mass-transfer resistance -Rate of electron-donor	-	[147]
Single chamber	- Two dimensional -Steady-state	Partial differential equation (PDE)	Single population	-Current generation -Biofilm thickness	- Presence/absence of NH_4	- Extracellular and intracellular	[148]
Single chamber	-Three dimensional -Steady-state	ODE PDE	Multiple population	-Substrate utilization yields -Standard potential of the redox -Mediator, ratio of suspended to biofilm cells	-Current -Voltage -Substrate concentration	External	[149]

Mathematical model-based optimization using computational methods is rare, and it is applied in this section using Pinto's model (2012) which is developed for a single

chamber MFC with air cathode inoculated with multi-cultural microbial community operating in the continuous-flow mode at a steady state. The main objective of this work is applying a single objective optimization method for three main performance criteria of MFC objective functions which are power density, current density and substrate removal efficiency. While multi-objective optimization is not covered as the functions found not to be conflicting with one another.

2.2.1. Computational Optimization tools

The optimization tools used in this study are Matlab and Microsoft Excel.

- **Microsoft Excel**

Solver is an add-in program in Microsoft Excel which can be used for optimization purposes conveniently. This optimization analysis using Solver is more complex than the one provided by Goal Seek analysis. Solver adds more value for the user by providing more options and control over the optimization problem. Goal seek provides for the optimization changing the objective function value to be set to a certain value by changing the decision parameters "unconstrained". While Solver provides the option of setting constraints over the decision parameters which can be in forms equalities, all different (dif) which adds to the constraints a condition that all decision variable values should be different at the optimal solution level, integer (int) values like (1,2, -1, etc..) within a small tolerance and binary (bin) which imposes a condition of having values of either 0 or 1 [150]. Minimum, maximum and set a value are the options provided by solver for the function to be optimized which can be one cell called the "objective cell". Also, decision parameters which are computed in the formulas and their values will be changed until the optimal value of the function can be found, require to be subjected to lower and upper limits. Therefore, Solver works to change the values of the decision parameters to satisfy the limits, satisfy the constraints and satisfy the

objective function being optimized. There are three solving methods by Solver to solve optimization problems: 1- Generalized Reduced Gradient (GRG), 2- LP simplex, 3- Evolutionary. LP simplex is used for solving linear problems while both GRG and Evolutionary are used for non-linear problems in which the former method is used for smooth non-linear and the latter used for non-smooth non-linear problems. Due to the complexity and non-linearity of MFC model which is based on non-linear ordinary differential equations, "Evolutionary" method is used for the optimization of all the three functions [151].

- **Matlab**

Fmincon is a nonlinear solver algorithm that is provided by Matlab optimization toolbox for solving constrained optimization multivariable functions that is supporting linear and non-linear constraints. While using this solver barrier method, tolerance, maximum iteration and tolerance of the function options can be configured. This function is mainly used for minimization purposes; however, it can be used for maximization by changing the sign of the function. The results of fmincon show generally a local minimum or local maximum. Interior point barrier method is used in this optimization problem, which helps in barrier parameter updating, which is time efficient for polynomial running and solving. Interior point is the default barrier method and there are other methods just as trust-region-reflective, 'active-se' and 'sqp-legacy', and 'sqp', however the default algorithm is used in this optimization problem as being considered as a faster method with more accurate results. ConstraintTolerance is used with additional options with fmincon optimization function, which is mainly set for the termination of the function by controlling the tolerance on the constraints. While MaxIterations is used for specifying the maximum number of iterations for the optimization problem. FunctionTolerance can be added for termination of the function

by controlling the tolerance on the value. Finally, plotting the optimization function with respect the iterations while the algorithm executes can be computed via using PlotFcn [151].

2.2.2. Single objective optimization

Optimization is the process of selecting the best value of a function by either minimizing or maximizing it regarding some criteria which should be satisfied. This can be carried out by changing some of the decision parameters simultaneously and systematically to capture the optimum value of the function under satisfying the constrains which in turn can be linear, non-linear, equality or non-equality. The decision parameters are chosen based on their expected impact on the objective function (function to be optimized) within a certain experimentally specified range [152]. From a mathematical perspective, the optimization problem can be formulated as follows:

Minimization/Maximization $f(x)$

Subject to:

$$g_i(x) \leq 0, \qquad i = 1,2, \dots \dots, m \tag{31}$$

$$h_j(x) = 0, \qquad j = 1,2, \dots \dots, p \tag{32}$$

While the decision variables (x values) are defined within a certain range for each as follows:

$$x_k^{LB} \leq x_k \leq x_k^{UB}, \qquad k = 1,2, \dots \dots, n \tag{33}$$

Where $f(x)$ is the objective function which is indented to be optimized over the values of the decision parameters; $g_i(x)$ represents the non-equality constraints which could be linear or non-linear; m is the number of the non-equality constraints; $h_j(x)$ represents equality constraints which could also be linear or non-linear; p is the number of the equality constraints such that m and p are greater than zero; x_k is the vector of design

parameters; x_k^{LB} is the lower bound of x_k parameter and x_k^{UB} is the upper bound of the same parameter and n is the number of the decision variables.

In this paper, the optimization problem is multi-variable, nonlinear and nonequality constrained problem. The optimization of this model was carried out using MATLAB as well as Microsoft excel solver. Three main objective functions have been optimized (maximized), power density (PD) (mW/L), substrate removal efficiency (SRE) (%) and current density (CD) (mA/L). The optimum operating conditions were found by varying the decision parameters with the specified range for each [153]. The model is set as follows:

- **Maximized objective functions:**

The power density of MFC, the removal efficiency and current density can be calculated as [1]:

$$PD_{MFC}\left(\frac{mW}{L}\right) = \frac{I_{MFC} * E_{MFC}}{V} \quad (34)$$

$$SRE(\%) = \frac{S_0 - S}{S_0} \times 100\% \quad (35)$$

$$CD_{MFC}\left(\frac{mA}{L}\right) = \frac{\frac{E_{OCV} - \eta_{conc}}{R_{ext} + R_{int}}}{V} \quad (36)$$

- **Subject to (constraints):**

The fifth constraint was defined for maximum power density: explained in Appendix 2 Table 1.

1) $\frac{dS}{dt} = -q_a X_a - q_m X_m + D(S_0 - S) = 0$ (37)

2) $\frac{dX_a}{dt} = \mu_a X_a - k_{d,a} X_a - \alpha_a D X_a = 0$ (38)

3) $\frac{dX_m}{dt} = \mu_m X_m - k_{d,m} X_m - \alpha_m D X_m = 0$ (39)

4) $X_a + X_m - X_{max} = 0$ (40)

5) $R_{int} \approx R_{external}$ (41)

- **Decision variables**

Decision variables as stated before, they are the parameters which values are changed so that the optimum value of each of the objective functions is obtained individually. The decision variables are the dilution rate (D), external resistance (R_{ext}), substrate concentration (S), anodophilic cell concentration (X_a) and methanogenic cell concentration (X_m).

2.2.3. Results and discussion

For the optimum value of each of the objective functions, five decision variable values should be determined for the single chamber, membrane-less, multi-culture with biofilm consideration and air cathode. The numerical optimization problem is carried out using Matlab and Microsoft Excel solver, the results of all parameters from both methods are stated in Table 2-5. The system is carried out at steady-state conditions at a constant feed substrate concentration of 1000 mg/L. Multi-population microbial community is used in this model, which consists of methanogenic and anodophilic bacteria. Using a multi-population community gives many advantages such as increasing the resistance of the community to sever living states and sudden changes in the operational conditions in the biofilm, therefore it helps in sustaining the bacterial population [149].

It is worth mentioning that the system consists of anodophilic and methanogens, the optimum power density is never in methanogenic region, as the electrons are produced only by anodophilic microorganisms. And at these conditions, the oxidized mediator fraction per anodophilic is constant and equals to the expression below based on Pinto's (2012) model [1]:

$$M_{ox} = \frac{k_M}{\frac{\mu_{max,a}*(K_{S,m}+S)}{\mu_{max,m}*(K_{S,a}+S)}-1} \quad (42)$$

The value of M_{ox} after using Equation 42 is 0.52 mgM/mgX_a. Table 2-5 below shows

the lower bound, upper bound and optimum values for each of the decision parameters after the optimization problem was executed using both Matlab and Microsoft Excel solver. While Table 2-6 below shows the optimized functions values. Matlab optimization codes are in Appendix 3.

Table 0-5. Decision variables

Parameters	Units	Lower boundary (LB)	Upper boundary (UB)	Excel optimum value	MATLAB optimum value
Dilution rate (D)	1/day	1	9.99E+307	2.0	2.0
External resistance (Rext)	ohm	10	800	25.009	25.1
Substrate concentration (S)	mgS/L	0.01	999	0.01	0.0112
Anodophilic cell concentration (x_a)	mgXa/L	10	512.5	510.5	510.5
Methanogenic cell concentration (x_m)	mgXm/L	0.01	512.5	2.0	2.0

Power density function values per iterations using Matlab and Microsoft Excel are shown in Figures 2-7 and 2-8, respectively.

Table 0-6. Optimum values of power density and corresponding current density and removal efficiency

Function	Excel optimum value	MATLAB optimum value	Difference (%)
Optimized PD (mW/L)	157.383	157.297	8.6
CD at the optimized PD (mA/L)	250.85	250.83	2
SRE at optimized PD (%)	99.999	99.998	0.1

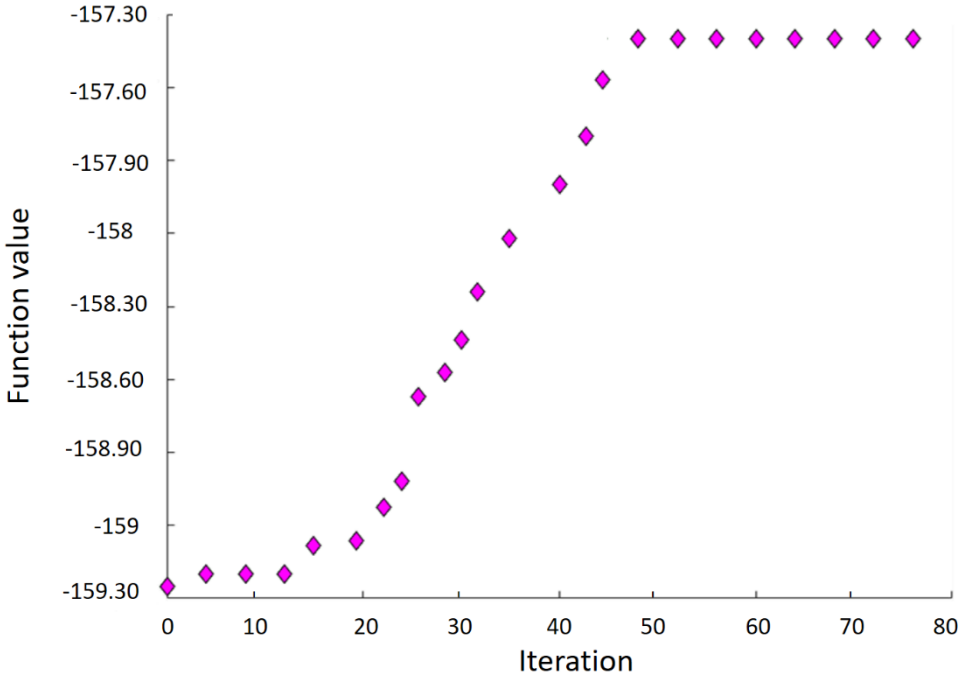

Figure 0-7. Power density value per iteration using Matlab

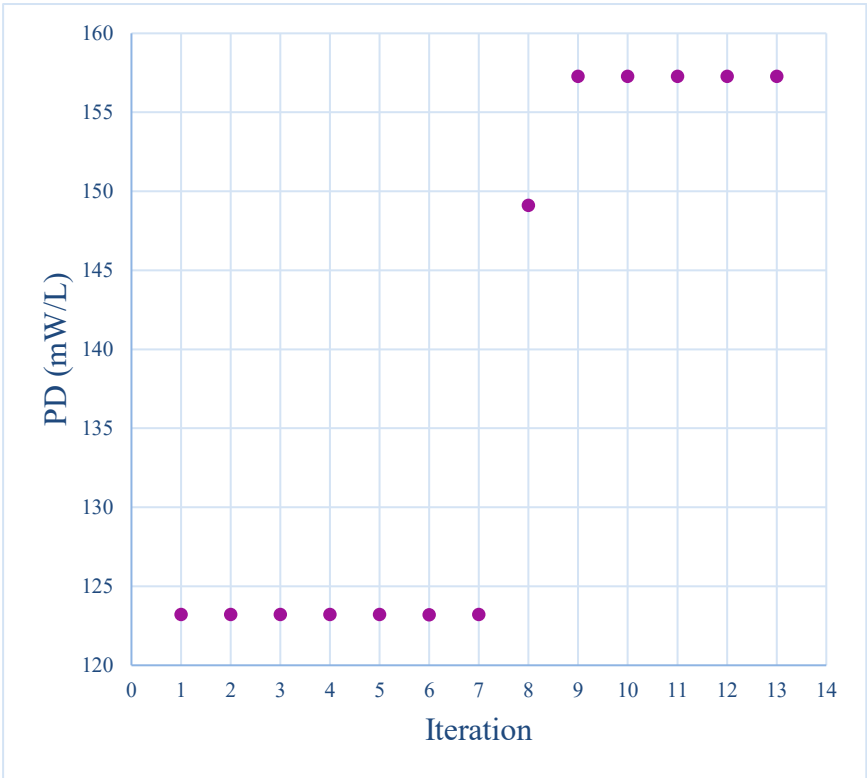

Figure 0-8. Power density value per iteration using Microsoft Excel

After optimization, it is concluded that all the objective functions are maximized at one point. Means that maximizing power density maximizes other two functions of current density and substrate removal efficiency. Almost the same results are obtained using both Excel and Matlab. The main issue in this optimization problem are the constraints and the optimization problem options so that the calculations are computed more accurately. In Pinto et al. (2012) model [1], they have mentioned that the optimum steady-state condition for the productivity (PD) of MFC the M_{ox} value is constant and equated to Equation 42 rather than solving the differential equation as a constraint which is represented in Equation 9. Also, the α value (the dimensionless biofilm retention constant) is defined differently from Pinto, R.P. et al. (2010) [15]. For the activation losses to be neglected in the calculations, the internal to the external resistances should be near one another values or equal. After optimizing the power density, the resulted external resistance is shown to be equal to the internal resistance. One of the main interesting points in the constrains is the summation of both microorganism ($x_a + x_m$) which should be greater than or equal to X_{max} (the maximum attainable biomass concentration). As stated previously, the co-existence of both species (anodophilics and methanogens) is assumed, this can be analysed by "competitive exclusion principle" which states that only one of the species can survive when a competence on the same substrate is the situation. This exclusion occurs due to using similar kinetics for competing species. Therefore, the results of the optimization should be allied with the equilibrium point in which the coexistence occur. The stable equilibrium point for MFC biofilm composition should satisfy the following condition for co-existence [1]:

$$0 < I_{MFC} \leq \overline{I_{MFC}} \quad (43)$$

Where I_{MFC} is the current produced from the MFC which is defined in Equation 21. For $\bar{I}_{MFC}$ is defined in Equation 44 below:

$$\overline{I_{MFC}} = q_{max,a} S \frac{M_{ox} X_{max}}{(K_M + M_{ox})} \frac{mV}{\gamma} \frac{FY_M}{(K_{s,a} + S)} + \frac{\eta_{conc}}{2R_{int}} \quad (44)$$

Also, β term which is defined as:

$$\beta = x_a \times \mu_m \quad (45)$$

For this stable point to take place the conditions of ($x_a + x_m = X_{max}$) should also be satisfied. I_{MFC} and $\overline{I_{MFC}}$ are both calculated as follows in Table 2-7:

Table 0-7. Different parameters values for ensuring optimization point stability

Parameter	Value
I_{MFC} (A)	0.01254
$\overline{I_{MFC}}$ (A)	0.06497
x_a (mg/L)	510.5
x_m (mg/L)	2.000
X_{max} (mg/L)	512.5
β	0.01914
$\mu_m X_{max}$	153.75

Comparing these values, it can be noticed that both ($0 < I_{MFC} \leq \overline{I_{MFC}}$), ($x_a + x_m = X_{max}$) and ($\beta < (\mu_m X_{max})$) are satisfied, therefore, the optimization point of the coexistence occurs and it is a stable point [1].

2.2.4. Results validation

For validating the results, the output of the optimization was compared with the analytical expressions of optimal productivity as stated in Pinto, R.P. et al. (2012) [1].

The optimum steady state current which corresponds the optimum productivity is given by the following expression:

$$I_{MFC} = I_{int}^{opt} - \frac{\eta_{conc}}{2R_{int}} \approx I_{int}^{opt} \qquad if\ I_{int}^{opt} \leq \bar{I}_{MFC} \tag{46}$$

$$\eta_{conc} = \frac{RT}{mF} ln\left(\frac{M_T}{M_T - M_{ox}}\right) \tag{47}$$

And if $I_{int}^{opt} \leq \bar{I}_{MFC}$ is applied, then there is a coexistence of both bacteria in the system between anodophilics and methanogens in the biofilm. The values of $\overline{I_{MFC}}$ and I_{int}^{opt} and the output I_{MFC} are given in Table 2-8 below.

Table 0-8. Values of MFC current

Parameter	Value
$\overline{I_{MFC}}$ (mA)	64.968
I_{int}^{opt} (mA)	12.543
I_{MFC} (mA)	12.542

From optimization results, power density value was 157.3 mW/L which shows that the produced power is 7.87mW. Then, the corresponding and optimized current is 12.54 mA. The steady state power productivity of MFC using the experimental results in Pinto, R.P. et al. (2012) model, the maximum current of 12.5 mA corresponds the maximum power of around 6.1 mA [1]. While the maximum power produced after optimization as stated earlier is 7.87mW. Main reason could be that in the model, the output substrate concentration was fixed to be 100 mg/L as a PID controller was used. Whereas, in this optimization problem the feed substrate concentration is fixed at 1000 mg/L and the substrate concentration value was optimized and found to be less than the value used in the model which was 0.01 mg/L. Therefore, more amount of substrate

consumed, and more power is produced. Also, the % of microorganisms from the maximum attainable bacterial concentration of both microorganisms in the biofilm was extracted from the experimental results in Pinto, R.P. et al. (2012) model. The optimized model shows a maximum power density at 99.6% of electricigenic bacterial concentration in the biofilm which show an output voltage of 627.6 mV which is compatible with what the expected from the experimental results [1].

2.2.5. Conclusions

In conclusion, a single-chamber microbial fuel cell with multi-population operating in continuous flow mode at steady-state was optimized. Single objective optimization was performed to maximize the generated power density, current density and substrate removal efficiency. Since all three functions are maximized together, this means that the functions are going in the same direction (increasing or decreasing together with respect different variables) and they are not conflicting with one another. hich is shown in the coming section of sensitivity analysis, therefore, the multi-objective optimization is not needed. The results of all three objectives showed that this optimization problem converges to a single point which maximizes all the functions. The Matlab optimization function, fmincon is used for single optimization problem simultaneously with Microsoft Excel solver. The performance of MFC described in this section depends mainly on the external resistance, anodophilic cell concentration and substrate concentration. The maximum PD produced obeying the range of conditions was 157.40 mW/L by both Matlab and Microsoft Excel which corresponds to a CD of 251 mA/L, 25.1 Ω external resistance, 510.5 mg/L anodophilic cell concentration and 2.0 1/d dilution rate. Finally, optimization is a powerful technique to predict the optimum operating and design conditions in terms of being practical, faster and economical.

CHAPTER 3: SENSITIVITY ANALYSIS

3.0. Sensitivity analysis

Measuring the quality of the parameters which can significantly impact the performance of MFC is crucial. This can be carried out by the means of performing sensitivity analysis on the system. This assists to evaluate the accuracy and quantify the uncertainty in the estimated empirical parameters of a model [154]. In addition, this can show the impact of multi-variate changes on the system. This is carried out by monitoring the output value of the objective function (function to be studied) and the extent to which each of the input parameter can affect its value, thus its uncertainty [155], [156]. The analysis method using sensitivity analysis is based on mathematical rules by generating values of the factor, then calculating the value of the output corresponds that mathematical model. If a small change in a certain input parameter has resulted in a relatively large change in the output; it is said that the output of the model is sensitive to this input parameter [157]–[159]. Ideally, both uncertainty and sensitivity analysis of a model should be run tandemly [160]–[162]. Figure 3-1 shows the interrelationship between uncertainty, sensitivity analysis and modelling.

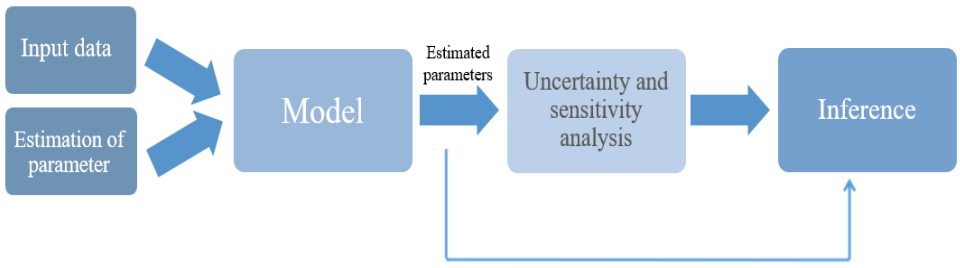

Figure 0-1. Representation of sensitivity analysis method

Figure 3-1 shows that a model which has input data (error-free for simplicity) from which the parameters are estimated using the specified model, then after the estimation; the best parameter values are considered. At this stage, the model is considered as a true

model and it is proceeded to the sensitivity analysis [163]–[165]. Finally, sensitivity analysis reveals which of the input parameters are the most important in impacting the uncertainty in the output objective function of the model then the values of sensitive parameters can be further optimized [166]. Therefore, sensitivity analysis is an important tool to reveal the factors most impact the output function [167]. This assists to evaluate the accuracy and quantify the uncertainty in the estimated model empirical parameters [168]. Two main types of sensitivity analysis can be carried out in studying any model. Local sensitivity analysis (LSA) and global sensitivity analysis (GSA) [169]. LSA is carrying out the sensitivity over one point in any selected parameter hyperspace while varying the selected parameter and held other parameters fixed [170]. Whereas GSA scans the entire defined range of all of the parameters of the study based on Monte Carlo simulation sampling techniques either systematic or random [163], [164]. Sobol', I. (1990) [171] determined that the sensitivity analysis assists the extent to which each input parameter impacts the uncertainty on the output functions. In addition, global sensitivity analysis reveals the leverage of the input factors stand-alone as well as their impact considering the interrelations between one another on the output function [158]. Sobol', I. (1967) [172] defined sensitivity analysis as the method of assigning variation of model outputs to different changes in input parameters. Generally, sensitivity analysis shows what happens to the output results if the main input are changed [176]. In this chapter, both LSA and GSA are computed on MFC model proposed by Pinto, R.P. et al. (2012) [1].

3.1.Local sensitivity analysis

Local sensitivity analysis is computed to study the impact of each of the decision parameters on the output function of power density once it is optimized. Therefore, for most of the studied decision parameters and other important parameters in this

optimization problem, a set of solutions were obtained and optimized for power and current density functions over a certain range of each for each of decision parameters. LSA is carried out by varying some of the selected parameters, while the others were held fixed. This is carried out over the described mathematical model of MFC using Microsoft Excel.

3.1.1. Results and discussion

1. Feed substrate concentration

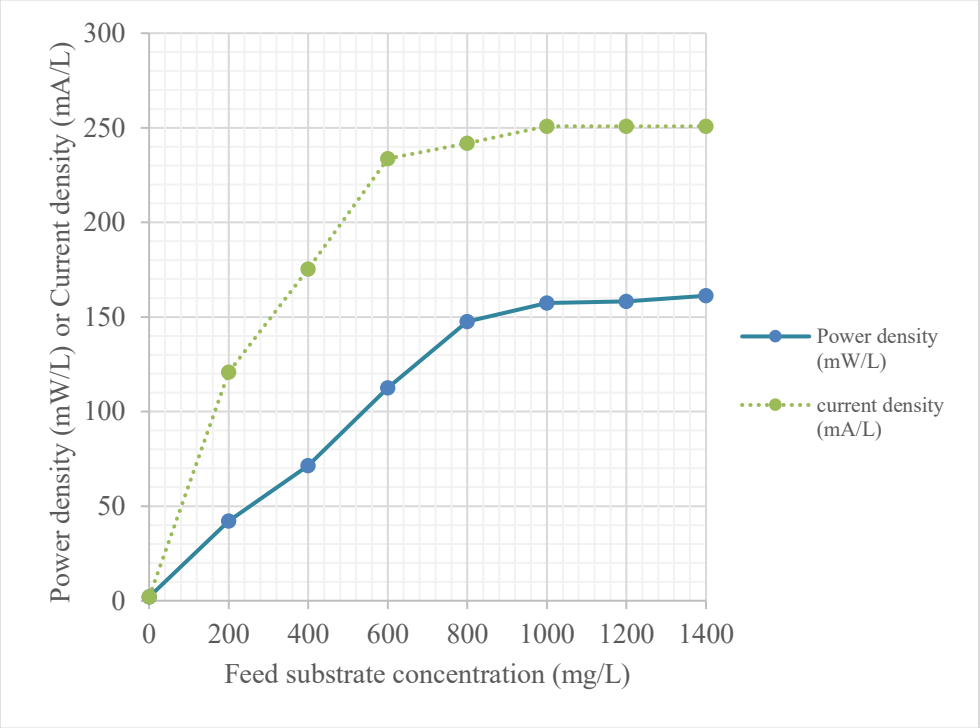

Figure 0-2. Impact of feed acetate concentration on the maximum produced power density (mW/L) and the corresponding current density (mA/L)

A set of solutions are provided for maximizing the power density function for some values of feed substrate concentration fed to the anode chamber. Figure 3-2 shows the impact of feed substrate concentration on the optimum value of produced power density and the corresponding value of the current density. From Figure 3-2, it can be noticed that the higher the feed substrate concentration in the feed the anode stream, the higher

the optimum produced power density in MFC predicted by the current used model and the higher the corresponding produced current density. This can be described by the Bulter-Volmer kinetic expression (Monod equation) represented by the reaction rate occurs in the anode chamber. The rate of the reaction depends on the substrate concentration, therefore, increasing the concentration results in a higher substrate oxidation producing a higher electron yield to be transferred to the cathode chamber available for the reduction. Therefore, a higher produced power and current density. From Figure 3-2, increasing the substrate concentration in the anode from 200 mg/L to 800 mg/L (four times), both the maximized power density was increased almost four folds and the corresponding current density was increased by 3.5 times. It is observed that at low feed substrate concentration (0-400) mg/L, the power density curve shows a linear correlation. A similar trend was observed in studies conducted by Abu-Reesh, I. (2020) [130] and Gil, G. et al. (2003) [174]. The former study showed that at low acetate concentration (0.5-2) mol/m^3, the optimized power density and its corresponding current density both show a linear behavior. Similarly, with the later study, COD concentration less than 50 mg/L show the same behavior. For higher concentrations, the relationship is non-linear described by modified Monod kinetics.

- **External resistance**

According to Jacobi's law [175], the optimal external resistance that maximizes the power density produced from a MFC should approach its internal resistance.

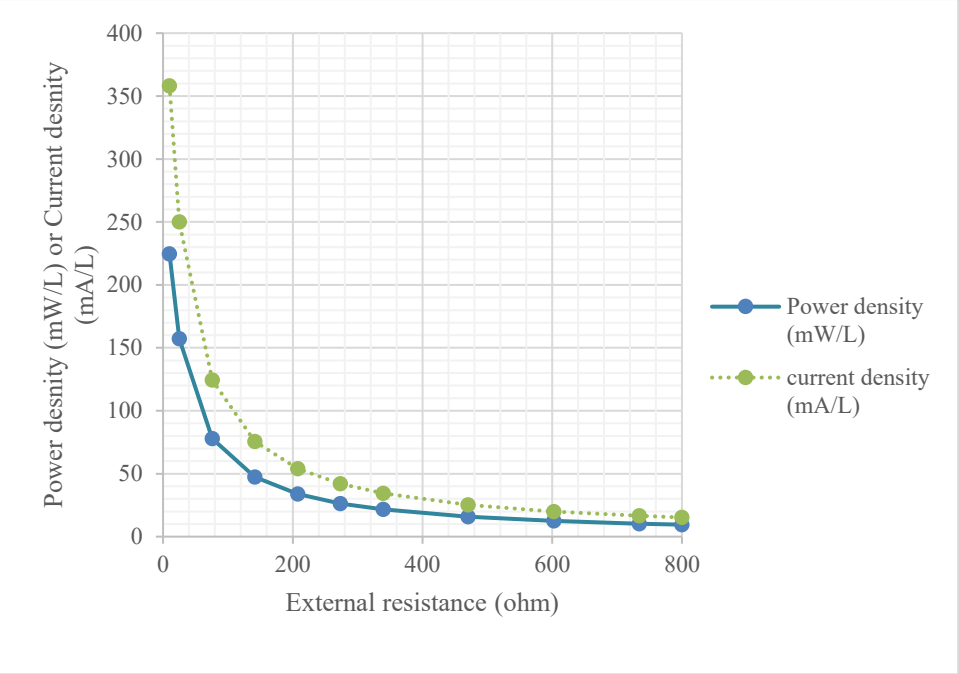

Figure 0-3. External resistance impact on the maximum produced power density (mW/L) and the corresponding current density (mA/L)

Operating MFC with a constant feed concentration of 1000 mg/L of acetate, the impact of external resistance was studied on the maximized power density and the corresponding optimized current density. MFC operated with different external resistance values across the MFC with a range (10-800) ohm. An important criterion for maximizing the power density in the current model is that the internal and the external resistances should be equal. As it is known, the external resistance is the opposing force for the flow of the current. It was observed that the lower the external resistance of MFC the higher the optimized power density and its corresponding current density. Therefore, power and current density are external resistance dependent. It can be noticed that optimized power density occurs at an external resistance of almost 25 Ω which is lower than that produced at 10 Ω. One of the reasons that the point does not lie at in the region of stable points which follow some criteria shown in chapter 2 in results and discussion part. As well as the condition of Jacob's law was not satisfied

which is the most critical condition. Increasing the external resistance resulted in increasing the voltage and decreasing the current, hence the current density. This can also be described by Ohm's law, and this is consistent with former studies. External resistance is one of the key factors that impact the performance of MFC and biofilm formation by impacting the rate of electrons transferred from the anode electrode impacting both the microbial metabolism and the biofilm [129], previously this impact was especially observed in the pure cultures, here it can be concluded that the external resistance has a significant impact on multiple cultures too. It can be confirmed from Figure 3-3 that both power and current density of MFC decrease in non-linear manner with increasing the external resistance. As stated earlier when analysing contour plots generated from mathematical modelling to predict the behaviour of power density VS external resistance, decreased external resistance is preferable to maximize the power generation in Pinto's (2012) model [1]. Some studies show a different manner for the relation of power density and external resistance such as Zhang et al. (2011) [131], while others agree with the results of this model. Gil, G. et al. (2003) [174] concluded that external resistance over than 500 ohm is determined as the rate limiting factor for proton transfer and power (current) production [174]. Different conclusions about the power density-external resistance relation are extracted from the proposed mathematical models which differs from one study to another and the interactions with the internal resistance which is not a system constant; and is dependent on the external resistance value. However, if the external resistance is very low initially, then the initial instantaneous current generated by the equilibrium potential will be higher than the sustainable rate of charge transfer to or from rate limiting electrode, however, this will not last too long, and the cell potential will be decreased to adjust to the rate limiting electrode (rate of charge transfer). Therefore, the sustainable generated power will be

less than the maximized power that can be generated. The opposite scenario happens if the initial external resistance is too high. For this reason, it is important to set the internal resistance value near or equal to the external resistance value for power maximization, which is called Jacobi's law [176]. It can be noticed that the external resistance shows the same behaviour regarding power density towards current density. Different studies were conducted studying the impact of external resistance on power density. Katuri et al. (2011) [131] showed interesting results that when the external resistance was increased from 0.1 kΩ to 1 kΩ, the power density increased to reach a maximum value of 10.1 mW/m^2, then further increase in external resistance (10-50) kΩ led to decrease in the generated power density, given that the internal resistance value of the system was 1 kΩ. While Lyon, D. et al. (2010) [177] conducted the same study operating under external resistance of 10 Ω -10 kΩ. The study revealed that the maximum power production was at an external resistance of 470 Ω given that the internal resistance was 300 Ω and the lowest power density was at external resistance of 10 Ω [177]. This reveals the power of Jacobi's law. External resistance while impacting the power production, it impacts the variable biocatalyst density, morphology and structure of biofilm too. At low external resistance, the anode potential will be high, therefore, more anodophilic bacteria are able to produce and transfer electrons to the electrode and gain more energy, this leads to denser and diverse anode biofilm. A study conducted by Ren, Z. et al. (2011) [178] observed the influence of external resistance on the structure of biofilm. They have obtained different biofilm densities and thickness under a range of external resistance from (10- 1000) Ω. Hence, observed comparable profiles of power density at different external resistance ranges. At low external resistance values, the electrcigenic bacteria were dominant in the biofilm due to high anode potential, and that was shown as in the system as rod-shaped

bacteria [178].

- **Dilution rate**

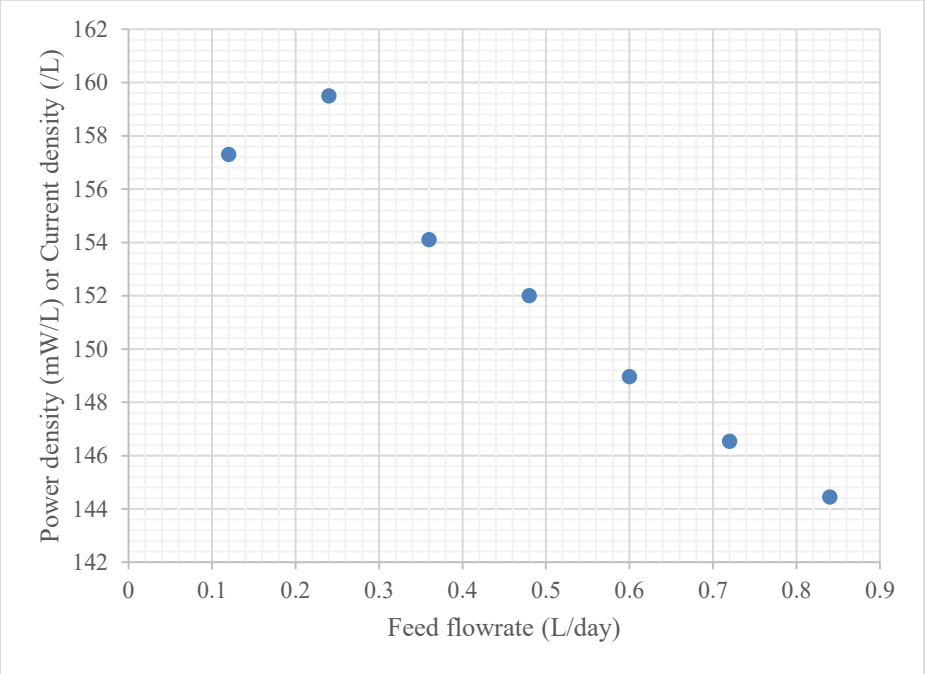

Figure 0-4. Feed Substrate flow rate impact on the maximum produced power density (mW/L)

While dilution rate (D) can be defined as the incoming flow rate of media to the anode over the volume of the anode. Increasing incoming flowrate will increase the dilution rate in the anode compartment. This impacts the maximum power density by impacting the rate of change of the substrate and anodophilic cell concentration. Increasing the flow rate of the feed will initially increase the maximized produced power density and the corresponding current density due to substrate limitation at flow rate. The maximized produced power density will decrease with increasing the flowrate and the dilution rate. As increasing the feed flowrate will decrease the hydraulic retention time allowing very limited time for bacterial growth and substrate removal producing limited number of electrons to be transferred and therefore low current and

power density. Decreasing the flowrate (increasing the hydraulic retention time), causes cell death due to the substrate limitation in the system. This ultimately affects the electrons production and transfer as well as the movement of hydrogen protons. As a result, the produced power and current densities decrease. This is shown in the Figure 3-4 in which the impact of the feed flowrate is shown on the optimum produced power density.

- **Fraction of oxidized mediator per total mediator concentration**

As stated earlier, increasing the external resistance will decrease the anode potential and its ability to transfer electrons to anode electrode. Table 3-1 shows the fraction of oxidized mediator concentration per anodophilic bacteria per total mediator concentration and the optimized power density and corresponding external resistance. As the previous sections illustrate, while decreasing the mediator concentration, the generated power decrease. In addition, the point corresponding the external resistance value of 10 Ω it does not satisfy Jacob's law for power production as stated earlier.

Table 0-1. Fraction of oxidized mediator per total mediator concentration (M_{ox}/M_T), the corresponding optimized power density (mW/L) and the resulted external resistance

Fraction of oxidized mediator per total mediator concentration	External resistance (Ω)	Power density (mW/L)
0.99	10	224.6
0.95	25	157.27
0.862	75	104.84
0.775	141.6	97.52
0.72	207.5	91.32
0.71	273.0	88.345
0.69	339.1	84.21
0.621	405	76.45
0.51	470.8	74.122
0.42	536.6	70.6
0.321	602.5	68.38
0.12	668.33	50.73
0.055	734.16	40.328
0.006	800	33.46

- **Bacterial community**

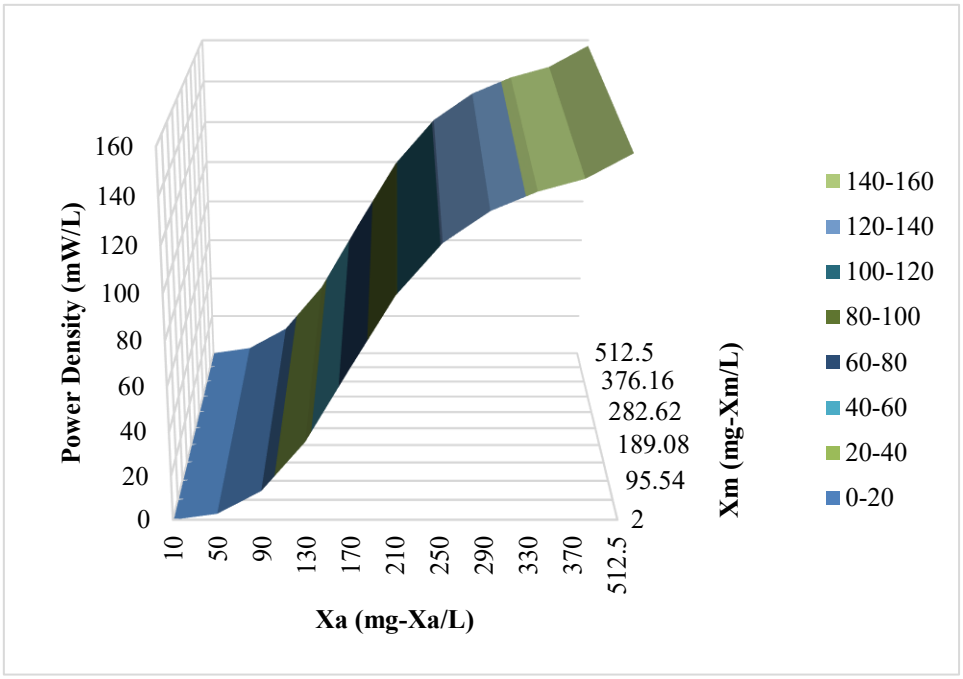

Figure 0-5. Anodophilic and methanogenic bacterial community impact on the maximum produced power density (mW/L)

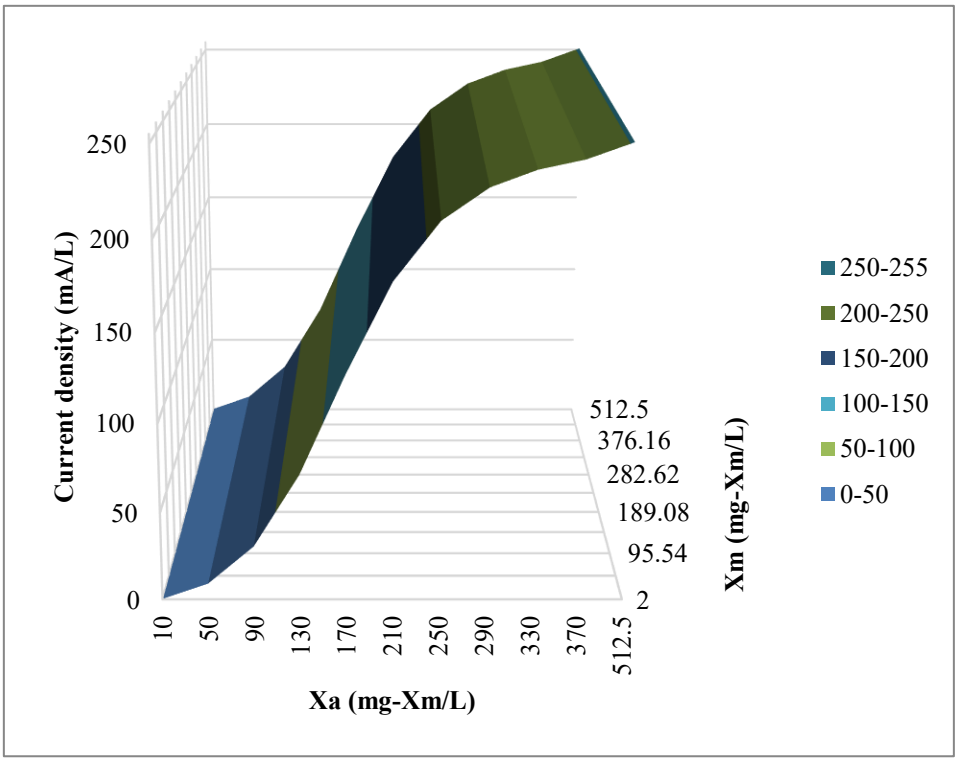

Figure 0-6. Anodophilic and methanogenic bacterial community impact on the maximum produced current density (mW/L)

Figures 3-5 and 3-6 show that both current and power density do have similar behaviour towards the concentration of the microorganisms. Add to that, both functions go in the same direction towards the maximum value of the function while changing X_a and X_m. Also, the graphs show that the optimum values for X_a and X_m while maximization both functions are the same. The maximum value of each of the functions takes place in the range of the minimum range value of X_m and towards almost the maximum limit of X_a. Also, it is revealed that the achieving maximum power density will guarantee maximum current density at high levels of X_a concentration. This is since anodophilics only produce electrons in the system, and high concentration of X_a ensure maximum current and power density.

3.2. Global sensitivity analysis

Global sensitivity analysis (GSA) scans the entire defined range of all of the parameters of the study based on Monte Carlo simulation sampling techniques either systematic or random [163], [164]. Sobol', I. (1990) [171] determined that the sensitivity analysis assists the extent to which each input parameter impacts the uncertainty on the output functions. In addition, GSA reveals the leverage of the input factors stand-alone as well as their impact considering the interrelations between one another on the output function [158]. As stated previously, MFCs have a strong non-linearity; Sobol-Saltelli method which is a variance-based method is used to evaluate the relative contribution of each of the parameters to the variance of the output function [171]. This method excluding the interrelations with other parameters in the first order indices and including all of the impacts and interrelation in the total order indices while taking into consideration the nonlinearity [179]. Yin, Y. et al. (2019) [180] expound the global sensitivity analysis based on variance method on a dual-chamber, single

population under steady state mode MFC. They studied the impact of eight parameters on the power density by conduct Sobol's indices. The results show that the cathodic charge transfer coefficient is the most crucial and impacting factor on the output, while the electrical conductivity of the aqueous solution is the least effective. By using the same methodology, a comprehensive global sensitivity analysis using variance-based method is carried out over Pinto, R.P. et al. (2012) [1] MFC model. In this section, first and total order sensitivity indices of six chosen parameters for optimization of a multi-population, single chamber with biofilm MFC operating at steady state mode were estimated. In addition, Monte Carlo simulations were used for predicting the behaviour of each of the parameters on the power density output [167].

3.2.1. Sensitivity indices using GSA

Global sensitivity analysis (GSA) is the variance-based analysis in which all the input factors are varied simultaneously over the whole range of interest allocating the uncertainty in the model output to the uncertainties of each of the input parameters. GSA is an important tool for decision making in complicated systems such as systems in environmental sciences in which many input factors have a strong interaction with one another [95], [181], [182]. Evaluating the individual impact of each parameter while the other inputs are constant produces non accurate results for the model output. In GSA, while evaluating the impacts of inputs on the model output, it can calculate both single impacts of individual factors called first-order indices and multiple impacts due to factors interactions with one another and it is called total-order indices. MFC is one of the convoluted systems in which many factors simultaneously affect the performance of the cell, which can cause multiple sources of uncertainty. To figure out the effect of these uncertain factors on the cell and on the population dynamics, GSA is performed. Therefore, GSA is becoming an essential tool for the assessment of

environmental systems [163], [169], [171], [182]–[185].

3.2.1.1. Sensitivity index estimation

In this study, the objective optimization function (output of the model) is the power density of MFC based on Pinto, R.P. et al. (2012) model [1]. Based on the proposed model, the variance of some constants defined in Table 1-10 on power density of MFC was studied. Global sensitivity analysis based on variance decomposition as a screening method which was suggested by Sobol is carried out. Variance based screening method (Sobol's) is better than the Morris method in terms of precise indices taking into consideration the interrelationships between the input parameters [186]. Screening is the process of sieving the factors and identifying the ones which are the least important in their impact on the output function and fix them within their feasible range [187]–[189]. In this part, the GSA is implemented based on variance-based screening and the sensitivity indices are approximated based on Sobol's method [171]. A critical point in such studies is the sample size selection. MFCs are complex systems, therefore, the sample size should not be too small so that the accuracy is lost or not too large and face difficulty to run the simulation. Based on the model input parameters (M), and the number of model evaluations (N) and the sample size (n), N is set as a function of M and n. Therefore, choosing the number of system's total evaluations can lead to the number of the sample size. Some methods use the direct relation between N and n and equate them (i.e. N=n) as it is used in this study [155], [164], [185], [190], [191].

- **Sobol's sequences**

Sobol indices is a method of estimation based on the variance calculations of the inputs of a mathematical model. Sobol' technique is basically an example of quasi-random low-discrepancy sequences [171]. These sequences are used for GSA extensively for their simplicity and accuracy. This was proposed first by the Russian

mathematician Ilya M. Sobol in 1967 [192]. The detailed GSA based on Sobol's method is as follows [155], [159]–[161], [164], [190], [193]:

$$Y_{output} = f(x_1, x_2, \dots) \tag{27}$$

Where: Y_{output} is the model output; f is the model function; x_1, x_2 are the chosen parameters to study their influence on the output function.

Based on the variance study, first-order and total-order coefficients are calculated as follows:

1- First-order indices:

$$S_i = \frac{Var_{x_i}\left(E_{x\sim i}(Y_{output}|x_i)\right)}{Var(Y_{output})} \tag{49}$$

2- Total indices can be described as:

$$S_{T\,i} = 1 - \frac{Var_{x_{\sim i}}\left(E_{xi}(Y_{output}|x\sim i)\right)}{Var(Y_{output})} \tag{50}$$

Where: (x_i) is a matrix of all parameters; ($x\sim_i$) is the matrix of all parameters but x_i; (Var_{x_i}) is the variance of argument (·) over x_i; (E_{xi}) is the mean of argument (·) over x_i;

($E_{x\sim i}$) is the mean of argument (·); ($Var_{x\sim_i}$) is the variance of argument (·).

Variance and mean value are calculated as follows:

$$Var_{x_i}\left(E_{x\sim i}\left(Y_{output}|x_i\right)\right) \approx \frac{1}{N}\sum_{j=1}^{N} f(B)_j \left(f\left(A_B^{(i)}\right)_j - f(A)_j\right) \tag{51}$$

$$E_{x\sim i}\left(Var_{x_i}\left(Y_{output}|x_{\sim i}\right)\right) \approx \frac{1}{2N}\sum_{j=1}^{N}\left(f(A)_j - f\left(A_B^{(i)}\right)_j\right)^2 \tag{52}$$

Where: (A and B) are matrices of size $N\times k$.

3.2.2. GSA Methodology

The methodology followed for the GSA in this study is as follows: the parameters to be studied were selected based on their expected impact on the power density (output function). After that the probability density function (PDF) of each

parameter was predicted for further Monte Carlo analysis. One key of getting good results is the choice of PDF type of each parameter. This represents a critical issue which needs an experience or knowledge in the field especially in MFC complicated models. Power density has a normal distribution with most of the factors with time [15], therefore, normal distribution is used for all of the parameters as a PDF. For global sensitivity analysis, Sobol's method was used to compute first and total order indices as the main method of the study. While double loop, Morris, Sobol and FAST methods were applied to compare different methods of calculating total indices. Finally, Monte Carlo simulations were run for each of the parameters to figure out the impact of each parameter on the power density. The methodology is shown in Figure 3-7.

3.2.3. Results and discussion

In this section the results of GSA which is applied on Pinto's MFC model are analysed and discussed. The impact of input parameters is evaluated under steady state conditions on power density of the cell. Most representative parameters have been chosen which may have an impact on the performance of MFC represented by the power density. Parameters are shown in Table 3-2 below. The studied parameters are: decay rate of anodophilics ($k_{d,a}$), half rate constant of anodophilic microorganism ($K_{s,a}$), curve steepness factor (K_r), mediator half rate constant (k_M), anodophilic specific growth rate ($\mu_{max,a}$) and number of electrons transferred per mole of mediator (m). The selection of parameters was based on the fact that anodophilics are the only organisms which contribute in electron production and transfer, thus impact the output power density production. The transfer of the electron is via two methods, the direct transfer and the indirect through the mediator, in turn the half rate of mediators constant is considered. Also, the number of the electrons transferred per mole of mediator as there are different mediators which can carry different amount of electrons. The initial

value used in the simulation initiation is the mean value of each of the parameters which is the proposed value in the model as it appears in Table 1-10, and the defined boundaries of both minimum and maximum values in Matlab are shown in Table 3-2 below.

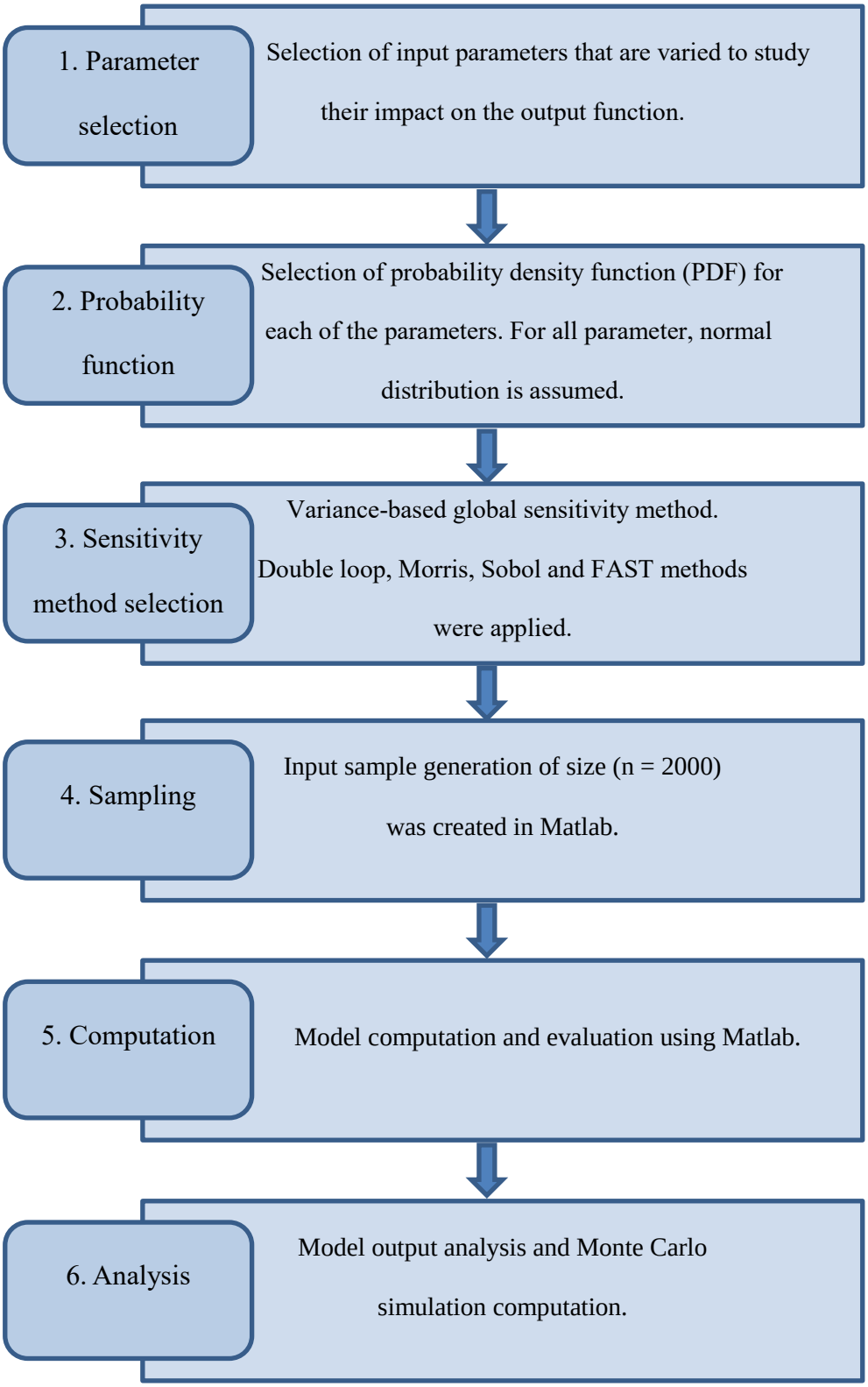

Figure 0-7. GSA methodology

Table 0-2. Selected parameters and their corresponding ranges for sensitivity analysis study

Parameter name	Symbol	Unit	Lower limit	Mean value	Upper limit
Decay rate of anodophilics	$k_{d,a}$	1/d	0.012	0.040	0.067
Half rate constant of anodophilic	$K_{s,a}$	mgS/L	6	20	34
Curve steepness factor	K_r	L/mgX_a	0.0018	0.006	0.0102
Mediator half rate constant	k_m	mgM/L	0.003	0.01	0.017
Maximum specific anodophilic growth rate	$\mu_{max,a}$	1/d	0.59	1.97	5.5
Number of electrons transferred per mole of mediator	m	$mole^-$ /molM	0	2	4

First-order and total-order sensitivity indices based on the variance (Sobol's) method are calculated for all parameters in response to their impacts on the power density output using Matlab. This is shown in Figure 3-8 below using a bar graph representation in which, blue colour represents the first-order indices while red colour represents the total-order indices. Also, Table 3-3 shows the values of the indices and the difference between them, as it is expected the total indices are greater than the first order. The indices reflect the degree of impact of the selected input parameters on the output function which is the power density of MFC. First-order indices reflect the level of impact of each parameter standalone on the output function. While the total-indices take into consideration the cross-interaction of all the variables with one another and

their effect on the output function (power density of MFC). The closer the value of the sensitivity coefficient (index) of the parameter to 1, the more sensitive it is to the output function.

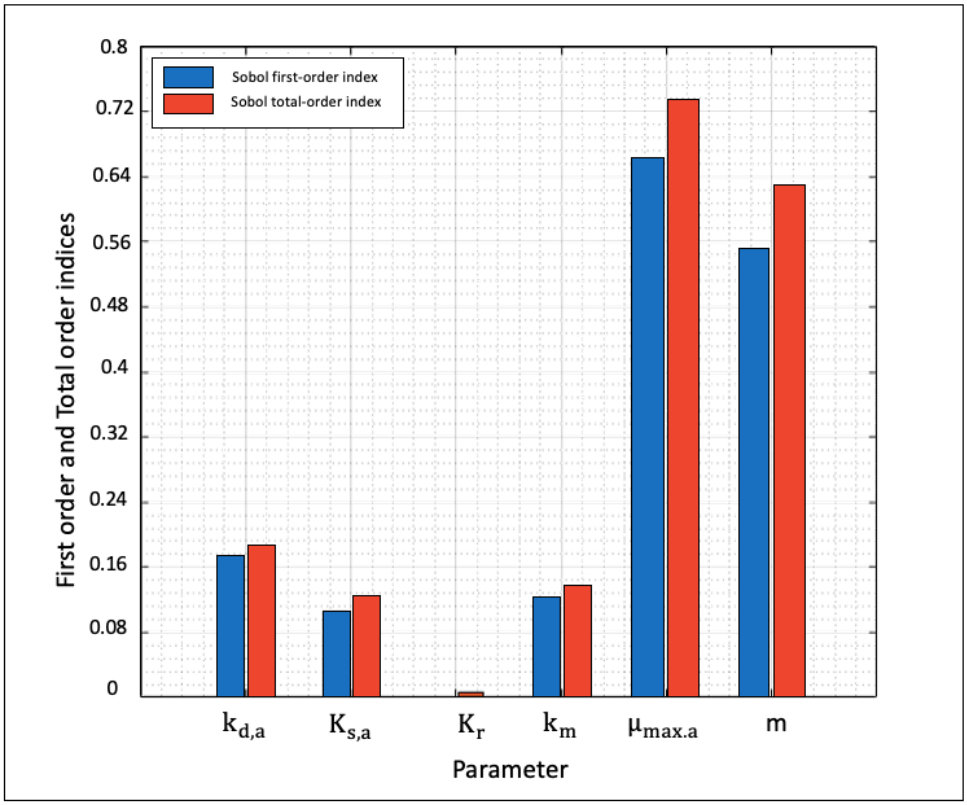

Figure 0-8. First and total order indices

The results of Figure 3-8 are shown in Table 3-3 as stated previously with showing the difference between the first and total-order indices. From Figure 3-8, the sequence of sensitivity of parameters based on their impact on power density can be determined as follows: The specific growth rate of anodophilic bacteria ($\mu_{max,a}$), number of electrons transferred per mole of mediator (m), decay rate of anodophilic bacteria ($k_{d,a}$), half rate constant of anodophilic bacteria ($K_{s,a}$), mediator half rate constant (k_m) and curve steepness factor (K_r). The difference between the first-order and total-order indices indicated that the factor has a larger impact on the power density

when interacts with other parameters. Among the parameters, $\mu_{max,a}$ has the greatest impact on the power density. This means that a small change in the value of this parameter will result in a large change in power density compared to other factors. While K_r has very weak impact on the power density as a stand-alone factor with a negligible impact on the power density when interacting with other parameters.

Table 0-3.First and total order indices

Parameter name	Symbol	Unit	First-order indices	Total-order indices	Difference
Decay rate of anodophilics	$k_{d,a}$	1/d	0.176	0.192	0.016
Half rate constant of anodophilic	$K_{s,a}$	mgS/L	0.112	0.127	0.015
Curve steepness factor	K_r	L/mgX_a	3.22×10^{-4}	1.76×10^{-3}	1.44×10^{-3}
Mediator half rate constant	k_m	mg M/L	0.128	0.144	0.016
Maximum specific anodophilic growth rate	$\mu_{max,a}$	1/d	0.664	0.736	0.072
Number of electrons transferred per mole of mediator	m	$mole^-$ /mol M	0.544	0.624	0.08

Decay rate constant of anodophilic bacteria ($k_{d,a}$), half rate constant of anodophilic bacteria ($K_{s,a}$) and mediator half rate constant (k_m) have near but fluctuating impacts on the power density. However, the difference between the first and total-order impacts for all the three factors is almost the same. Therefore, they have some variety in their impact; the lumped impact is almost the same on the power density function. Based on the studies conducted by Batstone, D.J. et al. (2000) [194] and Marcus, A. et al. (2007) [195] the value of decay rate of the biomass is 2% of the

maximum specific growth rate of the biomass. Therefore, the impact of this factor will be less than that of the maximum specific growth rate of the biomass. The net rate of biomass production consists of biomass production and decay. Increased decay rate of anodophilic bacteria means more bacteria which is responsible of producing electrons is lost. Thus, a lower power density could be produced. Half rate constant of anodophilic bacteria ($K_{s,a}$) represents the concentration of the substrate at which the growth rate equals half of the maximum growth rate in Monod kinetics. Therefore, $K_{s,a}$ is linked with the growth rate of anodophilic bacteria. Increasing $K_{s,a}$ decreases the growth rate of anodophilic bacteria, hence, decreased the power produced. Therefore, it is expected that both $K_{s,a}$ and $k_{d,a}$ have a decreasing relationship with power density production which is represented using Monte Carlo simulation in the next section. Mediator half rate constant (k_m) is the Monod constant when the oxidized mediator fraction per anodophilic bacteria is a limiting factor for the growth rate of anodophilic bacteria in addition to substrate concentration, and it is expected to have very similar manner as $K_{s,a}$, which is also represented by Monte Carlo scatterplots. Number of electrons transferred per mole of mediator (m) appeared to be one of the most impacting factors on the power density. There are many types of artificial mediators which differ in the number of electrons they can carry. Neutral Red (NR) is an artificial mediator that carries two electrons which is shown in Equation 53, while potassium ferricyanide ($Fe(CN_6)^{3-}$) carries one electron, the redox reaction is represented in Equation 54. Therefore, other mediators can be artificially produced to enhance the power productivity of MFC by carrying more electrons. It is worth mentioning that more than one type of mediator can be used in a MFC [196], if considering them as a group, then the number of electron transferred per one mole of the group would be increased, and this enhances the power production.

$$NR(oxidized) + H^+ + 2e^- => NR\ (reduced) \quad (53)$$

$$Fe(CN_6)^{3-} + e^- => Fe(CN_6)^{4-} \quad (54)$$

While curve steepness factor (K_r), has almost very negligible impact on the power produced from MFC and the research field of MFC can be placed elsewhere than studying the impact of this factor or the improvements its value. This is also shown in scatterplot of power density versus the curve steepness factor in Monte Carlo simulation. Finally, the maximum specific growth rate of anodophilics microorganism ($\mu_{max,a}$), this has empirical values that depend on the bacterial species used as well as the environmental conditions [197]. Also, $\mu_{max,a}$ is a result of the true yield of cell production and the maximum anodophilic reaction rate (maximum specific rate of substrate utilization). Therefore, to increase $\mu_{max,a}$, the yield can be increased by increasing the mass of the cell produced per mass of substrate consumed. Any small increase in the $\mu_{max,a}$ value will increase the value of power density as it is considered a sensitive factor for power density [198]. When the value of $\mu_{max,a}$ increases, the maximum growth rate of anodophilic bacteria increases, then, more bacteria are available to produce electrons if enough substrate is available. Therefore, an increasing relationship of $\mu_{max,a}$ with power density in Monte Carlo simulation is expected. In fact, both $K_{s,a}$ and $\mu_{max,a}$ are Monod kinetics parameters which are estimated using experimental methods. Therefore, a large uncertainty in expected to be associated with their values which are originated from the reaction conditions, number of samples and the measurement errors.

For total-order indices, several techniques for sampling are considered to tackle the most accurate results compared to Sobol's method which is shown in Figure 3-9. Sampling techniques which are used in this section are: Sobol, double-loop, Fourier

Amplitude Sensitivity Testing (FAST) and Morris. Sobol's sampling technique depends on the direct integral calculations. Which is then developed further to reveal Saltelli's approach by new formula which improved the computational accuracy and called Saltelli-Sobol. While the double loop approach is a simple approach and considered as an alternative for the direct techniques after the improvements in the algorithms suggested by Plischke. FAST is a variance-based GSA method which is based on the conditional variances. FAST is considered as one of the most efficient techniques to calculate sensitivities via Monte Carlo integration. However, FAST is limited to the calculations of total effects only [156]–[163], [165], [166], [171], [172], [179], [199]–[209]. Finally, Morris method can be used to calculate the first-order or total-order indices, however, it is an extension for LSA in the whole parameter range. Therefore, it does not rank the importance of impact of parameters on the model output in GSA and considered as a screening method only [210]. Figure 3-9 shows the different methods in calculating the total-indices. It can be noticed that almost all the three methods of double loop, Sobol and FAST are giving similar results. While Morris underestimates the total indices. Also, it is an indication that the results of GSA based on Sobol method on this model are correct as the other methods producing similar results.

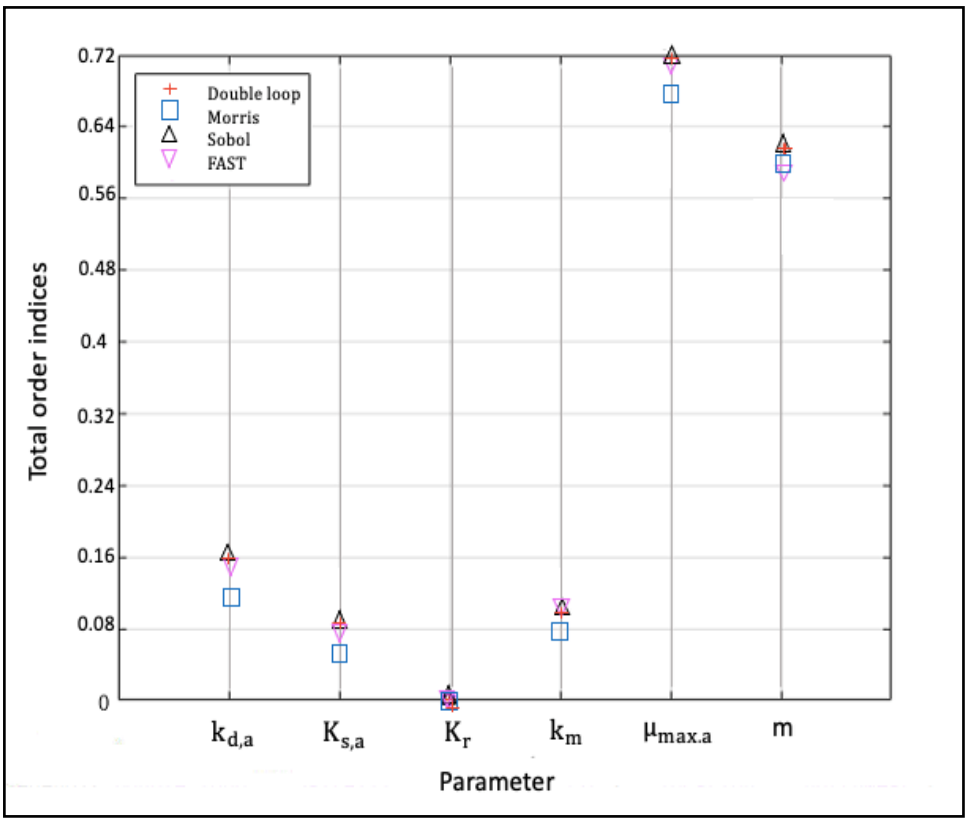

Figure 0-9.Total effects index using different data sampling methods

3.2.4. Monte Carlo simulation

In this section, Monte Carlo experiments are performed on MFC model. Monte Carlo is a method of sampling based on the repeated random values of the factors in the study from the distribution that they follow; so that the statistical behaviour of the output function is obtained. In addition, the factors assumed to be independent from one another so that the samples (input values) are extracted from the distribution they follow. In this study, normal distribution is assumed for all of the parameters under the study [162]–[166], [171], [172], [211]. If Y is assumed the output function (power density), then the input matrix for Y is as follows:

$$\mathrm{M} = \begin{bmatrix} z_1^{(1)} & z_2^{(1)} & \dots \\ \vdots & \vdots & z_r^{(2)} \\ z_1^{(N)} & \dots & z_r^{(N)} \end{bmatrix} \tag{55}$$

Then, calculating Y for each row using the model, then the output matrix is:

$$\mathrm{Y} = \begin{bmatrix} \mathrm{y}^1 \\ \mathrm{y}^{\mathrm{N}-1} \\ \mathrm{y}^{\mathrm{N}} \end{bmatrix} \tag{56}$$

With this Y matrix and the model inputs, a scatterplot can be produced for each of the model parameters and the output by projecting the N values of the selected output Y vs the N values for each of the input parameters. For MFC model, each of the parameter produce a scatterplot with the model output of power density. These scatterplots are crucial to investigate the behaviour of parameters on the output [210]. The scatterplots of the MFC power density versus the three factors of decay rate of anodophilic bacteria ($\mathrm{k_{d,a}}$), half rate constant of anodophilic bacteria ($\mathrm{K_{s,a}}$) and mediator half rate constant ($\mathrm{k_m}$) are represented in Figure 3-10.

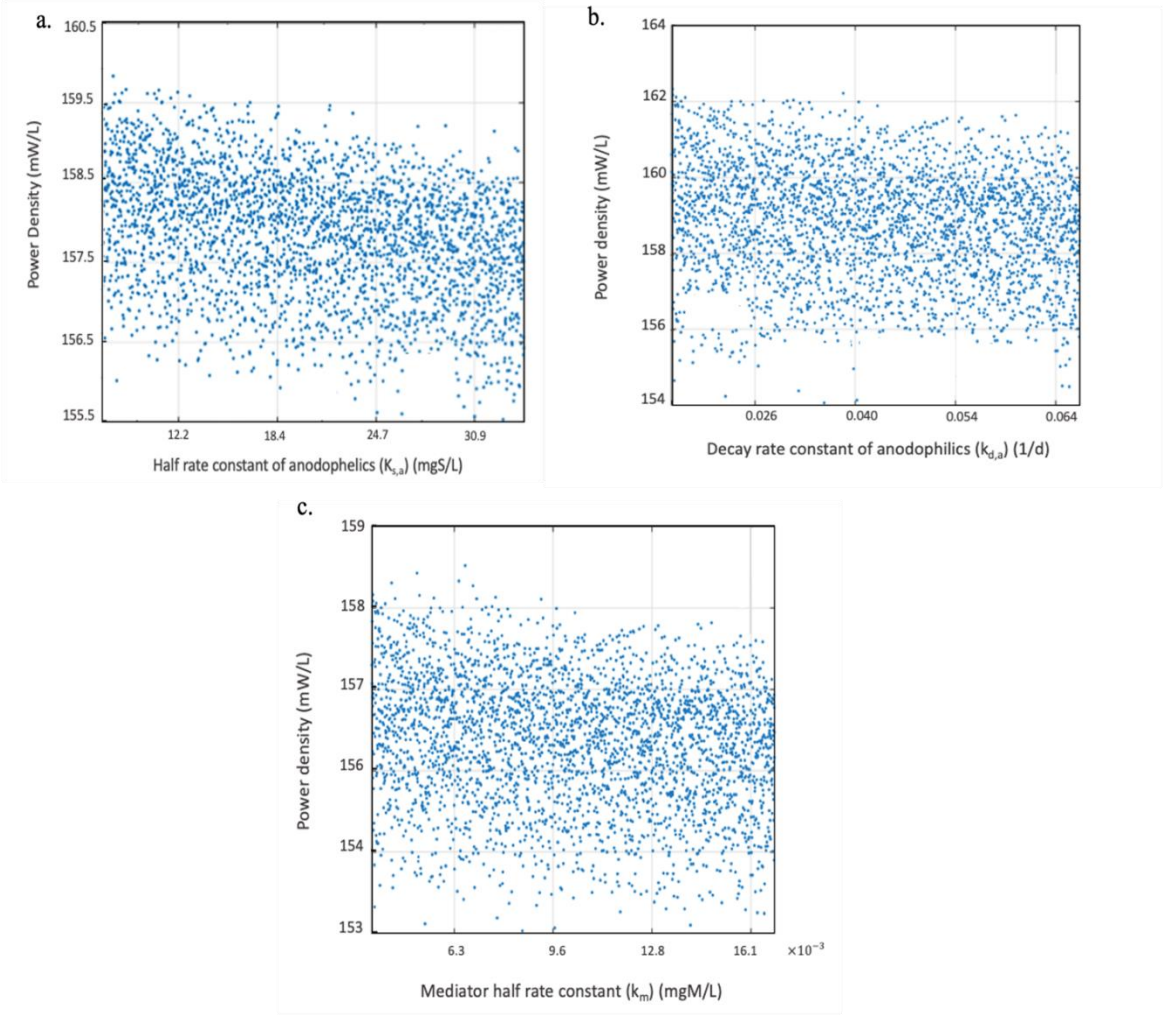

Figure 0-10. Scatterplots of MFC power density vs: a. Half rate constant of anodophilics ($K_{s,a}$). b. Decay rate constant of anodophilics ($k_{d,a}$). c. Mediator half rate constant (k_m)

Figure 3-10 show k_m, $K_{s,a}$ and $k_{d,a}$ relationship with power density using Monte Carlo representation. All the three factors show a discernible linear decreasing relationship with MFC power density. Increasing the decay rate of anodophilic microorganisms means increase in the loss of the active biomass, therefore, decrease in the number of biomass which can produce electrons. While half rate constant of anodophilics ($K_{s,a}$) represents the half saturation concentration in Monod equation

which describes the bacterial growth linked to the substrate consumption. $K_{s,a}$ is the concentration of substrate at which the specific growth rate of the microorganism (μ) becomes half of the maximum specific growth rate (μ_{max}). In addition, k_m represents the half rate constant for the Monod equation representing the oxidized mediators' impacts being a limiting factor for the growth rate of anodophilic bacteria as stated before. Therefore, its relationship with the power density is expected to be similar to $K_{s,a}$. While, for the curve steepness factor (K_r), the power density is found to be insensitive to this factor as shown in Figure 3-11. It can be noticed that the behaviour of this output function is almost constant at different values of the input and the scatterplot become as a horizontal line towards all the values of this input.

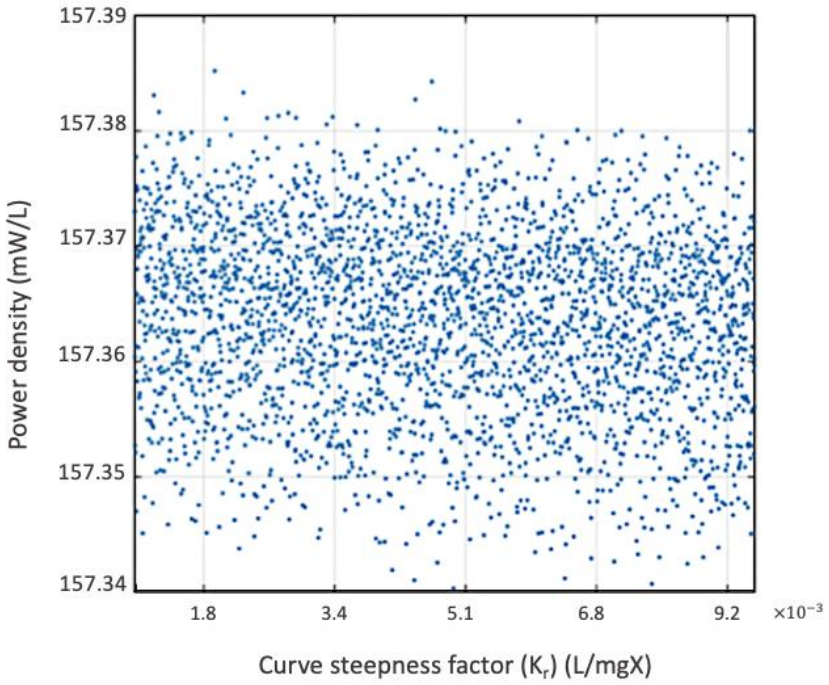

Figure 0-11. Scatterplot of power density vs curve steepness factor (K_r)

K_r is a constant which determines the curve steepness factor in the equation of

resistance which is identified experimentally in Pinto, R.P. et al. (2012) [1] by using the voltage measurements in MFC-1 operation. GSA revealed that power density is insensitive to this factor even though this factor is determined by the voltage values. The change in power density function due to the change in K_r is negligible as shown in Figure 3-11 which is only 0.04 mW/L for the whole range of the factor.

For maximum specific growth rate ($\mu_{max,a}$), a discernible strong nonlinear increasing pattern is shown for the power density. As stated previously, $\mu_{max,a}$ is an important Monod parameter for bacterial growth. As $\mu_{max,a}$ increased the growth rate of anodophilic bacteria which produce power increase through Monod equation which is shown below.

$$\mu_a = \mu_{max,a}\left(\frac{S}{S+K_{s,a}}\right)\left(\frac{M_{ox}}{k_m+M_{ox}}\right) \quad (57)$$

The relationship between μ_a, $\mu_{max,a}$ and the substrate (S), is non-linear increasing. Increasing $\mu_{max,a}$ increases the amount of the substrate concentration required to reach the maximum growth rate. Increasing the maximum growth rate and substrate in the system increases the power produced as the nutrient is available for anodophilics to oxidize and produce electrons. The relationship of the power density and $\mu_{max,a}$ is shown in Figure 3-12.

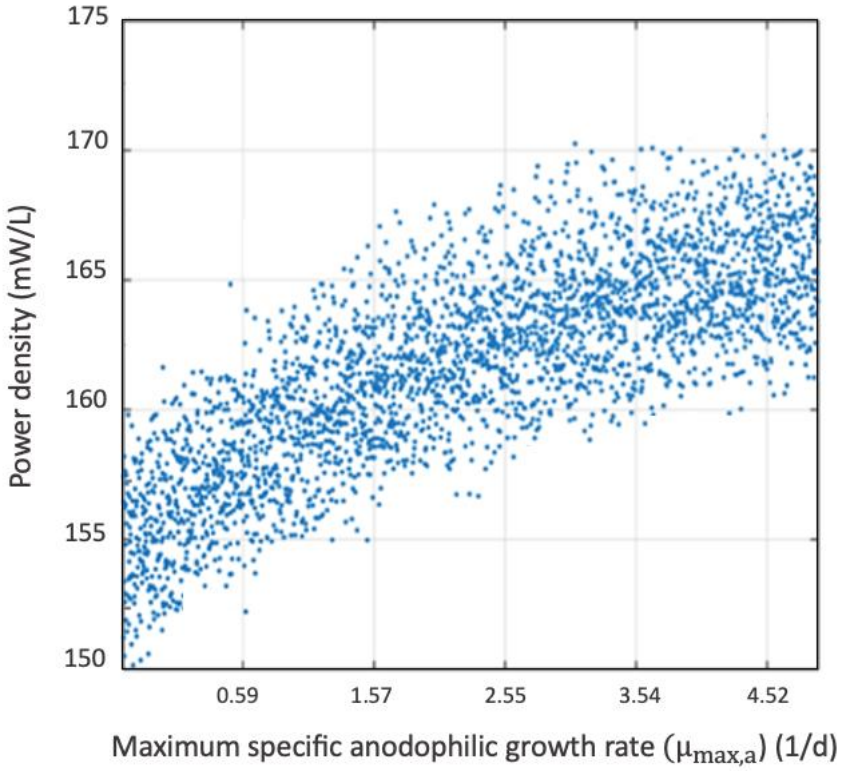

Figure 0-12. Scatterplot of power density vs maximum anodophilic specific growth rate ($\mu_{max,a}$)

For the last parameter which is the number of electrons to be transferred by the mediator, the power density has shown a discernible non-linear increasing relationship in the scatterplot that is shown below in Figure 3-13.

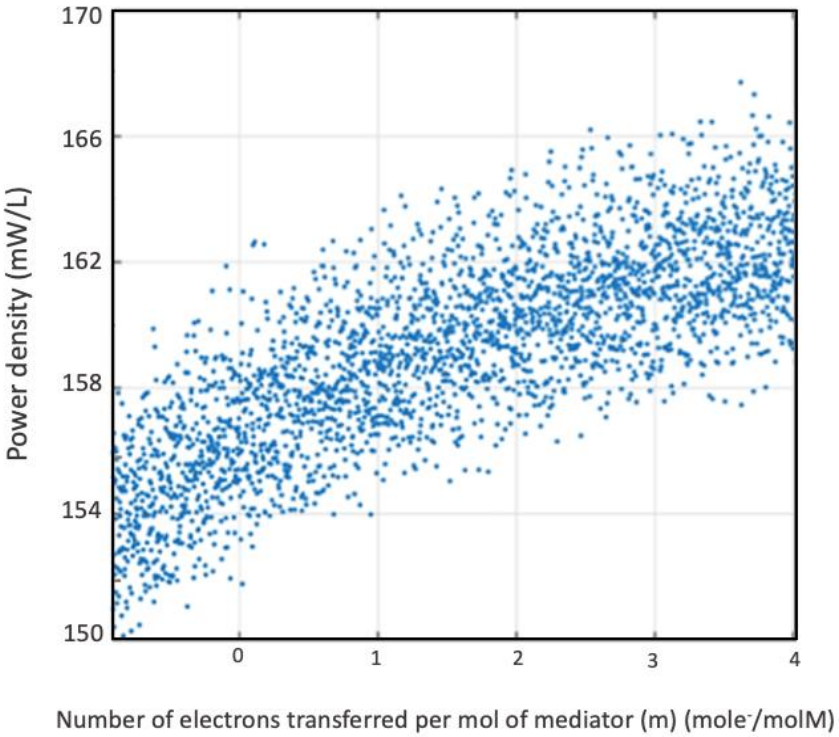

Figure 0-13. Scatterplot of power density vs number of electrons transferred per mole of mediator

The power density can be increased if the number of the electrons can be transferred per a mediator increase. This mainly depends on the type of the mediator used and partially the substrate. Artificial mediators vary in the number of electrons that they can carry. Therefore, increased the number of electrons transferred per mole of mediator enhances the amount of produced power. Figure 3-13 shows a discernible non-linear increasing relationship of power density and the number of electrons transferred per mole of mediator.

3.2.5. Conclusions

In conclusion, local and global sensitivity analysis are critical tool in revealing the impact of different parameters on output functions. Variance-based global sensitivity analysis using Sobol's method was applied on multi-population, single

chamber MFC in a continuous flow mode at steady state. The conducted study revealed the extent and pattern of influence of some selected parameters on the produced power density. The studied parameters were maximum specific anodophilic growth rate, half rate constant of anodophilics, curve steepness factor, mediator half rate constant, number of electrons transferred per mole of mediator and decay rate constant of anodophilic. GSA results showed that the maximum specific growth rate and number of electrons transferred per mole of mediator were the most impacting factors on power density and both have a discernible non-linear increasing relationship with power density using Monte Carlo simulation. Decay rate constant and half rate constant of anodophilics and mediator half rate constant had almost the same impact on the output function, and all showed a decreasing linear relationship with power density upon using Monte Carlo simulation. Finally, curve steepness factor had almost no impact on the results of power density. Monte Carlo simulation results agreed with the GSA in terms of revealing which factor can affect the power density of MFC using scatterplots. It can be concluded that global sensitivity analysis is very powerful tool and can be successfully applied for parameter analysis and optimization. This study can be utilized further to conduct uncertainty analysis and optimize the uncertain parameters.

4.0. Conclusions

In conclusion, MFCs are one of the renewable energy sources and sustainable wastewater treatment processes. Numerous factors impact the power generation performance of the cell. The optimization study showed that the studied model of single-chamber microbial fuel cell with multi-population operating in continuous flow mode at steady-state was optimized at a single point. The maximum PD was 157.40 mW/L by both Matlab and Microsoft Excel which corresponded to a CD of 251 mA/L, 25.1 Ω external resistance, 510.5 mg/L anodophilic cell concentration and 2.0 1/d dilution rate. The optimum point region was expected using RSM using Minitab prior the optimization by visualizing the model in contour plots. Local and global sensitivity analysis showed the most critical impacting factors on the performance of MFC. Local sensitivity analysis showed that the performance of MFC depends mainly on the external resistance and anodophilic cell concentration. Variance-based global sensitivity analysis coupled with Monte Carlo simulations revealed the impact of maximum specific anodophilic growth rate, half rate constant of anodophilics, curve steepness factor, mediator half rate constant, number of electrons transferred per mole of mediator and decay rate constant of anodophilic. GSA results showed that maximum specific growth rate and the number of electrons transferred per mole of mediator were the most impacting factors on power density by computing first order and total order indices. Monte Carlo simulation results agreed with the GSA in terms of revealing which factor can affect the power density of MFC using scatterplots. Finally, this study is critical and adds knowledge in couple areas in MFC vital field such as RSM, single objective optimization following computational methods and sensitivity analysis.

5.0. Reference

[1] R. P. Pinto, B. Tartakovsky, and B. Srinivasan, "Optimizing energy productivity of microbial electrochemical cells," *J. Process Control*, vol. 22, no. 6, pp. 1079–1086, 2012, doi: 10.1016/j.jprocont.2012.04.005.

[2] M. Alexander, "Biological Degradation and Bioremediation of Toxic Chemicals," *J. Environ. Qual.*, vol. 25, no. 1, pp. 204–205, 1996, doi: 10.2134/jeq1996.00472425002500010030x.

[3] C. Santoro, C. Arbizzani, B. Erable, and I. Ieropoulos, "Microbial fuel cells: From fundamentals to applications. A review," *J. Power Sources*, vol. 356, pp. 225–244, 2017, doi: 10.1016/j.jpowsour.2017.03.109.

[4] K. Rabaey, "Bioelectrochemical Systems: From Extracellular Electron Transfer to Biotechnological Application," *Water Intell. Online*, vol. 8, Dec. 2009, doi: 10.2166/9781780401621.

[5] A. Rinaldi, B. Mecheri, V. Garavaglia, S. Licoccia, P. Di Nardo, and E. Traversa, "Engineering materials and biology to boost performance of microbial fuel cells: A critical review," *Energy and Environmental Science*, vol. 1, no. 4. The Royal Society of Chemistry, pp. 417–429, Sep. 16, 2008, doi: 10.1039/b806498a.

[6] P. Aelterman, M. Versichele, M. Marzorati, N. Boon, and W. Verstraete, "Loading rate and external resistance control the electricity generation of microbial fuel cells with different three-dimensional anodes," *Bioresour. Technol.*, vol. 99, no. 18, pp. 8895–8902, Dec. 2008, doi: 10.1016/j.biortech.2008.04.061.

[7] A. R. Howgrave-Graham, A. J. L. Macario, and F. M. Wallis, "Quantitative analysis and mapping of micro-organisms in anaerobic digester granules using a combination of transmission electron microscopy with immunotechnology,"

1997.

[8] P. S, S. M, C. M, C. M, D. B. M, and C. J, “Microbial fuel cell application in landfill leachate treatment,” *J. Hazard. Mater.*, vol. 185, no. 2–3, pp. 763–767, Jan. 2011, doi: 10.1016/J.JHAZMAT.2010.09.086.

[9] P. S, S. M, C. M, B. MD, and C. J, “Simultaneous domestic wastewater treatment and renewable energy production using microbial fuel cells (MFCs),” *Water Sci. Technol.*, vol. 64, no. 4, pp. 904–909, 2011, doi: 10.2166/WST.2011.401.

[10] T. BAUCHOP and S. R. ELSDEN, “The growth of micro-organisms in relation to their energy supply.,” *J. Gen. Microbiol.*, vol. 23, pp. 457–469, 1960, doi: 10.1099/00221287-23-3-457.

[11] F. E. Mosey, “Mathematical modelling of the anaerobic digestion process: Regulatory mechanisms for the formation of short-chain volatile acids from glucose,” in *Water Science and Technology*, 1983, vol. 15, no. 8–9, pp. 209–232, doi: 10.2166/wst.1983.0168.

[12] D. J. Batstone, J. Keller, R. B. Newell, and M. Newland, “Modelling anaerobic degradation of complex wastewater. I: Model development,” *Bioresour. Technol.*, vol. 75, no. 1, pp. 67–74, Oct. 2000, doi: 10.1016/S0960-8524(00)00018-3.

[13] V. B. Oliveira, M. Simões, L. F. Melo, and A. M. F. R. Pinto, “A 1D mathematical model for a microbial fuel cell,” *Energy*, vol. 61, pp. 463–471, Nov. 2013, doi: 10.1016/J.ENERGY.2013.08.055.

[14] H. H. P. Fang, C. Ho-Kwong, and L. Yu-You, “Effect of degradation kinetics on the microstructure of anaerobic biogranules,” *Water Sci. Technol.*, vol. 32, no. 8, pp. 165–172, Oct. 1995, doi: 10.2166/wst.1995.0289.

[15] R. P. Pinto, B. Srinivasan, M. F. Manuel, and B. Tartakovsky, “A two-population

bio-electrochemical model of a microbial fuel cell," *Bioresour. Technol.*, vol. 101, no. 14, pp. 5256–5265, 2010, doi: 10.1016/j.biortech.2010.01.122.

[16] C. W. Lin, C. H. Wu, Y. H. Chiu, and S. L. Tsai, "Effects of different mediators on electricity generation and microbial structure of a toluene powered microbial fuel cell," *Fuel*, vol. 125, pp. 30–35, 2014, doi: 10.1016/j.fuel.2014.02.018.

[17] D. R. Bond, D. E. Holmes, L. M. Tender, and D. R. Lovley, "Electrode-reducing microorganisms that harvest energy from marine sediments," *Science (80-.).*, vol. 295, no. 5554, pp. 483–485, Jan. 2002, doi: 10.1126/science.1066771.

[18] H. Awad, M. Gar Alalm, and H. K. El-Etriby, "Environmental and cost life cycle assessment of different alternatives for improvement of wastewater treatment plants in developing countries," *Sci. Total Environ.*, vol. 660, pp. 57–68, Apr. 2019, doi: 10.1016/j.scitotenv.2018.12.386.

[19] D. R. Lovley, "The microbe electric: conversion of organic matter to electricity," *Current Opinion in Biotechnology*, vol. 19, no. 6. pp. 564–571, Dec. 2008, doi: 10.1016/j.copbio.2008.10.005.

[20] M. Behera and M. M. Ghangrekar, "Performance of microbial fuel cell in response to change in sludge loading rate at different anodic feed pH," *Bioresour. Technol.*, vol. 100, no. 21, pp. 5114–5121, Nov. 2009, doi: 10.1016/j.biortech.2009.05.020.

[21] I. M. Abu-Reesh, "Single-and multi-objective optimization of a dual-chamber microbial fuel cell operating in continuous-flow mode at steady state," *Processes*, vol. 8, no. 7, 2020, doi: 10.3390/pr8070839.

[22] D. Deb, R. Patel, and V. E. Balas, "A Review of Control-Oriented Bioelectrochemical Mathematical Models of Microbial Fuel Cells," *Process. 2020, Vol. 8, Page 583*, vol. 8, no. 5, p. 583, May 2020, doi:

10.3390/PR8050583.

[23] J. P. Sampson *et al.*, "A content analysis of career development theory, research, and practice - 2013," *Career Development Quarterly*, vol. 62, no. 4. Wiley Blackwell, pp. 290–326, Dec. 01, 2014, doi: 10.1002/j.2161-0045.2014.00085.x.

[24] C. G. Daughton, "Pharmaceuticals and the Environment (PiE): Evolution and impact of the published literature revealed by bibliometric analysis," *Science of the Total Environment*, vol. 562. Elsevier B.V., pp. 391–426, Aug. 15, 2016, doi: 10.1016/j.scitotenv.2016.03.109.

[25] "Scopus - Document search results," 2021. https://0-www2.scopus.com.mylibrary.qu.edu.qa/results/results.uri?sort=plf-f&src=s&nlo=&nlr=&nls=&sid=d8bbfb1bd9aae7353fac7351accc4c19&sot=b&sdt=cl&cluster=scosubtype%2C%22ar%22%2Ct%2C%22re%22%2Ct%2Bscolang%2C%22English%22%2Ct&sl=72&s=TITLE-ABS-KEY%28micr (accessed Oct. 11, 2021).

[26] "Wastewater treatment and renewable energy | Veolia." https://www.veolia.com/en/newsroom/thematic-reports/veolia-committed-climate/our-climate-solutions/wastewater-treatment-renewable-energy (accessed Sep. 26, 2021).

[27] M. S. Hamed, H. S. Majdi, and B. O. Hasan, "Effect of Electrode Material and Hydrodynamics on the Produced Current in Double Chamber Microbial Fuel Cells," *ACS Omega*, vol. 5, no. 18, pp. 10339–10348, May 2020, doi: 10.1021/acsomega.9b04451.

[28] E. Y. Konovalova *et al.*, "The microorganisms used for working in microbial fuel cells," in *AIP Conference Proceedings*, Apr. 2018, vol. 1952, no. 1, p. 020017, doi: 10.1063/1.5031979.

[29] B. E. Logan *et al.*, “Microbial fuel cells: Methodology and technology,” *Environmental Science and Technology*, vol. 40, no. 17. American Chemical Society, pp. 5181–5192, Sep. 01, 2006, doi: 10.1021/es0605016.

[30] E. J. Steen *et al.*, “Microbial production of fatty-acid-derived fuels and chemicals from plant biomass,” *Nature*, vol. 463, no. 7280, pp. 559–562, Jan. 2010, doi: 10.1038/nature08721.

[31] P. L. McCarty, J. Bae, and J. Kim, “Domestic wastewater treatment as a net energy producer-can this be achieved?,” *Environ. Sci. Technol.*, vol. 45, no. 17, pp. 7100–7106, Sep. 2011, doi: 10.1021/es2014264.

[32] D. Pant, G. Van Bogaert, L. Diels, and K. Vanbroekhoven, “A review of the substrates used in microbial fuel cells (MFCs) for sustainable energy production,” *Bioresource Technology*, vol. 101, no. 6. Elsevier, pp. 1533–1543, Mar. 01, 2010, doi: 10.1016/j.biortech.2009.10.017.

[33] C. Y. Chen, T. H. Tsai, P. S. Wu, S. E. Tsao, Y. S. Huang, and Y. C. Chung, “Selection of electrogenic bacteria for microbial fuel cell in removing Victoria blue R from wastewater,” *J. Environ. Sci. Heal. - Part A Toxic/Hazardous Subst. Environ. Eng.*, vol. 53, no. 2, pp. 108–115, Jan. 2018, doi: 10.1080/10934529.2017.1377580.

[34] Z. Naureen *et al.*, “Generation of Electricity by Electrogenic Bacteria in a Microbial Fuel Cell Powered by Waste Water,” *Adv. Biosci. Biotechnol.*, vol. 07, no. 07, pp. 329–335, 2016, doi: 10.4236/abb.2016.77031.

[35] L. Fan and S. Xue, “Overview on Electricigens for Microbial Fuel Cell,” *Open Biotechnol. J.*, vol. 10, no. 1, pp. 398–406, Dec. 2016, doi: 10.2174/1874070701610010398.

[36] H. Ren *et al.*, “A high power density miniaturized microbial fuel cell having

carbon nanotube anodes," *J. Power Sources*, vol. 273, pp. 823–830, Jan. 2015, doi: 10.1016/j.jpowsour.2014.09.165.

[37] M. Y. Xi and Y. P. Sun, "Preliminary study on E. coli microbial fuel cell and on-electrode taming of the biocatalyst," *Guocheng Gongcheng Xuebao/The Chinese J. Process Eng.*, vol. 8, no. 6, pp. 1179–1184, 2008.

[38] C. S. Kang, N. Eaktasang, D. Y. Kwon, and H. S. Kim, "Enhanced current production by Desulfovibrio desulfuricans biofilm in a mediator-less microbial fuel cell," *Bioresour. Technol.*, vol. 165, no. C, pp. 27–30, 2014, doi: 10.1016/j.biortech.2014.03.148.

[39] Q. YJ, Q. Y, Z. L, W. XS, and L. JH, "Biofilm promoted current generation of Pseudomonas aeruginosa microbial fuel cell via improving the interfacial redox reaction of phenazines," *Bioelectrochemistry*, vol. 117, pp. 34–39, Oct. 2017, doi: 10.1016/J.BIOELECHEM.2017.04.003.

[40] "Mechanism of energy generation of microbial fuel cells." https://www.researchgate.net/publication/286757963_Mechanism_of_energy_generation_of_microbial_fuel_cells (accessed Oct. 11, 2021).

[41] B. H. Kim *et al.*, "Enrichment of microbial community generating electricity using a fuel-cell-type electrochemical cell," *Appl. Microbiol. Biotechnol.*, vol. 63, no. 6, pp. 672–681, Feb. 2004, doi: 10.1007/s00253-003-1412-6.

[42] K. Rabaey, N. Boon, S. D. Siciliano, M. Verhaege, and W. Verstraete, "Biofuel cells select for microbial consortia that self-mediate electron transfer," *Appl. Environ. Microbiol.*, vol. 70, no. 9, pp. 5373–5382, Sep. 2004, doi: 10.1128/AEM.70.9.5373-5382.2004.

[43] J. Lee, N. T. Phung, I. S. Chang, B. H. Kim, and H. C. Sung, "Use of acetate for enrichment of electrochemically active microorganisms and their 16S rDNA

analyses," *FEMS Microbiol. Lett.*, vol. 223, no. 2, pp. 185–191, Jun. 2003, doi: 10.1016/S0378-1097(03)00356-2.

[44] "Bacteria - Bacterial metabolism | Britannica." Accessed: Oct. 03, 2021. [Online]. Available: https://www.britannica.com/science/bacteria/Bacterial-metabolism.

[45] A. A. Yaqoob, M. N. M. Ibrahim, M. Rafatullah, Y. S. Chua, A. Ahmad, and K. Umar, "Recent advances in anodes for microbial fuel cells: An overview," *Materials*, vol. 13, no. 9. Multidisciplinary Digital Publishing Institute (MDPI), May 01, 2020, doi: 10.3390/ma13092078.

[46] M. J. Angelaalincy, R. Navanietha Krishnaraj, G. Shakambari, B. Ashokkumar, S. Kathiresan, and P. Varalakshmi, "Biofilm Engineering Approaches for Improving the Performance of Microbial Fuel Cells and Bioelectrochemical Systems," *Front. Energy Res.*, vol. 6, p. 63, Jul. 2018, doi: 10.3389/fenrg.2018.00063.

[47] K. JM, M. DN, M. JM, M. FB, and K. GN, "Microbial Fuel Cells: Influence of External Resistors on Power, Current and Power Density," *J. Thermodyn. Catal.*, vol. 08, no. 01, 2017, doi: 10.4172/2157-7544.1000182.

[48] J. Menicucci, H. Beyenal, E. Marsili, R. A. Veluchamy, G. Demir, and Z. Lewandowski, "Procedure for determining maximum sustainable power generated by microbial fuel cells," *Environ. Sci. Technol.*, vol. 40, no. 3, pp. 1062–1068, Feb. 2006, doi: 10.1021/es051180l.

[49] S. Dharmalingam, V. Kugarajah, and M. Sugumar, "Membranes for microbial fuel cells," in *Biomass, Biofuels, Biochemicals: Microbial Electrochemical Technology: Sustainable Platform for Fuels, Chemicals and Remediation*, Elsevier, 2018, pp. 143–194.

[50] Y. Pan, X. Mo, K. Li, L. Pu, D. Liu, and T. Yang, “Iron-nitrogen-activated carbon as cathode catalyst to improve the power generation of single-chamber air-cathode microbial fuel cells,” *Bioresour. Technol.*, vol. 206, pp. 285–289, Apr. 2016, doi: 10.1016/j.biortech.2016.01.112.

[51] P. Kaewkannetra, W. Chiwes, and T. Y. Chiu, “Treatment of cassava mill wastewater and production of electricity through microbial fuel cell technology,” *Fuel*, vol. 90, no. 8, pp. 2746–2750, Aug. 2011, doi: 10.1016/j.fuel.2011.03.031.

[52] Y. Sun, Z. Z. Zhang, Y. M. Sun, and G. X. Yang, “One-pot pyrolysis route to Fe−N-doped carbon nanosheets with outstanding electrochemical performance as cathode materials for microbial fuel cell,” *Int. J. Agric. Biol. Eng.*, vol. 13, no. 6, pp. 207–214, Dec. 2020, doi: 10.25165/j.ijabe.20201306.5765.

[53] A. Iannaci, T. Pepè Sciarria, B. Mecheri, F. Adani, S. Licoccia, and A. D’Epifanio, “Power generation using a low-cost sulfated zirconium oxide based cathode in single chamber microbial fuel cells,” *J. Alloys Compd.*, vol. 693, pp. 170–176, 2017, doi: 10.1016/j.jallcom.2016.09.159.

[54] T. Yamashita and H. Yokoyama, “Molybdenum anode: A novel electrode for enhanced power generation in microbial fuel cells, identified via extensive screening of metal electrodes,” *Biotechnol. Biofuels*, vol. 11, no. 1, pp. 1–13, Feb. 2018, doi: 10.1186/s13068-018-1046-7.

[55] M. Lu and S. F. Y. Li, “Cathode reactions and applications in microbial fuel cells: A review,” *Critical Reviews in Environmental Science and Technology*, vol. 42, no. 23. Taylor & Francis Group, pp. 2504–2525, Jan. 01, 2012, doi: 10.1080/10643389.2011.592744.

[56] L. Zhang *et al.*, “Chemically activated graphite enhanced oxygen reduction and power output in catalyst-free microbial fuel cells,” *J. Clean. Prod.*, vol. 115, pp.

332–336, Mar. 2016, doi: 10.1016/j.jclepro.2015.12.067.

[57] S. Singha, T. Jana, J. A. Modestra, A. Naresh Kumar, and S. V. Mohan, “Highly efficient sulfonated polybenzimidazole as a proton exchange membrane for microbial fuel cells,” *JPS*, vol. 317, pp. 143–152, Jun. 2016, doi: 10.1016/J.JPOWSOUR.2016.03.103.

[58] N. V. Prabhu and D. Sangeetha, “Characterization and performance study of sulfonated poly ether ether ketone/Fe3O4 nano composite membrane as electrolyte for microbial fuel cell,” *Chem. Eng. J.*, vol. 243, pp. 564–571, May 2014, doi: 10.1016/J.CEJ.2013.12.103.

[59] Y. Feng, Q. Yang, X. Wang, Y. Liu, H. Lee, and N. Ren, “Treatment of biodiesel production wastes with simultaneous electricity generation using a single-chamber microbial fuel cell,” *Bioresour. Technol.*, vol. 102, no. 1, pp. 411–415, Jan. 2011, doi: 10.1016/j.biortech.2010.05.059.

[60] S. Chen, S. A. Patil, and U. Schröder, “A high-performance rotating graphite fiber brush air-cathode for microbial fuel cells,” *Appl. Energy*, vol. 211, pp. 1089–1094, Feb. 2018, doi: 10.1016/j.apenergy.2017.12.013.

[61] L. Bi, S. Ci, P. Cai, H. Li, and Z. Wen, “One-step pyrolysis route to three dimensional nitrogen-doped porous carbon as anode materials for microbial fuel cells,” *Appl. Surf. Sci.*, vol. 427, pp. 10–16, 2018, doi: 10.1016/j.apsusc.2017.08.030.

[62] S. Singh, A. Modi, and N. Verma, “Enhanced power generation using a novel polymer-coated nanoparticles dispersed-carbon micro-nanofibers-based air-cathode in a membrane-less single chamber microbial fuel cell,” *Int. J. Hydrogen Energy*, vol. 41, no. 2, pp. 1237–1247, 2016, doi: 10.1016/j.ijhydene.2015.10.099.

[63] A. Mehdinia, E. Ziaei, and A. Jabbari, “Facile microwave-assisted synthesized reduced graphene oxide/tin oxide nanocomposite and using as anode material of microbial fuel cell to improve power generation,” *Int. J. Hydrogen Energy*, vol. 39, no. 20, pp. 10724–10730, 2014, doi: 10.1016/j.ijhydene.2014.05.008.

[64] S. Zhao *et al.*, “Energy Resources: Three-dimensional graphene/Pt nanoparticle composites as freestanding anode for enhancing performance of microbial fuel cells,” *Sci. Adv.*, vol. 1, no. 10, Nov. 2015, doi: 10.1126/sciadv.1500372.

[65] M. Aghababaie, M. Farhadian, A. Jeihanipour, and D. Biria, “Effective factors on the performance of microbial fuel cells in wastewater treatment – a review,” *http://dx.doi.org/10.1080/09593330.2015.1077896*, vol. 4, no. 1, pp. 71–89, Jan. 2015, doi: 10.1080/09593330.2015.1077896.

[66] Y. G. Zhao *et al.*, “Effect of Substrate Conversion on Performance of Microbial Fuel Cells and Anodic Microbial Communities,” *Environ. Eng. Sci.*, vol. 34, no. 9, pp. 666–674, 2017, doi: 10.1089/ees.2016.0604.

[67] M. Rahimnejad, N. Mokhtarian, G. D. Najafpour, A. A. Ghoreyshi, and W. R. W. Daud, “Effective parameters on performance of microbial fuel cell,” *2nd Int. Conf. Environ. Comput. Sci. ICECS 2009*, no. November 2015, pp. 411–415, 2009, doi: 10.1109/ICECS.2009.23.

[68] M. Li *et al.*, “Microbial fuel cell (MFC) power performance improvement through enhanced microbial electrogenicity,” 2018, Accessed: Oct. 12, 2021. [Online]. Available: http://www.elsevier.com/open-access/userlicense/1.0/.

[69] L. Guang, D. A. Koomson, H. Jingyu, D. Ewusi-Mensah, and N. Miwornunyuie, “Performance of exoelectrogenic bacteria used in microbial desalination cell technology,” *Int. J. Environ. Res. Public Health*, vol. 17, no. 3, Feb. 2020, doi: 10.3390/IJERPH17031121.

[70] M. D. Yates *et al.*, “Convergent development of anodic bacterial communities in microbial fuel cells,” *ISME J.*, vol. 6, no. 11, pp. 2002–2013, May 2012, doi: 10.1038/ismej.2012.42.

[71] N. Kim, Y. Choi, S. Jung, and S. Kim, “Development of microbial fuel cells using Proteus vulgaris,” *Bull. Korean Chem. Soc.*, vol. 21, no. 1, pp. 44–48, 2000.

[72] Z. D. Liu, Z. W. Du, J. Lian, X. Y. Zhu, S. H. Li, and H. R. Li, “Improving energy accumulation of microbial fuel cells by metabolism regulation using Rhodoferax ferrireducens as biocatalyst,” *Lett. Appl. Microbiol.*, vol. 44, no. 4, pp. 393–398, Apr. 2007, doi: 10.1111/j.1472-765X.2006.02088.x.

[73] R. Mostafa, J. Tahere, D. Najafpour Ghasem, and G. A. Asghar, “EFFECT OF GLUCOSE CONCENTRATION ON PERFORMANCE OF MICROBIAL FUEL CELL,” *Environ. Res. Technol.*, p. 236, 2010, Accessed: Oct. 12, 2021. [Online]. Available: https://www.researchgate.net/publication/283349632_Effect_of_glucose_concentration_on_performance_of_microbial_fuel_cell.

[74] W. Wu, F. Yang, X. Liu, and L. Bai, “Influence of substrate on electricity generation of Shewanella loihica PV-4 in microbial fuel cells,” *Microb. Cell Fact.*, vol. 13, no. 1, pp. 1–6, May 2014, doi: 10.1186/1475-2859-13-69.

[75] “(PDF) Activated Sludge-based Microbial Fuel Cell for Bio-electricity Generation.” https://www.researchgate.net/publication/303913568_Activated_Sludge-based_Microbial_Fuel_Cell_for_Bio-electricity_Generation (accessed Oct. 12, 2021).

[76] R. Mike, “Microbial fuel cells: A new approach to waste-water treatment - EE

Publishers," *Energize*, 2018. https://www.ee.co.za/article/microbial-fuel-cells-a-new-approach-to-waste-water-treatment.html (accessed Oct. 12, 2021).

[77] A. K. Manohar and F. Mansfeld, "The internal resistance of a microbial fuel cell and its dependence on cell design and operating conditions," *Electrochim. Acta*, vol. 54, no. 6, pp. 1664–1670, Feb. 2009, doi: 10.1016/j.electacta.2008.06.047.

[78] P. Y. Zhang and Z. L. Liu, "Experimental study of the microbial fuel cell internal resistance," *J. Power Sources*, vol. 195, no. 24, pp. 8013–8018, Dec. 2010, doi: 10.1016/j.jpowsour.2010.06.062.

[79] H. Liu and B. E. Logan, "Electricity generation using an air-cathode single chamber microbial fuel cell in the presence and absence of a proton exchange membrane," *Environ. Sci. Technol.*, vol. 38, no. 14, pp. 4040–4046, Jul. 2004, doi: 10.1021/es0499344.

[80] M. Rahimnejad, G. Bakeri, G. Najafpour, M. Ghasemi, and S. E. Oh, "A review on the effect of proton exchange membranes in microbial fuel cells," *Biofuel Research Journal*, vol. 1, no. 1. pp. 7–15, 2014, doi: 10.18331/BRJ2015.1.1.4.

[81] M. Rahimnejad, T. Jafary, F. Haghparast, G. D. Najafpour, and A. A. Ghoreyshi, "Nafion as a nanoproton conductor in microbial fuel cells," *Turkish J. Eng. Environ. Sci.*, vol. 34, no. 4, pp. 289–291, 2010, doi: 10.3906/muh-1006-48.

[82] Y. Hindatu, M. S. M. Annuar, and A. M. Gumel, "Mini-review: Anode modification for improved performance of microbial fuel cell," *Renewable and Sustainable Energy Reviews*, vol. 73. Pergamon, pp. 236–248, Jun. 01, 2017, doi: 10.1016/j.rser.2017.01.138.

[83] M. Kodali, R. Gokhale, C. Santoro, A. Serov, K. Artyushkova, and P. Atanassov, "High Performance Platinum Group Metal-Free Cathode Catalysts for Microbial Fuel Cell (MFC)," *J. Electrochem. Soc.*, vol. 164, no. 3, p. H3041, Dec. 2016,

doi: 10.1149/2.0061703JES.

[84] M. Ghasemi, S. Shahgaldi, M. Ismail, B. H. Kim, Z. Yaakob, and W. R. Wan Daud, "Activated carbon nanofibers as an alternative cathode catalyst to platinum in a two-chamber microbial fuel cell," *Int. J. Hydrogen Energy*, vol. 36, no. 21, pp. 13746–13752, Oct. 2011, doi: 10.1016/J.IJHYDENE.2011.07.118.

[85] Y. Luo, F. Zhang, B. Wei, G. Liu, R. Zhang, and B. E. Logan, "Power generation using carbon mesh cathodes with different diffusion layers in microbial fuel cells," *J. Power Sources*, vol. 196, no. 22, pp. 9317–9321, Nov. 2011, doi: 10.1016/j.jpowsour.2011.07.077.

[86] C. Santoro, Y. Lei, B. Li, and P. Cristiani, "Power generation from wastewater using single chamber microbial fuel cells (MFCs) with platinum-free cathodes and pre-colonized anodes," *Biochem. Eng. J.*, vol. 62, pp. 8–16, Mar. 2012, doi: 10.1016/j.bej.2011.12.006.

[87] A. G. Capodaglio, D. Cecconet, and D. Molognoni, "An integrated mathematical model of microbial fuel cell processes: Bioelectrochemical and microbiologic aspects," *Processes*, vol. 5, no. 4, 2017, doi: 10.3390/pr5040073.

[88] N. Jayasinghe and R. Mahadevan, "Metabolic modeling of spatial heterogeneity of biofilms in microbial fuel cells," in *IFAC Proceedings Volumes (IFAC-PapersOnline)*, Jan. 2010, vol. 11, no. PART 1, pp. 215–220, doi: 10.3182/20100707-3-BE-2012.0050.

[89] A. Torrents, N. Godino, F. J. Campo, F. X. Muñoz, and J. Mas, "Influence of pH and Carbonate Buffering on the Performance of a Lactate Microbial Fuel Cell Results :," p. 14390, 2010, Accessed: Oct. 10, 2021. [Online]. Available: https://www.comsol.com/paper/influence-of-ph-and-carbonate-buffering-on-

the-performance-of-a-lactate-microbia-8752.

[90] D. A. Jadhav, A. A. Carmona-Martínez, A. D. Chendake, S. Pandit, and D. Pant, "Modeling and optimization strategies towards performance enhancement of microbial fuel cells," *Bioresource Technology*, vol. 320. 2021, doi: 10.1016/j.biortech.2020.124256.

[91] X. C. Zhang and A. Halme, "Modelling of a microbial fuel cell process," *Biotechnol. Lett.*, vol. 17, no. 8, pp. 809–814, Aug. 1995, doi: 10.1007/BF00129009.

[92] P. T. Ha, H. Moon, B. H. Kim, H. Y. Ng, and I. S. Chang, "Determination of charge transfer resistance and capacitance of microbial fuel cell through a transient response analysis of cell voltage," *Biosens. Bioelectron.*, vol. 25, no. 7, pp. 1629–1634, Mar. 2010, doi: 10.1016/J.BIOS.2009.11.023.

[93] D. Recio-Garrido, M. Perrier, and B. Tartakovsky, "Parameter estimation of a microbial fuel cell process control-oriented model," in *2014 22nd Mediterranean Conference on Control and Automation, MED 2014*, Nov. 2014, pp. 918–923, doi: 10.1109/MED.2014.6961491.

[94] B. E. Logan, "Exoelectrogenic bacteria that power microbial fuel cells," *Nat. Rev. Microbiol.*, vol. 7, no. 5, pp. 375–381, 2009, doi: 10.1038/nrmicro2113.

[95] G. Mohanakrishna, I. M. Abu-Reesh, S. Kondaveeti, R. I. Al-Raoush, and Z. He, "Enhanced treatment of petroleum refinery wastewater by short-term applied voltage in single chamber microbial fuel cell," *Bioresour. Technol.*, vol. 253, pp. 16–21, 2018, doi: 10.1016/j.biortech.2018.01.005.

[96] C. I. Torres, A. Kato Marcus, and B. E. Rittmann, "Kinetics of consumption of fermentation products by anode-respiring bacteria," *Appl. Microbiol. Biotechnol.*, vol. 77, no. 3, pp. 689–697, 2007, doi: 10.1007/s00253-007-1198-

z.

[97] A. Raychaudhuri and M. Behera, “Review of the Process Optimization in Microbial Fuel Cell using Design of Experiment Methodology,” *J. Hazardous, Toxic, Radioact. Waste*, vol. 24, no. 3, p. 04020013, Jul. 2020, doi: 10.1061/(asce)hz.2153-5515.0000503.

[98] B. Tartakovsky and S. R. Guiot, “A comparison of air and hydrogen peroxide oxygenated microbial fuel cell reactors,” in *Biotechnology Progress*, Jan. 2006, vol. 22, no. 1, pp. 241–246, doi: 10.1021/bp050225j.

[99] Y. Zhang and I. Angelidaki, “Submersible microbial fuel cell sensor for monitoring microbial activity and BOD in groundwater: Focusing on impact of anodic biofilm on sensor applicability,” *Biotechnol. Bioeng.*, vol. 108, no. 10, pp. 2339–2347, Oct. 2011, doi: 10.1002/BIT.23204.

[100] Y. Zeng, Y. F. Choo, B. H. Kim, and P. Wu, “Modelling and simulation of two-chamber microbial fuel cell,” *J. Power Sources*, vol. 195, no. 1, pp. 79–89, Jan. 2010, doi: 10.1016/j.jpowsour.2009.06.101.

[101] Y. J. He and Z. F. Ma, “A Data-Driven Gaussian Process Regression Model for Two-Chamber Microbial Fuel Cells,” *Fuel Cells*, vol. 16, no. 3, pp. 365–376, Jun. 2016, doi: 10.1002/fuce.201500109.

[102] S. Sundararajan, “Design of Experiments – A Primer,” *iSixSigma*, pp. 2–7, 2016, Accessed: Aug. 26, 2021. [Online]. Available: https://www.isixsigma.com/tools-templates/design-of-experiments-doe/design-experiments-%e2%80%93-primer/.

[103] M. A. Abdel-Rahman *et al.*, “One-factor-at-a-time and response surface statistical designs for improved lactic acid production from beet molasses by Enterococcus hirae ds10,” *SN Appl. Sci.*, vol. 2, no. 4, 2020, doi:

10.1007/s42452-020-2351-x.

[104] C. Ireland, “Fundamental Concepts In The Design of Experiments,” *Technometrics*, vol. 7, no. 4, pp. 652–653, 1965, doi: 10.1080/00401706.1965.10490308.

[105] J. Jacyna, M. Kordalewska, and M. J. Markuszewski, “Design of Experiments in metabolomics-related studies: An overview,” *J. Pharm. Biomed. Anal.*, vol. 164, pp. 598–606, 2019, doi: 10.1016/j.jpba.2018.11.027.

[106] A. Raychaudhuri and M. Behera, “Review of the Process Optimization in Microbial Fuel Cell using Design of Experiment Methodology,” *J. Hazardous, Toxic, Radioact. Waste*, vol. 24, no. 3, p. 04020013, Jul. 2020, doi: 10.1061/(ASCE)HZ.2153-5515.0000503.

[107] JMP, “Types of Design of Experiments | Introduction to Statistics | JMP,” *JMP.com*. 2020, Accessed: Aug. 28, 2021. [Online]. Available: https://www.jmp.com/en_ph/statistics-knowledge-portal/what-is-design-of-experiments.html.

[108] D. C. Woods and S. M. Lewis, “Design of experiments for screening,” in *Handbook of Uncertainty Quantification*, Springer International Publishing, 2017, pp. 1143–1185.

[109] A. N. 55 Analytical Methods Committee, “Experimental design and optimisation (4): Plackett-Burman designs,” *Anal. Methods*, vol. 5, no. 8, pp. 1901–1903, Mar. 2013, doi: 10.1039/c3ay90020g.

[110] J. Antony, *Design of Experiments for Engineers and Scientists*. 2003.

[111] Y. Chen, J. Luo, Y. Yan, and L. Feng, “Enhanced production of short-chain fatty acid by co-fermentation of waste activated sludge and kitchen waste under alkaline conditions and its application to microbial fuel cells,” *Appl. Energy*, vol.

102, pp. 1197–1204, Feb. 2013, doi: 10.1016/j.apenergy.2012.06.056.

[112] A. N. Z. Alshehri, “Statistical optimization of pentachlorophenol biodegradation and electricity generation simultaneously in mediator – less air cathode microbial fuel cell,” *J. Environ. Appl. Bioresearch*, vol. 03, no. 1, pp. 6–15, 2015, Accessed: Aug. 28, 2021. [Online]. Available: https://www.researchgate.net/publication/270338703_Statistical_optimization_of_pentachlorophenol_biodegradation_and_electricity_generation_simultaneously_in_mediator_-_less_air_cathode_microbial_fuel_cell.

[113] A. N. Al-Shehri, K. M. Ghanem, and S. M. Al-Garni, “Statistical Optimization of Medium Components to Enhance Bioelectricity Generation in Microbial Fuel Cell,” *Arab. J. Sci. Eng.*, vol. 38, no. 1, pp. 21–27, Nov. 2013, doi: 10.1007/s13369-012-0397-9.

[114] S. Pandit, S. Ghosh, M. M. Ghangrekar, and D. Das, “Performance of an anion exchange membrane in association with cathodic parameters in a dual chamber microbial fuel cell,” *Int. J. Hydrogen Energy*, vol. 37, no. 11, pp. 9383–9392, Jun. 2012, doi: 10.1016/J.IJHYDENE.2012.03.011.

[115] Q. Zhang, L. Zhang, H. Wang, Q. Jiang, and X. Zhu, “Simultaneous efficient removal of oxyfluorfen with electricity generation in a microbial fuel cell and its microbial community analysis,” *Bioresour. Technol.*, vol. 250, pp. 658–665, Dec. 2018, doi: 10.1016/j.biortech.2017.11.091.

[116] M. Behera and M. M. Ghangrekar, “Optimization of Operating Conditions for Maximizing Power Generation and Organic Matter Removal in Microbial Fuel Cell,” *J. Environ. Eng.*, vol. 143, no. 4, p. 04016090, Nov. 2017, doi: 10.1061/(asce)ee.1943-7870.0001179.

[117] B. Tartakovsky and S. R. Guiot, “A comparison of air and hydrogen peroxide

oxygenated microbial fuel cell reactors," in *Biotechnology Progress*, Jan. 2006, vol. 22, no. 1, pp. 241–246, doi: 10.1021/bp050225j.

[118] A. Almatouq and A. O. Babatunde, "Identifying optimized conditions for concurrent electricity production and phosphorus recovery in a mediator-less dual chamber microbial fuel cell," *Appl. Energy*, vol. 230, pp. 122–134, Nov. 2018, doi: 10.1016/j.apenergy.2018.08.108.

[119] P. Kumar and A. K. Mungray, "Microbial fuel cell: optimizing pH of anolyte and catholyte by using taguchi method," *Environ. Prog. Sustain. Energy*, vol. 36, no. 1, pp. 120–128, Jan. 2017, doi: 10.1002/ep.12459.

[120] X. Wang, Y. Tian, H. Liu, X. Zhao, and S. Peng, "Optimizing the performance of organics and nutrient removal in constructed wetland–microbial fuel cell systems," *Sci. Total Environ.*, vol. 653, pp. 860–871, Feb. 2019, doi: 10.1016/J.SCITOTENV.2018.11.005.

[121] R. L. PLACKETT and J. P. BURMAN, "THE DESIGN OF OPTIMUM MULTIFACTORIAL EXPERIMENTS," *Biometrika*, vol. 33, no. 4, pp. 305–325, Jun. 1946, doi: 10.1093/BIOMET/33.4.305.

[122] M. G. Ekpenyong, S. P. Antai, A. D. Asitok, and B. O. Ekpo, "Plackett-burman design and response surface optimization of medium trace nutrients for glycolipopeptide biosurfactant production," *Iran. Biomed. J.*, vol. 21, no. 4, pp. 249–260, Jul. 2017, doi: 10.18869/acadpub.ibj.21.4.249.

[123] T. Design and O. M. Experiments, "5.3.3.5. Plackett-Burman designs," pp. 3–5, 2016, Accessed: Aug. 29, 2021. [Online]. Available: https://www.itl.nist.gov/div898/handbook/pri/section3/pri335.htm.

[124] S. Bhattacharya, "Central Composite Design for Response Surface Methodology and Its Application in Pharmacy," *Response Surf. Methodol. Eng. Sci. [Working*

Title], Jan. 2021, doi: 10.5772/INTECHOPEN.95835.

[125] "Add axial points."

[126] B. Ait-Amir, P. Pougnet, and A. El Hami, "Meta-model development," *Embed. Mechatron. Syst.*, vol. 2, pp. 151–179, Jul. 2015, doi: 10.1016/B978-1-78548-014-0.50006-2.

[127] C. D. Montgomery, *Design and Analysis of Experiments - Douglas C. Montgomery - Google Books*. 463AD.

[128] M. Li *et al.*, "Microbial fuel cell (MFC) power performance improvement through enhanced microbial electrogenicity," *Biotechnology Advances*, vol. 36, no. 4. pp. 1316–1327, 2018, doi: 10.1016/j.biotechadv.2018.04.010.

[129] K. JM, M. DN, M. JM, M. FB, and K. GN, "Microbial Fuel Cells: Influence of External Resistors on Power, Current and Power Density," *J. Thermodyn. Catal.*, vol. 08, no. 01, p. 182, 2017, doi: 10.4172/2157-7544.1000182.

[130] I. M. Abu-Reesh, "Single-and multi-objective optimization of a dual-chamber microbial fuel cell operating in continuous-flow mode at steady state," *Processes*, vol. 8, no. 7, p. 839, Jul. 2020, doi: 10.3390/pr8070839.

[131] K. P. Katuri, K. Scott, I. M. Head, C. Picioreanu, and T. P. Curtis, "Microbial fuel cells meet with external resistance," *Bioresour. Technol.*, vol. 102, no. 3, pp. 2758–2766, 2011, doi: 10.1016/j.biortech.2010.10.147.

[132] L. Zhang, X. Zhu, J. Li, Q. Liao, and D. Ye, "Biofilm formation and electricity generation of a microbial fuel cell started up under different external resistances," *J. Power Sources*, vol. 196, no. 15, pp. 6029–6035, Aug. 2011, doi: 10.1016/J.JPOWSOUR.2011.04.013.

[133] W. C. Oakes, L. L. Leone, and C. G. Gunn, *Engineering your future: An introduction to engineering*. Great Lakes Press, 2004.

[134] S. Agarwal, “Computer based optimization techniques.”

[135] D. R. Lovley, “The microbe electric: conversion of organic matter to electricity,” *Current Opinion in Biotechnology*, vol. 19, no. 6. Elsevier Current Trends, pp. 564–571, Dec. 01, 2008, doi: 10.1016/j.copbio.2008.10.005.

[136] M. Sedighi, S. A. Aljlil, M. D. Alsubei, M. Ghasemi, and M. Mohammadi, “Performance optimisation of microbial fuel cell for wastewater treatment and sustainable clean energy generation using response surface methodology,” *Alexandria Eng. J.*, vol. 57, no. 4, pp. 4243–4253, 2018, doi: 10.1016/j.aej.2018.02.012.

[137] M. Esfandyari, M. A. Fanaei, R. Gheshlaghi, and M. A. Mahdavi, “Neural network and neuro-fuzzy modeling to investigate the power density and Columbic efficiency of microbial fuel cell,” *J. Taiwan Inst. Chem. Eng.*, vol. 58, pp. 84–91, Jan. 2016, doi: 10.1016/j.jtice.2015.06.005.

[138] M. Karimi Alavijeh, M. M. Mardanpour, and S. Yaghmaei, “One-dimensional Conduction-based Modeling of Bioenergy Production in a Microbial Fuel Cell Engaged with Multi-population Biocatalysts,” *Electrochim. Acta*, vol. 184, pp. 151–163, Dec. 2015, doi: 10.1016/j.electacta.2015.10.045.

[139] S. Luo, H. Sun, Q. Ping, R. Jin, and Z. He, “A Review of Modeling Bioelectrochemical Systems: Engineering and Statistical Aspects,” *Energies 2016, Vol. 9, Page 111*, vol. 9, no. 2, p. 111, Feb. 2016, doi: 10.3390/EN9020111.

[140] L. Zhao, J. Naviaux, J. Brouwer, and A. Hochbaum, “Modeling of polarization losses of a microbial fuel cell,” *ASME 2014 12th Int. Conf. Fuel Cell Sci. Eng. Technol. FUELCELL 2014 Collocated with ASME 2014 8th Int. Conf. Energy Sustain.*, 2014, doi: 10.1115/FUELCELL2014-6388.

[141] M. Sindhuja, N. S. Kumar, V. Sudha, and S. Harinipriya, “Equivalent circuit modeling of microbial fuel cells using impedance spectroscopy,” *J. Energy Storage*, vol. 7, pp. 136–146, Aug. 2016, doi: 10.1016/J.EST.2016.06.005.

[142] G. Hernández-Flores, H. M. Poggi-Varaldo, O. Solorza-Feria, M. T. Ponce Noyola, T. Romero-Castañón, and N. Rinderknecht-Seijas, “Tafel equation based model for the performance of a microbial fuel cell,” *Int. J. Hydrogen Energy*, vol. 40, no. 48, pp. 17421–17432, Dec. 2015, doi: 10.1016/J.IJHYDENE.2015.06.119.

[143] A. Abul, J. Zhang, R. Steidl, G. Reguera, and X. Tan, “Microbial fuel cells: Control-oriented modeling and experimental validation,” in *Proceedings of the American Control Conference*, Jul. 2016, vol. 2016-July, pp. 412–417, doi: 10.1109/ACC.2016.7524949.

[144] R.-G. D, P. M, and T. B, “Combined bioelectrochemical-electrical model of a microbial fuel cell,” *Bioprocess Biosyst. Eng.*, vol. 39, no. 2, pp. 267–276, Feb. 2016, doi: 10.1007/S00449-015-1510-8.

[145] M. Esfandyari, M. A. Fanaei, R. Gheshlaghi, and M. Akhavan Mahdavi, “Mathematical modeling of two-chamber batch microbial fuel cell with pure culture of Shewanella,” *Chem. Eng. Res. Des.*, vol. 117, pp. 34–42, Jan. 2017, doi: 10.1016/j.cherd.2016.09.016.

[146] R. Shankar, P. Mondal, and S. Chand, “Modelling and Simulation of Double Chamber Microbial Fuel Cell: Cell Voltage, Power Density and Temperature Variation with Process Parameters,” *Green*, vol. 3, no. 3–4, pp. 181–194, Oct. 2013, doi: 10.1515/GREEN-2012-0027.

[147] A. K. Marcus, C. I. Torres, and B. E. Rittmann, “Conduction-based modeling of the biofilm anode of a microbial fuel cell,” *Biotechnol. Bioeng.*, vol. 98, no. 6,

pp. 1171–1182, Dec. 2007, doi: 10.1002/bit.21533.

[148] N. Jayasinghe, A. Franks, K. P. Nevin, and R. Mahadevan, “Metabolic modeling of spatial heterogeneity of biofilms in microbial fuel cells reveals substrate limitations in electrical current generation,” *Biotechnol. J.*, vol. 9, no. 10, pp. 1350–1361, Oct. 2014, doi: 10.1002/biot.201400068.

[149] C. Picioreanu, I. M. Head, K. P. Katuri, M. C. M. van Loosdrecht, and K. Scott, “A computational model for biofilm-based microbial fuel cells,” *Water Res.*, vol. 41, no. 13, pp. 2921–2940, Jul. 2007, doi: 10.1016/j.watres.2007.04.009.

[150] “Excel Solver - How Integer, Binary and Alldifferent constraints affect solving | solver.” https://www.solver.com/excel-solver-how-integer-binary-and-alldifferent-constraints-affect-solving (accessed Sep. 01, 2021).

[151] M. Arguments, P. E. Parameters, S. Iterations, and C. Violate, “Find minimum of constrained nonlinear multivariable function (fmincon),” *Matlab Doc.*, no. x, p. 2014, 2016, Accessed: Sep. 01, 2021. [Online]. Available: https://www.mathworks.com/help/optim/ug/fmincon.html.

[152] Q. Wen, H. Zhang, Z. Chen, Y. Li, J. Nan, and Y. Feng, “Using bacterial catalyst in the cathode of microbial desalination cell to improve wastewater treatment and desalination,” *Bioresour. Technol.*, vol. 125, pp. 108–113, Dec. 2012, doi: 10.1016/j.biortech.2012.08.140.

[153] M. Mahrach, G. Miranda, C. León, and E. Segredo, “Comparison between single and multi-objective evolutionary algorithms to solve the knapsack problem and the travelling salesman problem,” *Mathematics*, vol. 8, no. 11, pp. 1–23, 2020, doi: 10.3390/math8112018.

[154] T. Lenhart, K. Eckhardt, N. Fohrer, and H. G. Frede, “Comparison of two different approaches of sensitivity analysis,” *Phys. Chem. Earth*, vol. 27, no. 9–

10, pp. 645–654, 2002, doi: 10.1016/S1474-7065(02)00049-9.

[155] R. L. Iman and W. J. Conover, “Small sample sensitivity analysis techniques for computer models, with an application to risk assessment,” *Commun. Stat. - Theory Methods*, vol. 9, no. 17, pp. 1749–1842, Jan. 1980, doi: 10.1080/03610928008827996.

[156] F. Cannavó, “Sensitivity analysis for volcanic source modeling quality assessment and model selection,” *Comput. Geosci.*, vol. 44, pp. 52–59, Jul. 2012, doi: 10.1016/j.cageo.2012.03.008.

[157] T. Homma and A. Saltelli, “Importance measures in global sensitivity analysis of nonlinear models,” *Reliab. Eng. Syst. Saf.*, vol. 52, no. 1, pp. 1–17, 1996, doi: 10.1016/0951-8320(96)00002-6.

[158] T. Homma and A. Saltelli, “Use of sobol’s quasirandom sequence generator for integration of modified uncertainty importance measure,” *J. Nucl. Sci. Technol.*, vol. 32, no. 11, pp. 1164–1173, 1995, doi: 10.1080/18811248.1995.9731832.

[159] S. Kucherenko and S. Song, “Different numerical estimators for main effect global sensitivity indices,” *Reliab. Eng. Syst. Saf.*, vol. 165, pp. 222–238, 2017, doi: 10.1016/j.ress.2017.04.003.

[160] E. Borgonovo, “A new uncertainty importance measure,” *Reliab. Eng. Syst. Saf.*, vol. 92, no. 6, pp. 771–784, Jun. 2007, doi: 10.1016/j.ress.2006.04.015.

[161] E. Triantaphyllou and A. Sánchez, “A sensitivity analysis approach for some deterministic multi-criteria decision-making methods,” *Decis. Sci.*, vol. 28, no. 1, pp. 151–194, 1997, doi: 10.1111/j.1540-5915.1997.tb01306.x.

[162] M. H. Chun, S. J. Han, and N. Il Tak, “An uncertainty importance measure using a distance metric for the change in a cumulative distribution function,” *Reliab. Eng. Syst. Saf.*, vol. 70, no. 3, pp. 313–321, 2000, doi: 10.1016/S0951-

8320(00)00068-5.

[163] W. P. Donders, J. Feinberg, and L. R. Hellevik, “Sensitivity analysis and uncertainty quantification,” pp. 1–53, 2015.

[164] G. E. P. Box and R. D. Meyer, “An analysis for unreplicated fractional factorials,” *Technometrics*, vol. 28, no. 1, pp. 11–18, Feb. 1986, doi: 10.1080/00401706.1986.10488093.

[165] H. Rabitz, M. Kramer, and D. Dacol, “Sensitivity Analysis in Chemical Kinetics,” *Annu. Rev. Phys. Chem.*, vol. 34, no. 1, pp. 419–461, Oct. 1983, doi: 10.1146/annurev.pc.34.100183.002223.

[166] D. J. Pannell, “Sensitivity analysis of normative economic models: Theoretical framework and practical strategies,” *Agric. Econ.*, vol. 16, no. 2, pp. 139–152, May 1997, doi: 10.1016/S0169-5150(96)01217-0.

[167] A. Saltelli, “Sensitivity analysis: Could better methods be used?,” *J. Geophys. Res. Atmos.*, vol. 104, no. D3, pp. 3789–3793, 1999, doi: 10.1029/1998JD100042.

[168] N. Bilal, “Implementation of Sobol’s Method of Global Sensitivity Analysis to a Compressor Simulation Model,” *22nd Int. Compress. Eng. Conf. Purdue*, pp. 1–10, 2014.

[169] S. Liu, *Global Sensitivity Analysis*, vol. 76, no. 3. 2008.

[170] F. Pianosi, F. Sarrazin, and T. Wagener, “A Matlab toolbox for Global Sensitivity Analysis,” *Environ. Model. Softw.*, vol. 70, pp. 80–85, 2015, doi: 10.1016/j.envsoft.2015.04.009.

[171] I. M. Soboĺ, “Quasi-Monte Carlo methods,” *Prog. Nucl. Energy*, vol. 24, no. 1–3, pp. 55–61, 1990, doi: 10.1016/0149-1970(90)90022-W.

[172] I. M. Sobol’, “On the distribution of points in a cube and the approximate

evaluation of integrals," *USSR Comput. Math. Math. Phys.*, vol. 7, no. 4, pp. 86–112, 1967, doi: 10.1016/0041-5553(67)90144-9.

[173] A. Saltelli, "Sensitivity analysis for importance assessment," *Risk Anal.*, vol. 22, no. 3, pp. 579–590, 2002, doi: 10.1111/0272-4332.00040.

[174] G. C. Gil *et al.*, "Operational parameters affecting the performannce of a mediator-less microbial fuel cell," *Biosens. Bioelectron.*, vol. 18, no. 4, pp. 327–334, Apr. 2003, doi: 10.1016/S0956-5663(02)00110-0.

[175] S. Potrykus, L. F. León-Fernández, J. Nieznański, D. Karkosiński, and F. J. Fernandez-Morales, "The influence of external load on the performance of microbial fuel cells," *Energies*, vol. 14, no. 3, 2021, doi: 10.3390/en14030612.

[176] J. Menicucci, H. Beyenal, E. Marsili, R. A. Veluchamy, G. Demir, and Z. Lewandowski, "Procedure for determining maximum sustainable power generated by microbial fuel cells," *Environ. Sci. Technol.*, vol. 40, no. 3, pp. 1062–1068, Feb. 2006, doi: 10.1021/es051180l.

[177] D. Y. Lyon, F. Buret, T. M. Vogel, and J. M. Monier, "Is resistance futile? Changing external resistance does not improve microbial fuel cell performance," *Bioelectrochemistry*, vol. 78, no. 1, pp. 2–7, Apr. 2010, doi: 10.1016/J.BIOELECHEM.2009.09.001.

[178] Z. Ren, H. Yan, W. Wang, M. M. Mench, and J. M. Regan, "Characterization of Microbial Fuel Cells at Microbially and Electrochemically Meaningful Time scales," *Environ. Sci. Technol.*, vol. 45, no. 6, pp. 2435–2441, Mar. 2011, doi: 10.1021/ES103115A.

[179] H. Akaike, "A New Look at the Statistical Model Identification," *IEEE Trans. Automat. Contr.*, vol. 19, no. 6, pp. 716–723, 1974, doi: 10.1109/TAC.1974.1100705.

[180] Y. Yin, C. Fu, and F. Ma, “Global Sensitivity Analysis of a Microbial Fuel Cell Model,” *Int. J. Electrochem. Sci.*, vol. 14, no. 11, pp. 10592–10606, 2019, doi: 10.20964/2019.11.55.

[181] M. Gavrilescu, “Environmental Biotechnology: Achievements, Opportunities and Challenges,” *Dyn. Biochem. Process Biotechnol. Mol. Biol.*, pp. 1–36, 2010.

[182] Y. Yin, C. Fu, and F. Ma, “Global Sensitivity Analysis of a Microbial Fuel Cell Model,” *Int. J. Electrochem. Sci.*, vol. 14, no. 11, pp. 10592–10606, 2019, doi: 10.20964/2019.11.55.

[183] I. M. SOBOL, “Sensitivity Estimates Nonlinear Mathematical Models,” vol. 1, no. 4, pp. 407–414, 1993.

[184] Y. Fan, E. Sharbrough, and H. Liu, “Quantification of the internal resistance distribution of microbial fuel cells,” *Environ. Sci. Technol.*, vol. 42, no. 21, pp. 8101–8107, 2008, doi: 10.1021/es801229j.

[185] M. D. McKay, R. J. Beckman, and W. J. Conover, “Comparison of three methods for selecting values of input variables in the analysis of output from a computer code,” *Technometrics*, vol. 21, no. 2, pp. 239–245, May 1979, doi: 10.1080/00401706.1979.10489755.

[186] G. Sin and K. V. Gernaey, “Improving the Morris method for sensitivity analysis by scaling the elementary effects,” *Comput. Aided Chem. Eng.*, vol. 26, pp. 925–930, 2009, doi: 10.1016/S1570-7946(09)70154-3.

[187] M. Jaxa-Rozen and J. Kwakkel, “Tree-based ensemble methods for sensitivity analysis of environmental models: A performance comparison with Sobol and Morris techniques,” *Environ. Model. Softw.*, vol. 107, pp. 245–266, 2018, doi: 10.1016/j.envsoft.2018.06.011.

[188] J. D. Herman, J. B. Kollat, P. M. Reed, and T. Wagener, “Technical Note:

Method of Morris effectively reduces the computational demands of global sensitivity analysis for distributed watershed models," *Hydrol. Earth Syst. Sci.*, vol. 17, no. 7, pp. 2893–2903, 2013, doi: 10.5194/hess-17-2893-2013.

[189] A. Saltelli and T. Homma, "Importance measures in global sensitivity analysis of model output," *Reliab. Eng. Sys. Saf.*, vol. 52, pp. 1–17, 1996.

[190] M. D. Morris, "Factorial sampling plans for preliminary computational experiments," *Technometrics*, vol. 33, no. 2, pp. 161–174, 1991, doi: 10.1080/00401706.1991.10484804.

[191] F. D. Baker and R. E. Bargmann, "Orthogonal central composite designs of the third order in the evaluation of sensitivity and plant growth simulation models," *J. Am. Stat. Assoc.*, vol. 80, no. 391, pp. 574–579, Sep. 1985, doi: 10.1080/01621459.1985.10478156.

[192] S. Liu, "Global Sensitivity Analysis: The Primer by Andrea Saltelli, Marco Ratto, Terry Andres, Francesca Campolongo, Jessica Cariboni, Debora Gatelli, Michaela Saisana, Stefano Tarantola," *Int. Stat. Rev.*, vol. 76, no. 3, pp. 452–452, 2008, doi: 10.1111/j.1751-5823.2008.00062_17.x.

[193] H. Ren, C. I. Torres, P. Parameswaran, B. E. Rittmann, and J. Chae, "Improved current and power density with a micro-scale microbial fuel cell due to a small characteristic length," *Biosens. Bioelectron.*, vol. 61, pp. 587–592, 2014, doi: 10.1016/j.bios.2014.05.037.

[194] D. J. Batstone, J. Keller, R. B. Newell, and M. Newland, "Modelling anaerobic degradation of complex wastewater. I: Model development," *Bioresour. Technol.*, vol. 75, no. 1, pp. 67–74, Oct. 2000, doi: 10.1016/S0960-8524(00)00018-3.

[195] A. K. Marcus, C. I. Torres, and B. E. Rittmann, "Conduction-based modeling of

the biofilm anode of a microbial fuel cell," *Biotechnol. Bioeng.*, vol. 98, no. 6, pp. 1171–1182, Dec. 2007, doi: 10.1002/bit.21533.

[196] P. Wang and H. Jia, "Power-Generation from Biorenewable Resources: Biocatalysis in Biofuel Cells," in *Bioprocessing for Value-Added Products from Renewable Resources*, Elsevier, 2007, pp. 507–525.

[197] A. Choi, B. D. Yoon, H. S. Kim, and H. M. Oh, "Growth and carbon fixation of cyanobacterium Spirulina platensis with different nitrogen sources," *Stud. Surf. Sci. Catal.*, vol. 153, pp. 581–584, 2004, doi: 10.1016/S0167-2991(04)80320-3.

[198] H. J. Jördening and J. Winter, *Environmental Biotechnology: Concepts and Applications*. 2005.

[199] S. Kucherenko and S. Song, "Different numerical estimators for main effect global sensitivity indices," *Reliab. Eng. Syst. Saf.*, vol. 165, pp. 222–238, 2017, doi: 10.1016/j.ress.2017.04.003.

[200] G. Glatting, P. Kletting, S. N. Reske, K. Hohl, and C. Ring, "Choosing the optimal fit function: Comparison of the Akaike information criterion and the F-test," *Med. Phys.*, vol. 34, no. 11, pp. 4285–4292, 2007, doi: 10.1118/1.2794176.

[201] B. W. Matthews, "Comparison of the predicted and observed secondary structure of T4 phage lysozyme," *BBA - Protein Struct.*, vol. 405, no. 2, pp. 442–451, Oct. 1975, doi: 10.1016/0005-2795(75)90109-9.

[202] T. M. Ludden, S. L. Beal, and L. B. Sheiner, "Comparison of the Akaike Information Criterion, the Schwarz criterion and the F test as guides to model selection," *J. Pharmacokinet. Biopharm.*, vol. 22, no. 5, pp. 431–445, Oct. 1994, doi: 10.1007/BF02353864.

[203] Z. Wang and P. Wang, "A double-loop adaptive sampling approach for sensitivity-free dynamic reliability analysis," *Reliab. Eng. Syst. Saf.*, vol. 142,

pp. 346–356, Jun. 2015, doi: 10.1016/j.ress.2015.05.007.

[204] N. Massey, “Feature tracking on the hierarchical equal area triangular mesh,” *Comput. Geosci.*, vol. 44, pp. 42–51, Jul. 2012, doi: 10.1016/j.cageo.2012.03.012.

[205] J. Cohen, “A Coefficient of Agreement for Nominal Scales,” *Educ. Psychol. Meas.*, vol. 20, no. 1, pp. 37–46, 1960, doi: 10.1177/001316446002000104.

[206] M. Battaglia and D. P. Hill, “Analytical modeling of gravity changes and crustal deformation at volcanoes: The Long Valley caldera, California, case study,” *Tectonophysics*, vol. 471, no. 1–2, pp. 45–57, Jun. 2009, doi: 10.1016/j.tecto.2008.09.040.

[207] J. H. Dieterich and R. W. Decker, “Finite element modeling of surface deformation associated with volcanism,” *J. Geophys. Res.*, vol. 80, no. 29, pp. 4094–4102, Oct. 1975, doi: 10.1029/jb080i029p04094.

[208] G. Adelfio, M. Chiodi, A. D’Alessandro, D. Luzio, G. D’Anna, and G. Mangano, “Simultaneous seismic wave clustering and registration,” *Comput. Geosci.*, vol. 44, pp. 60–69, Jul. 2012, doi: 10.1016/j.cageo.2012.02.017.

[209] G. J. McRae, J. W. Tilden, and J. H. Seinfeld, “Global sensitivity analysis-a computational implementation of the Fourier Amplitude Sensitivity Test (FAST),” *Comput. Chem. Eng.*, vol. 6, no. 1, pp. 15–25, 1982, doi: 10.1016/0098-1354(82)80003-3.

[210] M. Ye and M. C. Hill, *Global Sensitivity Analysis for Uncertain Parameters, Models, and Scenarios*, no. 2015. 2017.

[211] B. E. Rittmann, “Microbial ecology to manage processes in environmental biotechnology,” *Trends Biotechnol.*, vol. 24, no. 6, pp. 261–266, 2006, doi: 10.1016/j.tibtech.2006.04.003.

6.0. Appendices

6.1.Appendix 1: RSM tables

Table 1. Plackett–Burman Randomized screening design for the study

Run	Run type [a]	Blk	X_1[b]	X_2[b]	X_3[b]	X_4[b]	X_5[b]	X_6[b]	X_7[b]
1	O1	1	-	-	-	-	-	-	-
2	O2	1	-	-	-	+	+	+	-
3	S1	1	+α	0	0	0	0	0	0
4	O3	1	+	-	-	-	+	+	+
5	O4	1	+	+	-	+	+	-	+
6	S2	1	- α	0	0	0	0	0	0
7	O5	1	-	+	+	+	-	+	+
8	O6	1	-	+	-	-	-	+	+
9	O7	1	+	-	+	+	-	+	-
10	O8	1	-	+	+	-	+	-	-
11	C1	1	0	0	0	0	0	0	0
12	O9	1	+	+	+	-	+	+	-
13	O10	1	+	-	+	-	-	-	+
14	S3	2	0	0	+α	0	0	0	0
15	O11	2	+	-	+	+	-	+	-
16	O12	2	-	+	+	-	+	-	-
17	O13	2	+	-	-	-	+	+	+
18	C2	2	0	0	0	0	0	0	0
19	O14	2	+	+	-	+	+	-	+
20	O15	2	-	+	+	+	-	+	+
21	O16	2	+	+	-	+	-	-	-
22	S4	2	0	0	0	0	0	-α	0
23	O17	2	+	+	+	-	+	+	-

24	S5	2	0	0	0	+α	0	0	0
25	O18	2	-	-	-	-	-	-	-
26	O19	2	-	+	-	-	-	+	+

[a] O =orthogonal design points, C = centre points, S = axial points.

[b] 0 = centre value, +1 = high value, 1 = low value, (+/−)α = star point value.

Where: X_1: feed substrate concentration (mg/L); X_2: dilution rate (1/day); X_3: external resistance (ohm); substrate concentration (mg/L); anodophelic bacteria concentration (mg/L); methanogenic bacteria concentration (mg/L); Mediator concentration per anodophelic bacteria concentration (mg M/mg Xa).

Table 0. ANOVA of screening design for all the response functions

Term	Effect	Coef.	SE Coef.	T-value	P-value	VIF
1. Power density						
Feed substrate Conc. (mg/L)	47.78	23.89	9.98	2.39	0.029	1.42
Dilution rate (1/d)	-22.12	-11.06	8.69	-1.27	0.221	1.08
Rext. (Ohm)	-77.42	-38.71	8.51	-4.55	0.000	1.04
Subs. Conc. (mg/L)	49.3	24.7	11.1	2.23	0.040	1.56
Anod.Conc.(mgXa/L)	103.25	51.63	8.69	5.94	0.000	1.08
Meth.Conc.(mgXm/L)	13.98	6.99	8.40	0.83	0.418	1.01
Mediator Conc.(mgM/mgXa)	16437	8218	2127	3.86	0.001	1.08
Ct Pt		-64.8	31.2	-2.08	0.054	1.07
2. Current density						
I. Sub. Conc. (mg/L)	2344	1172	490	2.39	0.029	1.42
Dilution rate (1/d)	-1085	-543	426	-1.27	0.221	1.08
Rext. (Ohm)	-3797	-1899	417	-4.55	0.000	1.04
Subs. Conc. (mg/L)	2420	1210	542	2.23	0.040	1.56

Anod.Conc.(mgXa/L)	5064	2532	426	5.94	0.000	1.08
Meth.Conc.(mgXm/L)	686	343	412	0.83	0.418	1.01
Mediator Conc.(mgM/mgXa)	806213	403106	104306	3.86	0.001	1.08
Ct Pt		-3180	1531	-2.08	0.054	1.07
3. Substrate removal efficiency						
I. Sub. Conc. (mg/L)	38.19	19.10	7.29	2.62	0.019	1.42
Dilution rate (1/d)	19.56	9.78	6.35	1.54	0.143	1.08
Rext. (Ohm)	-13.20	-6.60	6.21	-1.06	0.304	1.04
Subs. Conc. (mg/L)	-109.26	-54.63	8.08	-6.76	0.000	1.56
Anod.Conc.(mgXa/L)	-19.56	-9.78	6.35	-1.54	0.143	1.08
Meth.Conc.(mgXm/L)	-3.17	-1.58	6.14	-0.26	0.800	1.01
Mediator Conc.(mgM/mgXa)	-3299	-1650	1553	-1.06	0.304	1.08
Ct Pt		-26.0	22.8	-1.14	0.271	1.07

Table 1. ANOVA from CCD for all the functions

Source	DF	Adj SS	Adj MS	F-Value	P-Value
1. Power density					
Model	27	649744	24065	114.60	0.000
Linear	**6**	**289196**	**48199**	**229.53**	**0.000**
Rext (ohm)	1	150028	150028	714.45	0.000
Anod. Conc. (mg/L)	1	138981	138981	661.84	0.000
Square	**6**	**30293**	**5049**	**24.04**	**0.000**
Rext (ohm)*Rext (ohm)	1	15364	15364	73.16	0.000
2-Way Interaction	**15**	**186122**	**12408**	**59.09**	**0.000**
Rext (ohm)*Anod. Conc. (mg/L)	1	185552	185552	883.62	0.000
R^2 (%)			98.04		
2. Current density					

Model	27	1659822	61475	12.61	0.000
Linear	**6**	**197683**	**32947**	**6.76**	**0.000**
Rext (ohm)	1	79043	79043	16.21	0.000
Anod. Conc. (mg/L)	1	117724	117724	24.14	0.000
Square	**6**	**143047**	**23841**	**4.89**	**0.000**
Dilution (1/D)*Dilution (1/D)	1	97555	97555	20.01	0.000
Rext (ohm)*Rext (ohm)	1	289	289	0.06	0.008
2-Way Interaction	**15**	**923381**	**61559**	**12.62**	**0.000**
I. Sub. Conc.(mg/L)*Dilution (1/D)	1	12	12	20	0.00019
I. Sub. Conc.(mg/L)*Rext (ohm)	1	87123	87123	17.87	0.000
I. Sub. Conc.(mg/L)*Sub. Conc.(mg/L)	1	182	182	14	0.00012
I. Sub. Conc.(mg/L)*Anod. Conc. (mg/L)	1	132	132	30	0.00010
I. Sub. Conc.(mg/L)*Meth. Conc. (mg/L)	1	92483	92483	18.97	0.000
Dilution (1/D)*Rext (ohm)	1	142565	142565	29.24	0.000
Dilution (1/D)*Sub. Conc.(mg/L)	1	242	242	25	0.00012
Dilution (1/D)*Anod. Conc. (mg/L)	1	34955	34955	7.17	0.0009
Dilution (1/D)*Meth. Conc. (mg/L)	1	35022	35022	7.18	0.0009
Rext (ohm)*Sub. Conc.(mg/L)	1	592	592	12	0.0017

Rext (ohm)*Anod. Conc. (mg/L)	1	310983	310983	63.78	0.000
Rext (ohm)*Meth. Conc. (mg/L)	1	34955	34955	7.17	0.0009
Sub. Conc.(mg/L)*Anod. Conc. (mg/L)	1	82200	82200	16.86	0.000
Sub. Conc.(mg/L)*Meth. Conc. (mg/L)	1	69188	69188	14.19	0.000
Anod. Conc. (mg/L)*Meth. Conc. (mg/L)	1	45	45	12	0.0009
R^2 (%)			94.02		
3. Substrate removal efficiency					
Model	27	122026	4519.50	2.25275E+09	0.000
Linear	**6**	**7009**	**1168.15**	**5.82267E+08**	**0.000**
I. Sub. Conc.(mg/L)	1	1683	1682.92	8.38856E+08	0.000
Sub. Conc.(mg/L)	1	2127	2126.63	1.06002E+09	0.000
Square	**6**	**2839**	**473.10**	**2.35818E+08**	**0.000**
I. Sub. Conc.(mg/L)*I. Sub. Conc.(mg/L)	1	481	480.77	2.39639E+08	0.000
Sub. Conc.(mg/L)*Sub. Conc.(mg/L)	1	0	0.00	3.09	0.0001
2-Way Interaction	**15**	**499**	**33.24**	**16566656.58**	**0.000**
I. Sub. Conc.(mg/L)*Sub. Conc.(mg/L)	1	496	495.77	2.47117E+08	0.000
R^2 (%)			99.9		

6.2.Appendix 2: Jackobi's Law and power density

Power density maximization:

Current: $I = \frac{V}{R_{int} + R_{ext}}$

Voltage: $V = IR$

Power: $P = IV = IIR_{ext} = I^2 R_{ext} = \left(\frac{V}{R_{int} + R_{ext}}\right)^2 R_{ext} = \frac{V^2}{(R_{ext} + R_{int})^2} R_{ext} = \frac{V^2 R_{ext}}{R_{ext}^2 + 2R_{ext}R_{int} + R_{int}^2} =$

$\frac{V^2 R_{ext}}{R_{ext} + 2R_{int} + \frac{R_{int}^2}{R_{ext}}}$

$\frac{dP}{dR_{ext}} = \frac{d}{dR_{ext}}\left(\frac{V^2 R_{ext}}{R_{ext} + 2R_{int} + \frac{R_{int}^2}{R_{ext}}}\right) = -\frac{R_{int}^2}{R_{ext}^2} + 1$

For maximum power density, the rate of change is zero, therefore:

$\frac{dP}{dR_{ext}} = -\frac{R_{int}^2}{R_{ext}^2} + 1 = 0$

$\frac{R_{int}^2}{R_{ext}^2} = 1$

$R_{ext}^2 = R_{int}^2$

$R_{ext} = R_{int}$

6.3. Appendix 3: Matlab optimization codes

Run file

```
%Optimizing energy productivity of microbial electrochemical cells
(2012)
clc
clear
format long e

%       S0                                  D                       Rext
S                   Xa                              Xm
x0=   [1000;                                  1.00;                   10;
10;             510.5;                                  10 ];
lb=   [1000;                                 1;                       10;
10;                 10;                                 0.1 ];
ub=   [1000;                                inf;                     800;
999;              512.5;                            512.5 ];
Aeq=[];
Beq=[];
A=[];
B=[];
options     =     optimoptions('fmincon','Display','iter','Algorithm','
interior-point','MaxFunEval',2000000000,'MaxIter',
50000000,'ConstraintTolerance',1.000000e-
02,'Plotfcn',@optimplotfval);
[x,fval,exitflag,output]=
fmincon(@objfunN,x0,A,B,Aeq,Beq,lb,ub,@consfunN)
```

Objective file

```
%Optimizing energy 144roductivity of microbial electrochemical cells
(2012)
%Mox: is constant as the system is in the co-existance region
function f=objfunN(x)
%=================================================================
============================================================
%Decision parameters
%x(1)                                                Feed substrate
concentration S0 (mg-S/L)
%x(2)                                                 Dilution rate
(1/day)
%x(3)                                                      External
resistance (ohm)
%x(4)                                                    Substrate
concentration S (mg-S/L)
%x(5)                                                  Anodophelic
cell concentration Xm(mg-Xm/L)
%x(6)                                                 Methanoginic
cell concentration Xm(mg-Xm/L)
%=================================================================
============================================================
%Constants
m=2;                                                          %Electron
```

```
transferred per mol of mediator (moll e/mol M)
F=96485.33;                                                    %Faraday
Constant (A.s/mol)
R= 8.314472;                                                  %Ideal gas
constant (J/mol.K)
KR=0.024;                                                   %Factor (L/mg-
X)
Kr=0.024;
Emax= 0.68;                                                    %Max Open
circuit potential (V)
Emin= 0.01;                                                    %Min Open
circuit potential (V)
Rmax= 2025;                                                     %Maximum
internal resistance (Ohm)
Rmin=25;                                                        %Minimum
internal resistance (Ohm)
T= 303.15;                                                  %MXC operating
temperature (K)
V= 0.05;                                                          %Anode
compartment volume (L)
mumaxa= 1.97;                                                       %Max
electricigenic growth rate (1/day)
mumaxm=0.3;                                                         %Max
methanogenic growth rate (1/day)
Kaa=20;                                                       %Half rate
constant of electricigenic (mg-A/L)
Kam=80;                                                       %Half rate
constant of methanogenic (mg-A/L)
MT= 0.05;                                                      %Mediator
fraction (mg-M/mg-X)
KM=0.01;                                                       %Mediator
half rate constant (mg-M/L)
%=================================================================
==============================
KM1=(mumaxa*(Kam+x(4)));
KM2=(mumaxm*(Kaa+x(4)));
Mox=((KM)/(((KM1)/(KM2))-1));
M=Mox/MT;

eta= ((R*T)/(m*F))*log(1/(1-M));                             %Concentration
losses (V)
Eoc=Emin+((Emax-Emin)*exp((-1)/(KR*x(5))));                   %Open circuit
potential (V)
Rint=Rmin+(Rmax-Rmin)*exp(-Kr*x(5));                             %Internal
resistance (ohm)
CU=(Eoc-eta)/(Rint+x(3));                                      %Current of
MFC (A)
%=================================================================
==============================
%Power density is calculated as= (Current* Voltage)/volume
%Calculatig Voltage(V)
Volt=Eoc-eta;
%Function to be optimized
%Power Density (mW/L)
%f=-1000*(((CU)*Volt)/(V));                                    %PD in (mW/L)
%f=-((x(1)-x(4))/(x(1)));
f=-1000*(Eoc-eta)/(Rint+x(3));                                    %Current
of MFC (A)

%=================================================================
============================================================
```

Constraints file

```
%Optimizing energy producivity of microbial electrochemical cells
(2012)
%Mox: is constant as the system is in the co-existance region
%Non-Linear constraints
function [c, ceq ]= consfunN(x)
%================================================================
============================================================
%Decision parameters
%x(1)                                                  Feed substrate
concentration S0 (mg-S/L)
%x(2)                                                   Dilution rate
(1/day)
%x(3)                                                        External
resistance (ohm)
%x(4)                                                     Substrate
concentration S (mg-S/L)
%x(5)                                                    Anodophelic
cell concentration Xm(mg-Xm/L)
%x(6)                                                    Methanoginic
cell concentration Xm(mg-Xm/L)
%================================================================
============================================================
%Constants
qmaxa=13.14;                                                      %Max
electricigenic reation rate (mg-A/mg-Xa.day)
qmaxm=14.12;                                                      %Max
methanogenic reation rate (mg-A/mg-Xm.day)
mumaxa= 1.97;                                                     %Max
electricigenic growth rate (1/day)
mumaxm=0.3;                                                       %Max
methanogenic growth rate (1/day)
KAa=20;                                                        %Half rate
constant of electricigenic (mg-A/L)
KAm=80;                                                        %Half rate
constant of methanogenic (mg-A/L)
m=2;                                                            %Electron
transfered per mol of mediator (moll e/mol M)
F=96485.33;                                                      %Faraday
Constant (A.s/mol)
R= 8.314472;                                                   %Ideal gas
constant (J/mol.K)
Y= 663400;                                                      %Mediator
molar mass (mg-M/mol M)
MT= 0.05;                                                       %Mediator
fraction (mg-M/mg-X)
KM=0.01;                                                        %Mediator
half rate constant (mg-M/L)
KR=0.024;                                                         %Factor
(L/mg-X)
Kr=0.024;
Emax= 0.68;                                                     %Max Open
circuit potential (V)
Emin= 0.01;                                                     %Min Open
circuit potential (V)
Rmax= 2025;                                                      %Maximum
internal resistance (Ohm)
YM= 34.85;                                                     %Yield (mg-
M/mg-A)
```

```
Xmax= 512.5;                                                    %Anode
biofilm space limiatation (mg-X/L)
T= 303.15;                                                  %MXC operating
temperature (K)
V= 0.05;                                                        %Anode
compartment volume (L)
Kda= 0.04;                                                    %Decay rate
of anodophilic microorganisms (1/day)
Kdm= 0.002;                                                   %Decay rate
of methanogenic microorganisms (1/day)
Rmin=25;                                                        %Minimum
internal resistance (Ohm)
Kx=0.40;                                                     %Steepness
factor in calculating Alpha equation factor
%=================================================================
==============================
%Electro-chemical Equations

KM1=(mumaxa*(KAm+x(4)));
KM2=(mumaxm*(KAa+x(4)));
Mox=((KM)/(((KM1)/(KM2))-1));
M=Mox/MT;

mua= mumaxa*((x(4))/(x(4)+KAa))*((M)/(M+(KM/MT)));
mum=mumaxm*((x(4))/(KAm+x(4)));
qa= qmaxa*((x(4))/(x(4)+KAa))*((M)/(M+(KM/MT)));
qm= qmaxm*((x(4))/(KAm+x(4)));

if (x(5)+x(6)>=Xmax)
alpha=(((mua*x(5))+(mum*x(6)))/((x(5)+x(6))));
else
    alpha=0;
end


%=================================================================
==============================
eta= ((R*T)/(m*F))*log(1/(1-M));                            %Concentration
losses (V)
Eoc=Emin+((Emax-Emin)*exp((-1)/(KR*x(5))));                  %Open circuit
potential (V)
Rint=Rmin+(Rmax-Rmin)*exp(-Kr*x(5));                            %Internal
resistance (ohm)
CU=(Eoc-eta)/(Rint+x(3));                                     %Current of
MFC (A)
%=================================================================
==============================
%Non-linear constraints
%1- Equality non-linear Constraints
%ceq1= dS/dt
ceq1=(-qa*x(5))-(qm*x(6))+(x(2)*(x(1)-x(4)));
%ceq2= dXa/dt
ceq2= (mua*x(5))-(Kda*x(5))-(alpha*x(2)*x(5));
%ceq3= dXm/dt
ceq3= (mum*x(6))-(Kdm*x(6))-(alpha*x(2)*x(6));
%Linear equality constraint
%ceq4= Xm+Xa=Xmax
ceq4= x(5)+x(6)-512.5;
%ceq5=Rint=Rext
ceq5=Rint-x(3);
```

```
ceq =[ceq1;

      ceq2;

      ceq3;

      ceq4;

      ceq5];
%Non-linear, Non-equality constraint

c= ((eta-Eoc));
```